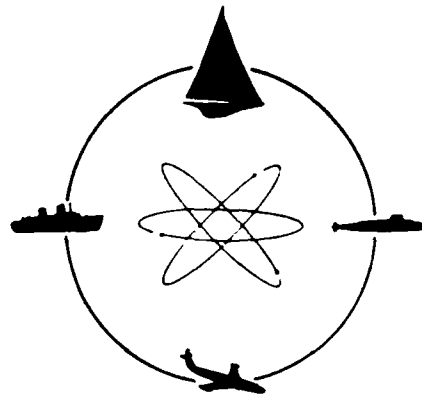


AD 1870

12

TR-2275



# DAVIDSON LABORATORY

Technical Report SIT-DL-82-9-2275  
December 1982

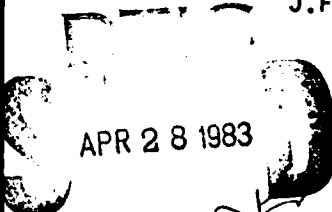
AN INVESTIGATION OF THE APPLICABILITY OF  
THE THIRD DEGREE FUNCTIONAL POLYNOMIAL MODEL  
TO NON-LINEAR SHIP MOTIONS PROBLEMS

by  
J.F. Dalzell



STEVENS INSTITUTE  
OF TECHNOLOGY

CASTLE POINT STATION  
HOBOKEN, NEW JERSEY 07030



**A**  
APPROVED FOR PUBLIC RELEASE:  
DISTRIBUTION UNLIMITED

Reproduction in whole or in part is  
permitted for any purpose of the  
United States Government.

88 04 28 1 16

TR-2275



UNCLASSIFIED

SECURITY CLASSIFICATION OF THIS PAGE(When Data Entered)

cont

nonlinearities was carried out for random excitation. The qualitative influence of cubic nonlinearities on random time domain response as well as response spectra are discussed. A first attempt was made at cross-tri-spectral identification of cubic response from samples of random excitation and response. Though this attempt was partially successful, the numerical method employed was not satisfactory in an important way and further development is indicated.



Account for the  
Number of  
In the  
A  
Special



UNCLASSIFIED

SECURITY CLASSIFICATION OF THIS PAGE(When Data Entered)

STEVENS INSTITUTE OF TECHNOLOGY  
DAVIDSON LABORATORY  
Castle Point Station, Hoboken, New Jersey 07030

Report SIT-DL-82-9-2275

December 1982

AN INVESTIGATION OF THE APPLICABILITY OF  
THE THIRD DEGREE FUNCTIONAL POLYNOMIAL MODEL  
TO NON-LINEAR SHIP MOTIONS PROBLEMS

by  
J.F. Dalzell

This research was carried out under the  
Naval Sea Systems Command  
General Hydromechanics Research Program  
SR 023-01-01 administered by the  
David W. Taylor Naval Ship Research and Development Center  
under  
Contract N00014-81-K-0231  
(Davidson Laboratory Project 4937/113)

APPROVED FOR PUBLIC RELEASE: DISTRIBUTION UNLIMITED

Reproduction in whole or in part is permitted  
for any purpose of the United States Government.

APPROVED: 

Daniel Savitsky  
Acting Director

## TABLE OF CONTENTS

INTRODUCTION.....	1
THE FUNCTIONAL SERIES MODEL.....	6
Generalities.....	6
The Functional Series.....	6
Impulse and Frequency Response Functions.....	8
THE THIRD DEGREE FUNCTIONAL POLYNOMIAL.....	10
DETERMINISTIC IDENTIFICATION OF FREQUENCY RESPONSE FUNCTIONS.....	11
FREQUENCY DOMAIN SIMULATION OF A CUBIC SYSTEM.....	20
SIMULATED IMPULSE RESPONSES.....	28
TIME DOMAIN COMPUTATIONS: PRACTICAL MATTERS.....	36
SIMULATION OF RESPONSE TO RANDOM EXCITATION.....	38
THE SPECTRUM OF RESPONSE TO RANDOM EXCITATION.....	50
IDENTIFICATION THEORY FOR THE RANDOM CASE.....	63
CROSS-TRI-SPECTRAL ESTIMATION.....	75
CROSS-BI-SPECTRAL IDENTIFICATION OF THE QUADRATIC FREQUENCY RESPONSE FUNCTION.....	85
TRIAL CROSS-TRI-SPECTRAL IDENTIFICATIONS.....	91
CONCLUDING REMARKS.....	98
RECOMMENDATIONS.....	101
REFERENCES.....	102
APPENDIX A: EXPECTED VALUES OF PRODUCTS OF ZERO MEAN GAUSSIAN EXCITATION.....	105
APPENDIX B: THE $n$ -DIMENSIONAL PARSEVAL FORMULA.....	107
PRINCIPAL NOTATION.....	108

## INTRODUCTION

In the past 2½ decades the approach outlined by St. Denis and Pierson (Reference 1)\* for the estimation of oscillatory ship motion statistics in irregular seas has become firmly established in engineering practice. This approach applies strictly only to ship responses which can be assumed to be linear functions of wave height. The credibility of the approach was established by exercising experimentally as many as possible of the mathematical consequences of the basic mathematical model. In particular it was found possible to a) synthesize observed responses in irregular waves in both time and frequency domains by means of responses obtained in regular waves, and b) identify the fundamental linear response functions from observations in both irregular and transient waves (Reference 2)\*.

In general, when non-linear responses become of importance there is no agreed universal model for dealing with the irregular sea case. However, when the non-linearities may be considered "weak" in some sense one of the conceptual approaches which have been proposed has considerable attraction. This is the functional series model. Among the attractions are that the model is suitable for any reasonably well behaved wave input (regular, transient or random) and since the model contains the completely linear system as a special case it appears to be a logical extension of present practice. In addition, prediction methods for scalar response spectra are available and it appears that the statistics of maxima may be approximated. Finally, it is possible to closely relate the functions required by the model to deterministic hydromechanical analyses and experiment because the effects of hydrodynamic "memory" which complicate the usual analysis are automatically accounted for.

---

\*1. St. Denis, M. and Pierson, W.J., "On the Motions of Ships in Confused Seas," SNAME Vol. 61, 1953.

\*2. Dalzell, J.F., "The Input-Output Approach to Seakeeping Problems: Review and Prospects," T.&R. Symposium S-3, Seakeeping 1953-1973, Society of Naval Architects and Marine Engineers, October 1973.

References 3\* through 7\* represent a contracted bibliography of some of the fundamental mathematical background to the model and References 8\* and 9\* discuss some of the potential for application to seakeeping problems.

In practical use the functional series must be truncated at some degree of non-linearity, thus becoming a functional polynomial. Within the last decade the functional polynomial model of degree two has been applied with some success to the non-linear ship responses in the un-restored modes of motion, in particular to added resistance, slow drift oscillations, etc. By drawing upon the analytical background

- 
- \*3. Weiner, N., "Non-Linear Problems in Random Theory," The Technology Press of MIT and John Wiley and Sons, Inc., 1958.
  - \*4. Barrett, J.F., "The Use of Functionals in the Analysis of Non-Linear Physical Systems," Journal of Electronics and Control, 15, No. 6, December 1963.
  - \*5. George, D.A., "Continuous Non-Linear Systems," Doctoral Dissertation, Department of Electrical Engineering, MIT, July 1959.
  - \*6. Ku, Y.H., and Wolf, A.A., "Volterra-Weiner" Functionals for the Analysis of Non-Linear Systems," Journal of Franklin Institute, 281, No. 1, January 1966.
  - \*7. Bedrosian, E. and Rice, S.O., "The Output Properties of Volterra Systems (Non-Linear Systems with Memory) Driven by Harmonic and Gaussian Inputs," Proceedings of the IEEE, Vol. 59, No. 12, December 1971.
  - \*8. Vassilopoulos, L.A., "The Application of Statistical Theory of Non-Linear Systems to Ship Motion Performance in Random Seas," Ship Control Systems Symposium, Annapolis, November 1966.
  - \*9. Bishop, R.E.D., Burcher, R.K., and Price, W.G., "The Uses of Functional Analysis in Ship Dynamics," Proceeding, Royal Society of London, A. 332, 1973.

afforded by References 10\* through 13\* it was possible to develop practical means of doing cross-bi-spectral analyses of towing tank observations of added resistance, Reference 14\*, and following this a demonstration, Reference 15\*, that a) the non-linear added resistance frequency response function can be identified from irregular wave experiments via cross-bi-spectral analysis, b) the mean added resistance and the spectrum of resistance can be synthesized from the linear and non-linear frequency response functions, c) that time histories of added resistance can be synthesized according to the functional polynomial model, and, d) that hydrodynamic theory can be developed for the required frequency response functions (Reference 16)\*.

- 
- \*10. Tick, L.J., "The Estimation of the "Transfer Functions" of Quadratic Systems," *TECHNOMETRICS*, 3, No. 4, 1961.
- \*11. Hasselman, K., "On Non-Linear Ship Motions in Irregular Waves," *JSR* 10, No. 1, 1966.
- \*12. Shaman, Paul, "Bi-Spectral Analysis of Stationary Time Series," Scientific Paper #18, Statistical Laboratory, School of Engineering and Sciences, N.Y.U., January 1964.
- \*13. Rosenblatt, M. and Van Ness, J.W., "Estimates of the Bi-Spectrum of Stationary Random Processes," Technical Report 11, Nonr 562(29)/11, Division of Applied Mathematics, Brown University, Providence, R.I., March 1964.
- \*14. Dalzell, J.F., "Cross-Bi-Spectral Analysis: Application to Ship Resistance in Waves," *Journal of Ship Research*, Vol. 18, No. 1, March 1974, pp. 62-72.
- \*15. Dalzell, J.F., "Application of the Functional Polynomial Model to the Ship Added Resistance Problem," Eleventh Symposium on Naval Hydrodynamics, University College, London, 1976.
- \*16. Dalzell, J.F. and Kim, C.H., "An Analysis of the Quadratic Frequency Response for Added Resistance," *Journal of Ship Research*, Vol. 23, No. 3, September 1979.

It is becoming clear that even when the functional polynomial model is not explicitly assumed the results of many investigations of the second order forces on ships (References 17\* and 18\* for example) are compatible with the functional polynomial model of the second degree. It is equally clear that this "linear+quadratic" model will not suffice for non-linear response problems where the non-linearity affects the amplitude at excitation frequency of oscillatory response to harmonic excitation. (In the "linear plus quadratic" or second degree system the non-linearities only produce new response frequency components.) Thus it is logical to consider applying the functional polynomial of degree three to some seakeeping problems. It is realistic to consider whether this is necessary since the theoretical hydrodynamicist would consider the non-linearities of the added (cubic) degree to be "third-order". Despite the implications of the words "third-order", "third-order" forces on heaving cylinders have been found (Reference 19)\* not to be negligibly small for large heave amplitudes and in fact magnitudes approaching those of "first-order" or linear forces have been reported. The work of References 20\* and 21\*

- 
- \*17. Newman, J.N., "Second Order Slowly Varying Forces on Vessels in Irregular Waves," International Symposium on the Dynamics of Marine Vehicles and Structures in Waves, University College, London, April 1974.
- \*18. Pinkster, J.A. and van Oortmerssen, G., "Computation of the First and Second Order Wave Forces on Bodies Oscillating in Regular Waves," Proceedings of the Second International Conference on Numerical Ship Hydrodynamics, University of California, pp. 136-156, September 1977.
- \*19. Tasai, F. and Koteratama, W., "Non-Linear Hydrodynamic Forces Acting on Cylinders Heaving on the Surface of a Fluid," Reports of the Research Institute for Applied Mechanics, Vol. XXIV, No. 77, 1976.
- \*20. Dalzell, J.F., "A Note on the Form of Ship Roll Damping," SIT-DL-76-1887, Davidson Laboratory, Stevens Institute of Technology, May 1976, (Also: Journal of Ship Research, Vol. 22, No. 3, September 1978).
- \*21. Dalzell, J.F., "Estimation of the Spectrum of Non-Linear Ship Rolling: The Functional Series Approach," SIT-DL-76-1894, Davidson Laboratory, Stevens Institute of Technology, May 1976, AD-A031 055/7G1.

has shown that if some of the long accepted ideas about non-linear ship rolling are to be accommodated by the functional polynomial approach, the polynomial must be at least of degree three. Thus there was encouragement in prior work to consider further the applicability of the third degree model to seakeeping problems.

The main avenue of establishing credibility in the cases of linear and linear+quadratic systems was through the capability of decomposing observations in irregular seas by analysis. In the linear case this has been through cross-spectral analysis. In the linear+quadratic case this has been through cross-bi-spectral analysis. In the linear+quadratic+cubic case (the functional polynomial of degree three) the analysis approach is not established.

The objectives of the present work were to further explore the applicability of the third degree functional polynomial to seakeeping problems and to attempt the development of an analysis approach by which third degree non-linearities in the response of ships to random waves might be interpreted and characterized.

## THE FUNCTIONAL SERIES MODEL

Generalities

The mathematical applications involved in the present work were first expressed by Wiener, Reference 3, and have since been slowly amplified and simplified for engineering purposes to a point that specialized text book coverage has begun to appear (Reference 22\* for example). All the fundamental mathematical development has taken place in the context of system or communication theory where typically a "system" has a single "input" or excitation and a single "output" or response. Clearly, the general seakeeping problem is more complicated since in that case the physical ship system is conceptually excited by elemental wave components arriving simultaneously from a continuous range of headings--the ship in short crested seas may at the very least be considered a multiple input system. For present purposes however the single excitation assumption must be made, and this translates into the case of long crested seas. In the event that the ship has forward speed, additional specializations must be made in order that the available mathematical background be utilized. These are that the mapping of wave frequency into encounter frequency be essentially single valued, and that the excitation be defined at a point which translates with the ship. These specializations correspond to what is usually done in towing tank experiments as well as the specializations customary in hydromechanical analyses. Essentially, the restrictions imposed by the available systems background suggest applicability to a useful (but not all inclusive) sub-class of sea-keeping problems.

The Functional Series

Within the class of problems so defined it will be possible to identify a response,  $Y(t)$ , of interest (a function of time,  $t$ ) and an excitation,  $X(t)$ , which is typically identified as a wave

---

\*22. Rugh, W.J., "Nonlinear System Theory; The Volterra/Wiener Approach," Johns Hopkins University Press, 1981.

elevation. Thus for present purposes it is reasonable to assume that the excitation,  $X(t)$ , is a zero mean function whether it be random or deterministic. Thus, following References 14, 15, 21, as a first step it is hypothesized that the response,  $Y(t)$ , is a sufficiently regular function that it may at least be expanded in an infinite functional series:

$$Y(t) = \sum_{n=0}^{\infty} \int \int \cdots \int \left[ g_n(t_1, t_2, \dots, t_n) X(t-t_1) \cdots X(t-t_n) dt_1 dt_2 \cdots dt_n \right] \quad (1)$$

(Omission of limits on integrals here and throughout this report signify limits of  $-\infty$  and  $+\infty$ .)

Each term in the series as written above is homogeneous functional of degree  $n$ . The terms are said to be homogeneous because a change in  $X(t)$  to  $c X(t)$  (where  $c$  is constant) results in multiplication of the term of degree  $n$  by  $(c^n)$ . The kernels,  $g_n(t_1 \cdots t_n)$ , are "time invariant", since they are considered to be functions only of time differences. In the present application, the wave system varies with time, but not the ship. Consequently the properties of the ship are contained wholly within the kernels.

Reference 4 indicates that the series expansion is unique if all kernels are completely symmetrical in the variables; that is

$$g_n(t_1, t_2, \dots, t_n) = g_n(t_2, t_3, \dots, t_n, t_1) \cdots \quad (2)$$

for any rearrangement of the variables  $t_j$ . (No loss of generality results from this restriction.)

According to Reference 6, the functional series converges for bounded excitation so long as the sum of integrals of the absolute value of all kernels is less than  $+\infty$ . The same is true with stochastic excitation, if in addition the input is strictly stationary with bounded moments of all orders. One physical way of looking at the convergence restrictions on the kernels is that the "memory" of the ship must not be enormously long, a restriction intuitively

acceptable for most if not all seakeeping responses. The restrictions on the excitation are those which have been tacitly accepted for some time in seakeeping research.

So long as the series, Equation 1, converges, its value is that of the kernel of zeroth degree ( $g_0$ ) when the excitation,  $X(t)$ , is zero. In the present context, responses in the absence of waves are not of interest so that the first term in the series may be dropped in all subsequent development.

#### Impulse and Frequency Response Functions

The kernels in Equation 1 may be considered as describing the system through a series of  $n^{\text{th}}$  degree impulse response functions. It is presumed that each impulse response function is sufficiently smooth and integrable so that there is no trouble about existence of an  $n$ -fold Fourier transform. Accordingly, it is assumed that to each  $n^{\text{th}}$  degree impulse response function there corresponds an  $n^{\text{th}}$  degree frequency response function,  $G_n(\omega_1, \omega_2 \dots \omega_n)$ . The transform pairs relating impulse and frequency response functions may be defined as follows:

$$g_n(t_1, t_2 \dots t_n) = \frac{1}{(2\pi)^n} \int \int \dots \int G_n(\omega_1, \omega_2 \dots \omega_n) \text{Exp} \left[ i \sum_{j=1}^n \omega_j t_j \right] d\omega_1 d\omega_2 \dots d\omega_n \quad (3)$$

$$G_n(\omega_1, \omega_2 \dots \omega_n) = \int \int \dots \int g_n(t_1, t_2 \dots t_n) \text{Exp} \left[ -i \sum_{j=1}^n \omega_j t_j \right] dt_1 dt_2 \dots dt_n \quad (4)$$

(where the  $\omega_j$  are circular frequencies).

The first degree frequency response function is the familiar linear one. The second degree frequency response function is the one treated in References 14, 15, and 16 in an application to added resistance. Regardless of the degree, the basic importance of the transform of the impulse response function is the same; that is, convolution in the time domain usually corresponds to multiplication in the frequency domain, and (perhaps more importantly in the present context) the typical hydromechanical seakeeping analysis ends up in the frequency domain.

As a consequence of the assumed symmetry of the impulse response functions and the transform, Equation 4, the  $n^{\text{th}}$  degree frequency response function is also symmetric in its arguments. That is,

$$G_n(\omega_1, \omega_2, \dots, \omega_n) = G_n(\omega_2, \omega_1, \dots, \omega_n) \dots$$

for any and all rearrangements of the  $\omega_j$ . Additionally, because the impulse response functions are real:

$$G_n(-\omega_1, -\omega_2, \dots, -\omega_n) = G_n^*(\omega_1, \omega_2, \dots, \omega_n)$$

where the star denotes the complex conjugate, and all arguments on the left hand side are negative.

## THE THIRD DEGREE FUNCTIONAL POLYNOMIAL

It is clear from the form of Equation 1 that the complexity of any answer which might result would increase geometrically with the order of the term. Consequently, it is hoped that the non-linearities in any given system are weak enough that the series may be truncated at a relatively few terms, in which case it is termed a "functional polynomial". The objective of the present work is to investigate the applicability of the functional polynomial of the third degree to seakeeping problems. Truncating Equation 1 at  $n = 3$  results in the fundamental time domain mathematical model for present purposes:

$$\begin{aligned}
 Y(t) = & \int g_1(t_1)X(t-t_1)dt_1 \\
 & + \int \int g_2(t_1, t_2)X(t-t_1)X(t-t_2)dt_1 dt_2 \\
 & + \int \int \int g_3(t_1, t_2, t_3)X(t-t_1)X(t-t_2)X(t-t_3)dt_1 dt_2 dt_3
 \end{aligned} \tag{5}$$

This model is the same as that of References 14 and 15 with the functional of third degree added. Though it may seem physically and intuitively justifiable to accept convergence of the series, Equation 1, the acceptance of the functional polynomial, Equation 5, as an adequate engineering approximation hinges purely upon how well it works in practice with whatever problem is at hand. The series itself, Equation 1, is thought applicable only to weakly nonlinear systems. If the system responds critically to a given level of excitation (as for instance a "jump" or an instability in the sense of the Hill equation) many terms in the series would be necessary for even a rough approximation and practical application is doubtful. On the other hand (apart from the added resistance/slow drift phenomena which are quadratic non-linearities) in many seakeeping situations where nonlinearities might be expected a purely linear treatment often yields results which appear within reason, and the model of Equation 5 may represent an improvement.

## DETERMINISTIC IDENTIFICATION OF FREQUENCY RESPONSE FUNCTIONS

Given the polynomial, Equation 5, and the Fourier transform definition, Equation 4, there are three frequency response functions of interest in the present problem:

$$\begin{aligned} \text{(Linear)} &\rightarrow G_1(\omega) \\ \text{(Quadratic)} &\rightarrow G_2(\omega_1, \omega_2) \\ \text{(Cubic)} &\rightarrow G_3(\omega_1, \omega_2, \omega_3) \end{aligned}$$

The interpretation of  $G_1(\omega)$  is of course identical to that of pure linear theory, it is simply the normalized amplitude and phase of linear steady state system response to sinusoidal excitation. The quadratic response,  $G_2(\omega_1, \omega_2)$ , has been interpreted in References 14 and 15, and what nominally remains is to interpret the cubic frequency response function. In words,  $G_2(\omega_1, \pm\omega_2)$  expresses the normalized steady state response at frequencies  $(\omega_1 \pm \omega_2)$  to two cosinusoids of frequencies  $\omega_1$  and  $\omega_2$ , due to interaction of the two frequency components. The units of  $G_2(\omega_1, \omega_2)$  are (response unit)/(excitation unit)<sup>2</sup>. Similarly,  $G_3(\omega_1, \pm\omega_2, \pm\omega_3)$  expresses the normalized steady state response at frequencies  $(\omega_1 \pm \omega_2 \pm \omega_3)$  to three cosinusoids of frequencies  $\omega_1$ ,  $\omega_2$  and  $\omega_3$ , due to interaction of the three frequency components. The units of  $G_3(\omega_1, \omega_2, \omega_3)$  are (response unit)/(excitation unit)<sup>3</sup>.

When the polynomial of third degree, Equation 5, is considered to be the system there arise some serious complications not present in the second degree model considered in References 14 and 15. For this reason it is thought best to clarify the contents of the last paragraph in stages which correspond to "experiments" of increasing complexity.

If the system is completely linear  $[g_2(t_1, t_2)$  and  $g_3(t_1, t_2, t_3) = 0$  in Equation 5] experimental characterization takes the form of exciting the system with

$$\hat{X}(t) = A \cos(\omega t - \epsilon) \quad (6a)$$

and interpreting the steady state response as:

$$\hat{Y}(t) = A \operatorname{Re} [G_1(\omega) \operatorname{Exp}(it\omega - i\epsilon)] \quad (6b)$$

from which the linear frequency response function  $G_1(\omega)$  may be derived by a frequency analysis. It should be noted that  $\epsilon$  is an arbitrary phase angle inserted in Equation 6a to reflect the situation which is normally inherent in the reduction of observations from a physical experiment. In linear theoretical analyses much the same process is followed except that "A" is customarily taken to be unity, " $\epsilon$ " as zero, and the excitation written as

$$\hat{X}(t) = \text{Exp} [it\omega]$$

with the understanding that the real part of the resulting complex solution for  $\hat{Y}(t)$  is to be taken. The result is identical in form to Equation 6b, and the theoretical expression for  $G_1(\omega)$  may be extracted. It should be remarked before proceeding further that the customary theoretical representation of excitation as a complex quantity with the real part of the resulting response "understood" is a completely valid procedure only for linear systems. Application of this procedure to nonlinear systems of the present type results in an incomplete answer at best. In order to produce theoretical analyses compatible with physical experiment for the present nonlinear system the excitation must be carried as an explicitly real quantity, or as sums of complex quantities and their conjugates.

Returning to the nonlinear system, Equation 5, the simplest "experiment" is to excite the system with a single cosinusoid just as in the characterization of the fully linear system. Thus, as before:

$$\hat{X}(t) = \text{Excitation} = A \cos (\omega t - \epsilon) \quad (7a)$$

Expressing Equation 7a as  $(A/2) [\text{Exp} (it\omega - \epsilon) + \text{Exp} (-it\omega + \epsilon)]$ , substitution into Equation 5, application of the Fourier transform definition, Equation 4, and consideration of symmetries, results in the following expression for the response of the nonlinear system to the single cosinusoid, Equation 7a:

$$\begin{aligned} \text{Response} = \hat{Y}(t) = \text{Re} \left[ \{AG_1(\omega) + \frac{3}{4} A^3 G_3(\omega, \omega, -\omega)\} \text{Exp}(it\omega - i\epsilon) \right] \\ + \frac{1}{2} A^2 \text{Re} \left[ G_2(\omega, -\omega) \right] \\ + \frac{1}{2} A^2 \text{Re} \left[ G_2(\omega, \omega) \text{Exp}(it2\omega - i2\epsilon) \right] \\ + \frac{1}{4} A^3 \text{Re} \left[ G_3(\omega, \omega, \omega) \text{Exp}(it3\omega - i3\epsilon) \right] \end{aligned} \quad (7b)$$

The complication mentioned earlier is immediately apparent in the first term of Equation 7b. The cubic nonlinearity may produce response at the excitation frequency as well as at the third harmonic of the excitation. While the values of the functions  $G_2(\omega, \omega)$  and  $G_2(\omega, -\omega)$ , and the values of  $G_3(\omega, \omega, \omega)$  may in principle be inferred by a frequency analysis of a single experiment, more than one experiment is required to separate  $G_1(\omega)$  and  $G_3(\omega, \omega, -\omega)$ . The complication, however, may not arise in theoretical analysis because  $G_3(\omega, \omega, -\omega)$  is the component which varies as excitation amplitude cubed.

Continuing the discussion of Equation 7b, the quantity most reduced and extracted in seakeeping experiments in waves corresponds to the ratio of amplitude of response at frequency  $\omega$  to amplitude of a regular wave of frequency  $\omega$ . In terms of Equation 7b this ratio is:

$$R(\omega) = |G_1(\omega) + \frac{3}{4} A^2 G_3(\omega, \omega, -\omega)| \quad (8)$$

When  $G_3(\omega, \omega, -\omega)$  is zero,  $R(\omega)$  is  $|G_1(\omega)|$  and is invariant with excitation amplitude as would be expected for a system of second degree. When the cubic nonlinearity is present the amplitude can vary with excitation amplitude in a variety of ways, since in general both  $G_1(\omega)$  and  $G_3(\omega, \omega, -\omega)$  are complex and this must be taken account of prior to performing the absolute value. If the ratio of real and imaginary parts of  $G_1(\omega)$  is the same as the corresponding ratio for  $G_3(\omega, \omega, -\omega)$ ,  $R(\omega)$ , (an "equivalent" linear response ratio) could be quadratic in excitation amplitude.

Because the single cosinusoid experiment involves only specialized portions of the quadratic and cubic frequency response functions it is clear that more complicated "experiments" must be carried out to define the remaining portions, and these take the form of dual and triple "tone" experiments where the excitation is taken as the sum of 2 and 3 cosinusoids.

Because of the cubic term the dual tone experiment outlined in Reference 15 takes a more complicated form. In particular the excitation,  $\tilde{X}(t)$ , is assumed to be composed of two cosinusoids of different amplitudes  $A_1$  and  $A_2$ , and different frequencies  $\omega_1$  and  $\omega_2$  as shown at the top of

Table 1. In order to be consistent with physical experiments, arbitrary phases  $\epsilon_1$  and  $\epsilon_2$  are included. The response,  $\tilde{Y}(t)$ , to the dual tone excitation,  $\tilde{X}(t)$  is shown in the lower part of Table 1. The result is derived exactly as indicated for Equation 7b, the assumed excitation is substituted in Equation 5 in complex form, the transform definition, Equation 4, is applied, and as much advantage as possible is taken of symmetry. A further complication about the response at the excitation frequencies is evident from the first three terms in the expression for  $\tilde{Y}(t)$ , Table 1. To illustrate, the response at frequency  $\omega_1$  is written out as follows:

$$\text{Re} \left[ \left\{ A_1 G_1(\omega_1) + \frac{3}{4} A_1^3 G_3(\omega_1, \omega_1, -\omega_1) + \frac{3}{2} A_1^2 A_2 G_3(\omega_2, -\omega_2, \omega_1) \right\} \text{Exp}(it\omega_1 - i\epsilon_1) \right]$$

The first two terms inside the curly brackets are the same as in the corresponding term of the single sinusoid experiment, the third represents a third degree interaction between the two frequency components. The fourth through seventh lines of the response in Table 1 are the same as the quadratic terms described in Reference 15.

The eighth line involves the third harmonics of the two excitation frequencies as would be expected from the single tone experiments, Equation 7b. The last four lines involve a frequency of a new form; that is,

$$2\omega_i \pm \omega_j$$

and the corresponding special values of quadratic frequency response function,  $G_3(\omega_i, \omega_i, \pm\omega_j)$ .

Table 2 indicates the response of the system of Equation 5 to a three tone excitation. In this case all the types of frequency components noted in the two tone experiment reappear. Essentially, the results of Table 1 are repeated for all the possible combinations of two of three frequencies. The last four lines of the response shown in Table 2 involve four new frequencies:

$$(\omega_1 + \omega_2 + \omega_3)$$

$$(\omega_1 + \omega_2 - \omega_3)$$

$$(\omega_1 - \omega_2 + \omega_3)$$

$$(\omega_2 + \omega_3 - \omega_1)$$

TABLE 1  
RESULTS OF THE TWO COSINUSOID EXPERIMENT

$$\text{Excitation} = \bar{X}(t) = A_1 \cos(\omega_1 t - \epsilon_1) + A_2 \cos(\omega_2 t - \epsilon_2)$$

$$\text{Response} = \bar{Y}(t)$$

$$\begin{aligned}
 &= \sum_{j=1}^2 \text{Re} \left[ A_j G_1(\omega_j) + \frac{3}{4} A_j^3 G_3(\omega_j, \omega_j, -\omega_j) \right] \text{Exp}(it\omega_j - i\epsilon_j) \\
 &+ \frac{3}{2} A_1^2 A_2 \text{Re} \left[ G_3(\omega_1, -\omega_1, \omega_2) \text{Exp}(it\omega_2 - i\epsilon_2) \right] \\
 &+ \frac{3}{2} A_2^2 A_1 \text{Re} \left[ G_3(\omega_2, -\omega_2, \omega_1) \text{Exp}(it\omega_1 - i\epsilon_1) \right] \\
 &+ \frac{1}{2} A_1^2 G_2(\omega_1, -\omega_1) + \frac{1}{2} A_2^2 G_2(\omega_2, -\omega_2) \\
 &+ \sum_{j=1}^2 \frac{1}{2} A_j^2 \text{Re} \left[ G_2(\omega_j, \omega_j) \text{Exp}(it2\omega_j - i2\epsilon_j) \right] \\
 &+ A_1 A_2 \text{Re} \left[ G_2(\omega_1, \omega_2) \text{Exp}\{it(\omega_1 + \omega_2) - i(\epsilon_1 + \epsilon_2)\} \right] \\
 &+ A_1 A_2 \text{Re} \left[ G_2(\omega_2, -\omega_1) \text{Exp}\{it(\omega_2 - \omega_1) - i(\epsilon_2 - \epsilon_1)\} \right] \\
 &+ \sum_{j=1}^2 \frac{1}{4} A_j^3 \text{Re} \left[ G_3(\omega_j, \omega_j, \omega_j) \text{Exp}(it3\omega_j - i3\epsilon_j) \right] \\
 &+ \frac{3}{4} A_1^2 A_2 \text{Re} \left[ G_3(\omega_1, \omega_1, \omega_2) \text{Exp}\{it(2\omega_1 + \omega_2) - it(2\epsilon_1 + \epsilon_2)\} \right] \\
 &+ \frac{3}{4} A_1^2 A_2 \text{Re} \left[ G_3(\omega_1, \omega_1, -\omega_2) \text{Exp}\{it(2\omega_1 - \omega_2) - it(2\epsilon_1 - \epsilon_2)\} \right] \\
 &+ \frac{3}{4} A_1 A_2^2 \text{Re} \left[ G_3(\omega_2, \omega_2, \omega_1) \text{Exp}\{it(2\omega_2 + \omega_1) - it(2\epsilon_2 + \epsilon_1)\} \right] \\
 &+ \frac{3}{4} A_1 A_2^2 \text{Re} \left[ G_3(\omega_2, \omega_2, -\omega_1) \text{Exp}\{it(2\omega_2 - \omega_1) - it(2\epsilon_2 - \epsilon_1)\} \right]
 \end{aligned}$$

TABLE 2

## RESULTS OF THE THREE COSINUSIOD EXPERIMENT

$$\text{Excitation} = \hat{X}(t) = \sum_{j=1}^3 A_j \cos(\omega_j t - \epsilon_j)$$

$$\text{Response} = \hat{Y}(t)$$

$$\begin{aligned} &= \sum_{j=1}^3 \text{Re} \left[ \left\{ A_j G_1(\omega_j) + \frac{3}{4} A_j^3 G_3(\omega_j, \omega_j, -\omega_j) \right\} \text{Exp}(i\omega_j t - i\epsilon_j) \right] \\ &+ \frac{3}{2} \sum_{k=1}^3 \sum_{j \neq k}^3 A_j^2 A_k \text{Re} \left[ G_3(\omega_j, -\omega_j, \omega_k) \text{Exp}(i\omega_k t - i\epsilon_k) \right] \\ &+ \sum_{j=1}^3 \frac{1}{2} A_j^2 G_2(\omega_j, -\omega_j) \\ &+ \sum_{j=1}^3 \frac{1}{2} A_j^2 \text{Re} \left[ G_2(\omega_j, \omega_j) \text{Exp}(i2\omega_j t - i2\epsilon_j) \right] \\ &+ \sum_{j=1}^2 \sum_{k=j+1}^3 A_j A_k \text{Re} \left[ G_2(\omega_k, \omega_j) \text{Exp}(i\omega_k t + i\omega_j t - i(\epsilon_k + \epsilon_j)) \right] \\ &+ \sum_{j=1}^2 \sum_{k=j+1}^3 A_j A_k \text{Re} \left[ G_2(\omega_k, -\omega_j) \text{Exp}(i\omega_k t - i\omega_j t - i(\epsilon_k - \epsilon_j)) \right] \\ &+ \sum_{j=1}^3 \frac{1}{4} A_j^3 \text{Re} \left[ G_3(\omega_j, \omega_j, \omega_j) \text{Exp}(i3\omega_j t - i3\epsilon_j) \right] \\ &+ \sum_{k=1}^3 \sum_{j \neq k}^3 \frac{3}{4} A_j^2 A_k \text{Re} \left[ G_3(\omega_j, \omega_j, \omega_k) \text{Exp}(i(2\omega_j + \omega_k)t - i(2\epsilon_j + \epsilon_k)) \right] \\ &+ \sum_{k=1}^3 \sum_{j \neq k}^3 \frac{3}{4} A_j^2 A_k \text{Re} \left[ G_3(\omega_j, \omega_j, -\omega_k) \text{Exp}(i(2\omega_j - \omega_k)t - i(2\epsilon_j - \epsilon_k)) \right] \\ &+ \frac{3}{2} A_1 A_2 A_3 \text{Re} \left[ G_3(\omega_1, \omega_2, \omega_3) \text{Exp}(i(\omega_1 + \omega_2 + \omega_3)t) \text{Exp}(-i(\epsilon_1 + \epsilon_2 + \epsilon_3)) \right] \\ &+ \frac{3}{2} A_1 A_2 A_3 \text{Re} \left[ G_3(\omega_1, \omega_2, -\omega_3) \text{Exp}(i(\omega_1 + \omega_2 - \omega_3)t) \text{Exp}(-i(\epsilon_1 + \epsilon_2 - \epsilon_3)) \right] \\ &+ \frac{3}{2} A_1 A_2 A_3 \text{Re} \left[ G_3(\omega_1, -\omega_2, \omega_3) \text{Exp}(i(\omega_1 - \omega_2 + \omega_3)t) \text{Exp}(-i(\epsilon_1 - \epsilon_2 + \epsilon_3)) \right] \\ &+ \frac{3}{2} A_1 A_2 A_3 \text{Re} \left[ G_3(-\omega_1, \omega_2, \omega_3) \text{Exp}(i(\omega_3 + \omega_2 - \omega_1)t) \text{Exp}(-i(\epsilon_3 + \epsilon_2 - \epsilon_1)) \right] \end{aligned}$$

The first is the triple sum frequency which is associated with the value of  $G_3(\omega_1, \omega_2, \omega_3)$  in the positive octant of tri-frequency space (and by symmetry the negative octant). The three remaining frequencies are associated with the cubic frequency response functions in the remaining six octants of tri-frequency space.

Thus in principle the three tone experiment, repeated for enough combinations of the three frequencies, can completely define the cubic frequency response function. If the frequencies chosen are incommensurate a very precise frequency analysis can in principle allow the identification of  $G_3(\omega_1, \omega_2, \omega_3)$  by picking out only the response at the sum frequency. This is the attitude expressed in the systems literature, Reference 22 for example.

The results in Table 2 suggest how an analytical identification of the various frequency response functions may be made. Essentially the analytical problem amounts to the consideration of the response to three superimposed cosinusoids, and the comparison of the resulting complex coefficients of each of the various time factors with the corresponding terms in Table 2.

In the experimental case of interest here (towing tank experiments) finite tank length tends to limit the overall length of experiment, and the incommensurate frequency approach might well be very difficult. If it is possible to choose excitation frequencies such that a complex periodic wave form results, relatively simple frequency analysis might serve as a data reduction procedure. To indicate the dimension of the problem in a more concrete way, all the expected frequencies in the response to 1, 2 and 3 cosinusoids have been listed in Table 3. In the single tone experiment there are 4 expected frequencies, in the two tone case there are 13, and in the three tone case 32.

Tables 1 through 3 together suggest how the deterministic identification problem might be approached. The first step would be to run single tone experiments to isolate  $G_1(\omega)$ ,  $G_2(\omega, -\omega)$ ,  $G_2(\omega, \omega)$ ,  $G_3(\omega, \omega, -\omega)$ , and  $G_3(\omega, \omega, \omega)$  as noted in the discussion of Equation 7b

TABLE 3

FREQUENCIES PRESENT IN THE RESPONSE TO THE p COSINUSOID EXPERIMENT

p = 1		p = 2		p = 3	
Frequency	Interaction	Frequency	Interaction	Frequency	Interaction
$\omega_1$	Linear&Cubic	$\omega_1$	Linear&Cubic	$\omega_1$	Linear&Cubic
0	Quadratic	$\omega_2$	"	$\omega_2$	"
$2\omega_1$	"	0	Quadratic	$\omega_3$	"
$3\omega_1$	Cubic	$2\omega_1$	"	0	Quadratic
		$2\omega_2$	"	$2\omega_1$	"
		$\omega_1 + \omega_2$	"	$2\omega_2$	"
		$\omega_1 - \omega_2$	"	$2\omega_3$	"
		$3\omega_1$	Cubic	$\omega_1 + \omega_2$	"
		$3\omega_2$	"	$\omega_1 + \omega_3$	"
		$2\omega_1 + \omega_2$	"	$\omega_2 + \omega_3$	"
		$2\omega_1 - \omega_2$	"	$\omega_2 - \omega_1$	"
		$2\omega_2 + \omega_1$	"	$\omega_3 - \omega_1$	"
		$2\omega_2 - \omega_1$	"	$\omega_3 - \omega_2$	"
				$3\omega_1$	Cubic
				$3\omega_2$	"
				$3\omega_3$	"
				$2\omega_2 + \omega_1$	"
				$2\omega_3 + \omega_1$	"
				$2\omega_1 + \omega_2$	"
				$2\omega_3 + \omega_2$	"
				$2\omega_1 + \omega_3$	"
				$2\omega_2 + \omega_3$	"
				$2\omega_2 - \omega_1$	"
				$2\omega_3 - \omega_1$	"
				$2\omega_1 - \omega_2$	"
				$2\omega_3 - \omega_2$	"
				$2\omega_1 - \omega_3$	"
				$2\omega_2 - \omega_3$	"
				$\omega_1 + \omega_2 + \omega_3$	"
				$\omega_1 + \omega_2 - \omega_3$	"
				$\omega_1 - \omega_2 + \omega_3$	"
				$\omega_3 + \omega_2 - \omega_1$	"

(Experiments with more than one excitation amplitude would be required to separate  $G_1(\omega)$  and  $G_3(\omega, \omega, -\omega)$ .) In principle, once these special cases are identified it would be possible to progress to the two tone experiment. It will be noted from Table 3 that in the two tone experiment seven of the 13 frequency components involve values of response functions derivable from the single tone experiment. Thus the concentration would be upon the quadratic sum and difference frequencies and the cubic terms arising from two tone interactions. The object of the two tone experiment would thus be to identify  $G_2(\omega_1, \omega_2)$ ,  $G_2(\omega_1, -\omega_2)$ , the special values of the cubic response function of the form  $G_3(\omega_j, \omega_j, \pm\omega_k)$ , and to separate the excitation frequency response  $G_3(\omega_j, -\omega_j, \omega_k)$  from the linear and cubic response obtained in the single tone experiment. Again in principle, the one and two tone experiments would serve to identify all but the last four frequency components of the three tone experiment so that there would be a reduction of the problem of selecting three excitation frequencies such that all the 32 frequencies shown for the three tone experiments would be distinct.

FREQUENCY DOMAIN SIMULATION  
OF A CUBIC SYSTEM

In order to proceed much further with the present work it was desirable to produce a specific example of a system of the third degree in order to see what qualitative features a cubic nonlinearity might introduce into the response to random waves, and to enable the simulation of the "data" which would be necessary in a later attempt at identification. A reasonable course of action was suggested by the work of Reference 21 where a modified form of the classic single degree of freedom roll equation was expanded in a functional series.

Thus for present purposes it was assumed that the response,  $Y(t)$ , and the excitation,  $X(t)$ , of the simulated system were related by the following differential equation:

$$\sum_{j=1}^3 \left[ A_j \{\ddot{Y}(t)\}^j + B_j \{\dot{Y}(t)\}^j + C_j \{Y(t)\}^j \right] = X(t) \quad (9)$$

where  $A_j$ ,  $B_j$  and  $C_j$  are constants and  $A_1$ ,  $B_1$  and  $C_1$  are not zero so that the system can contain a significant linear response. In Reference 21 the constants corresponding to  $j=2$  were taken to be zero so that no quadratic nonlinearities were present, the equation was expanded in a functional series to fifth degree and the frequency response functions were derived by the incommensurate frequency technique of Reference 7. For present purposes an expansion up to the third degree was wanted and thus most of the work required for the present case is documented in Reference 21. Applying the incommensurate frequency approach of Reference 7 to Equation 9, and truncating the results at the third degree to be consistent with the cubic model, Equation 5, results in the following expressions for the simulated linear, quadratic and cubic frequency response functions:

$$\hat{G}_1(\omega) = 1/D_1(i\omega) \quad (10)$$

$$\hat{G}_2(\omega_1, \omega_2) = -D_2(-\omega_1, \omega_2) \hat{G}_1(\omega_1) \hat{G}_1(\omega_2) \hat{G}_1(\omega_1 + \omega_2) \quad (11)$$

$$\begin{aligned}
\hat{G}_3(\omega_1, \omega_2, \omega_3) = & -\hat{G}_1(\omega_1 + \omega_2 + \omega_3) \left[ D_3(-i\omega_1\omega_2\omega_3) \hat{G}_1(\omega_1) \hat{G}_1(\omega_2) \hat{G}_1(\omega_3) \right. \\
& + \frac{2}{3} D_2(-\omega_1(\omega_2 + \omega_3)) \hat{G}_2(\omega_2, \omega_3) \hat{G}_1(\omega_1) \\
& + \frac{2}{3} D_2(-\omega_2(\omega_1 + \omega_3)) \hat{G}_2(\omega_1, \omega_3) \hat{G}_1(\omega_2) \\
& \left. + \frac{2}{3} D_2(-\omega_3(\omega_1 + \omega_2)) \hat{G}_2(\omega_1, \omega_2) \hat{G}_1(\omega_3) \right] \quad (12)
\end{aligned}$$

where the auxillary function is defined:

$$D_n(\alpha) = A_n \alpha^2 + B_n \alpha + C_n \quad (13)$$

Some remarks are perhaps in order before proceeding further. It may be noted in Equations 11 and 12 that the expressions for the quadratic and cubic frequency response functions involve all the response and auxillary functions of lesser degree. Unfortunately, this continues on for frequency response functions of higher degree so that, despite the fact that the exponent,  $j$ , of Equation 9 is limited to 3, frequency response functions of all degrees may be derived for Equation 9. In effect, Equations 10 through 12 are not a complete solution. This is not too bothersome in the present context since the postulated model, Equation 5, assumes that all response functions of greater degree than three are zero, and since all that is wanted here are a set of response functions which have the required symmetry, and which may be evaluated.

Given the coefficients of Equation 9, numerical evaluation of Equations 10 through 12 is straightforward. What was wanted for the present work was one fairly reasonable system, and the selection of the coefficients was partly arbitrary and partly trial and error. The coefficients  $A_1$ ,  $B_1$ ,  $C_1$  were arbitrarily fixed as follows:

$$A_1 = 1/(2\pi)^2$$

$$B_1 = 1/4\pi$$

$$C_1 = 1$$

These choices define a simple linear single degree of freedom system in which the response amplitude ratio is unity at zero frequency and 2.0

at resonance. The resonant frequency is  $2\pi$  radians/second. Thus the linear subsystem was made generally similar to a lightly damped heave response to waves or a relatively heavily damped roll response to wave slope. The implied time scale (resonant period of 1 second) is typical of small model testing. It may be noted in Equations 10 through 12 that if  $\hat{G}_1(\omega_k)$  is zero,  $\hat{G}_2(\omega_k, \omega_2)$  and  $\hat{G}_3(\omega_k, \omega_2, \omega_3)$  will also be zero for any choice of  $\omega_3$  and  $\omega_2$ . For the numerical work to be later described it was thought to be of advantage to make sure that the quadratic and cubic frequency response functions would go to zero if the absolute value of any frequency argument exceeded some cutoff value. Accordingly, in the numerical evaluation of  $\hat{G}_1(\omega)$ , provision was made to multiply the computed value of  $\hat{G}_1(\omega)$  in the range  $7\pi < |\omega| < 8\pi$  by a factor decreasing linearly from unity to zero. In effect,  $\hat{G}_1(\omega)$  was computed in accordance with Equation 10 in the range  $-7\pi < \omega < 7\pi$ , the computed value outside this range was attenuated to zero at  $|\omega| = 8\pi$ , and  $\hat{G}_1(\omega)$  was set equal to zero for  $|\omega| > 8\pi$ .

The next step was to select the quadratic coefficients  $A_2$ ,  $B_2$ ,  $C_2$ , in Equation 9. For lack of better information, the intention was to produce a quadratic frequency response function qualitatively similar to those shown in References 15 and 16. Qualitatively, the functions in those references are double humped in the bi-frequency plane. Generally, the maximum absolute value of  $\hat{G}_2(\omega, \omega)$  defines the maximum of one hump and  $\hat{G}_2(\omega, -\omega)$  the maximum of the other. The function tends to zero for bi-frequency  $(0,0)$  and to be small for large values of either frequency component. Given the values of  $A_1$ ,  $B_1$ ,  $C_1$  established previously,  $\hat{G}_2(\omega, \omega)$  and  $\hat{G}_2(\omega, -\omega)$  were evaluated in accordance with Equation 11 for trial and error selections of  $A_2$ ,  $B_2$  and  $C_2$ . The first conclusion was that  $C_2$  should be zero if  $\hat{G}_2(0,0)$  was to be zero. With an initial selection of  $A_2$  and  $B_2$  which yielded reasonable qualitative behavior of  $\hat{G}_2(\omega, \omega)$  and  $\hat{G}_2(\omega, -\omega)$ , the entire function was computed. It was found that the  $A_2$  coefficient produced relatively significant values of response at large values of frequency argument ( $|\omega_1| \neq |\omega_2|$ ) which made the function qualitatively dissimilar to that desired, and this coefficient was finally also zeroed. The final selection of quadratic coefficients was as follows:

$$A_2 = C_2 = 0$$

$$B_2 = -0.265 A_1$$

This choice yielded the overall qualitative behavior desired, a maximum value of  $\hat{G}_2(\omega, -\omega)$  of about unity at  $\omega \approx 2\pi$ , and a maximum value of  $|\hat{G}_2(\omega, \omega)|$  of  $\approx 0.33$  at the same frequency. Noting Equation 7b, for single tone excitation of unity amplitude, these values imply a shift in the mean of about 1/2 and a second harmonic of about 1/6.

Given the linear and quadratic frequency response functions, the coefficients  $A_3$ ,  $B_3$ ,  $C_3$  were to be selected in order to complete the simulated system. In this case there was no previous qualitative guidance available since no mapping of the cubic frequency response function for any system was available. It seemed reasonable to select these coefficients upon the basis of the single tone response, Equation 7b; that is, to compute  $|\hat{G}_1(2\pi) + 0.75 \hat{G}_3(2\pi, 2\pi, -2\pi)|$ , which is the amplitude of the response at the resonant frequency to unity amplitude excitation at resonance. The objective was to select coefficients which would make this result about 4/3, (2/3 of the linear response amplitude) on the assumption that this might yield an "equivalent" linear frequency response resembling something which might have been experienced in ship motions experiments. Initial trial and error numerical work showed that the  $A_3$  coefficient had to nearly vanish in order to achieve the desired result. It was suspected, as in the quadratic case, that a non zero  $A_3$  coefficient would produce significant values of  $G_3(\omega_1, \omega_2, \omega_3)$  for high frequency arguments. A preliminary mapping of the function with non-zero  $A_3$  tended to confirm this and the final values of coefficients selected were:

$$A_3 = 0$$

$$B_3 = 0.0032 B_1$$

$$C_3 = 0.0075 C_1$$

With this selection the maximum absolute value of  $G_3(\omega, \omega, -\omega)$  was 0.92 and the maximum absolute value of  $G_3(\omega, \omega, \omega)$  was about 0.11; that is, the third harmonic response to single tone excitation would be about

1/9 the amplitude of the contribution to the fundamental frequency. This last is not inconsistent with ship motions experiments where significant third harmonic response is rare or un-noticed. The non-zero  $C_3$  coefficient produces a slight static softening effect which is also not inconsistent with ship hydrostatics.

As has been previously implied, one of the main motives for the present work has been the experimental situation where the normalized response amplitude is not invariant with excitation amplitude as it should be for a purely linear system. It was thus of interest to evaluate the normalized response ("equivalent" linear response) for the simulated system.  $R(\omega)$  of Equation 8 was evaluated for a number of excitation amplitudes ("A" of Equation 7a) and the results are plotted in Figures 1 and 2. The evaluations were carried out at frequency steps of  $\pi/10$ , the actual results are plotted as points and straight lines are drawn between. The amplitude range chosen was  $A = 0$  to 5. The somewhat surprising range of the results suggested the presentation in Figures 1 and 2. The frame at the top of Figure 1 covers the range  $0 \leq A \leq 2$ , the frame at the bottom extends the range to 3, and Figure 2 extends the amplitude range to 4 and 5. It is clear from the figures that the cubic nonlinearities which would be noticeable in an experiment with the simulated system are concentrated about the linear resonance. Normalized response above  $\omega = 12$  is essentially invariant with excitation amplitude. That below  $\omega \approx 3.5$  is weakly dependent on amplitude. The decrease of the normalized response near resonance is about as might be expected from the method of choosing coefficients, up to an excitation amplitude of 2. Above this amplitude the trend of response reverses and the normalized response grows steadily with excitation amplitude. The radical trends shown in Figure 2 probably have no qualitative parallel in known sea-keeping experiments. On the otherhand the qualitative and quantitative behavior shown at the top of Figure 1 for an excitation amplitude range up to about 1.0 has been seen quite a lot, and it is conceivable physically that nonlinearities could produce inflections in the normalized response at a given frequency, as implied in the lower frame of Figure 1.

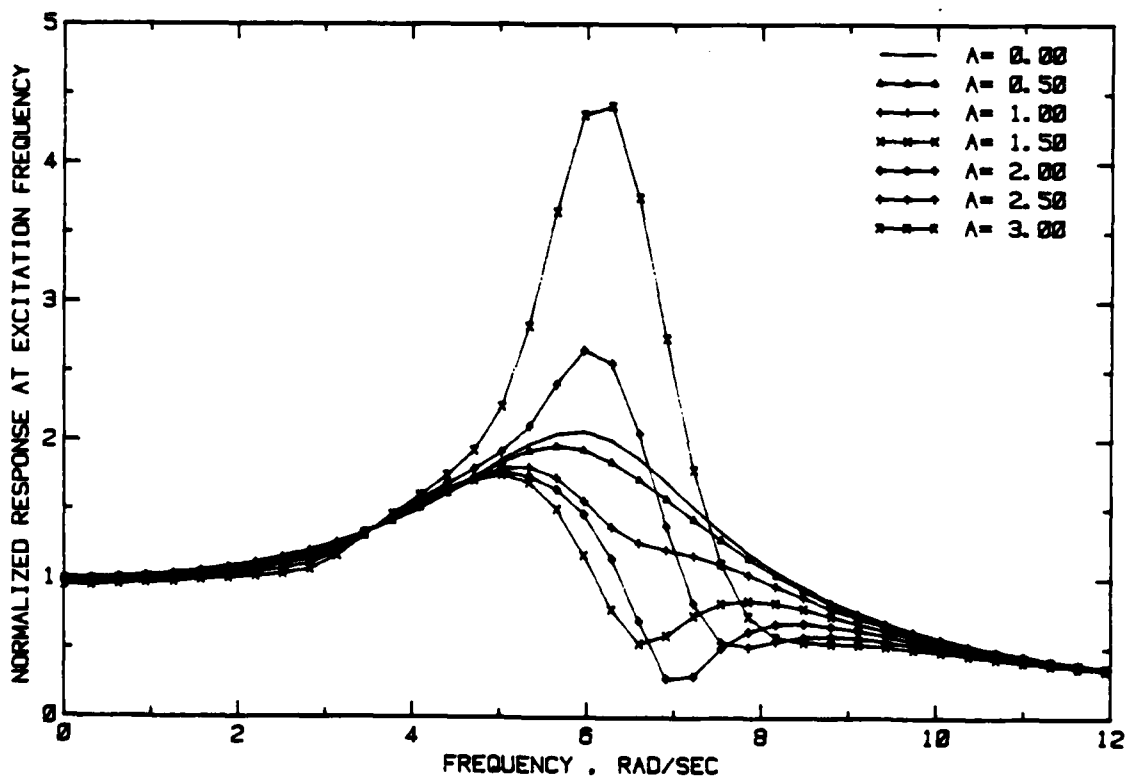
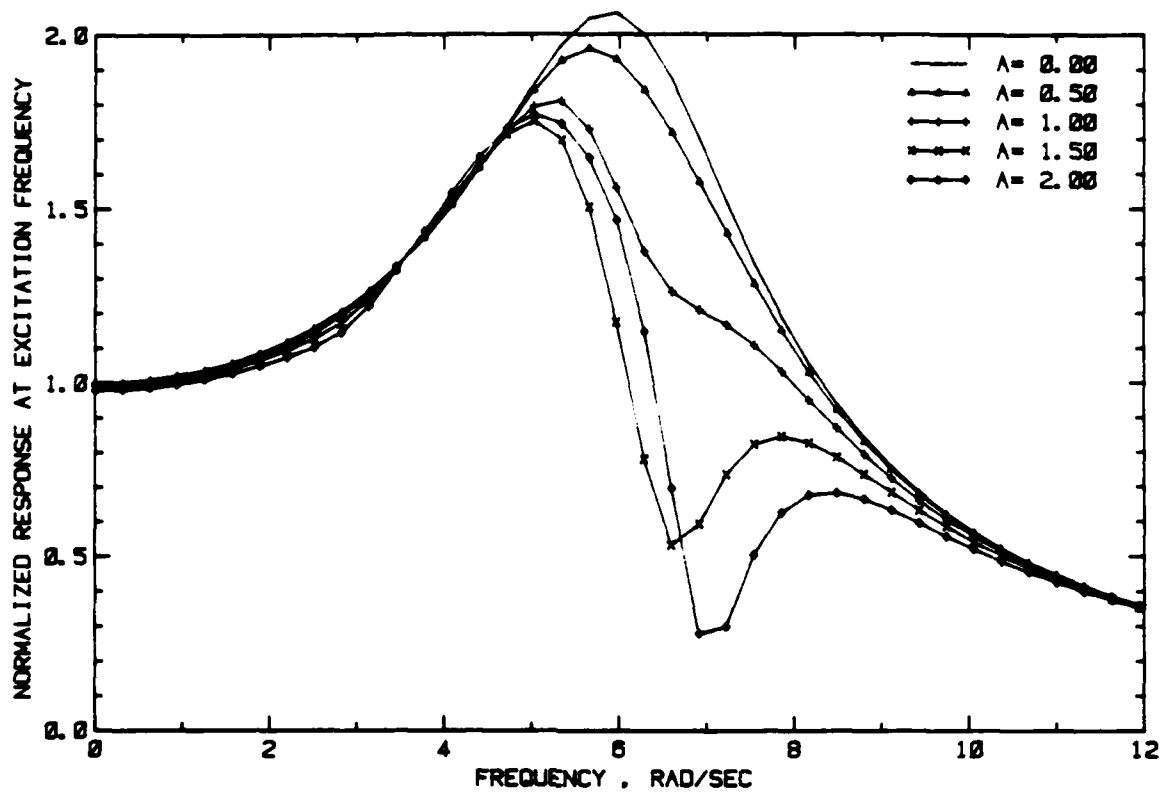


FIGURE 1 NORMALIZED RESPONSE OF THE SIMULATED SYSTEM AT THE EXCITATION FREQUENCY TO VARIOUS EXCITATION AMPLITUDES

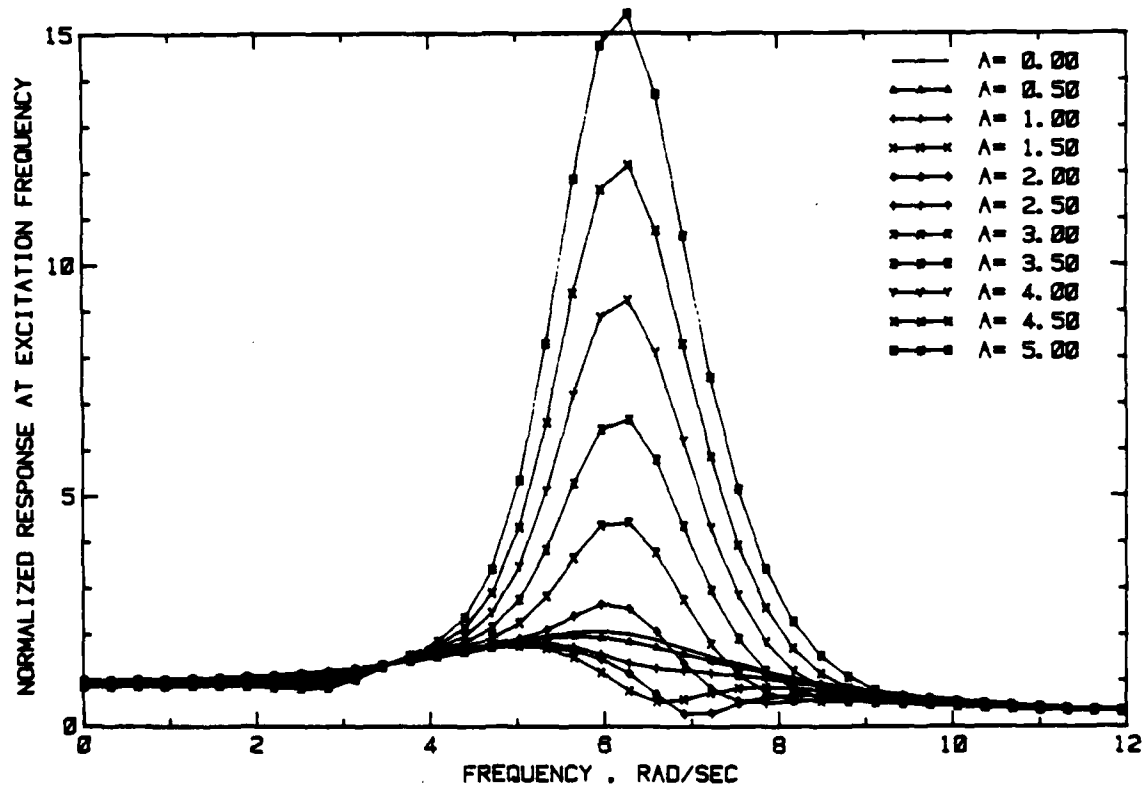
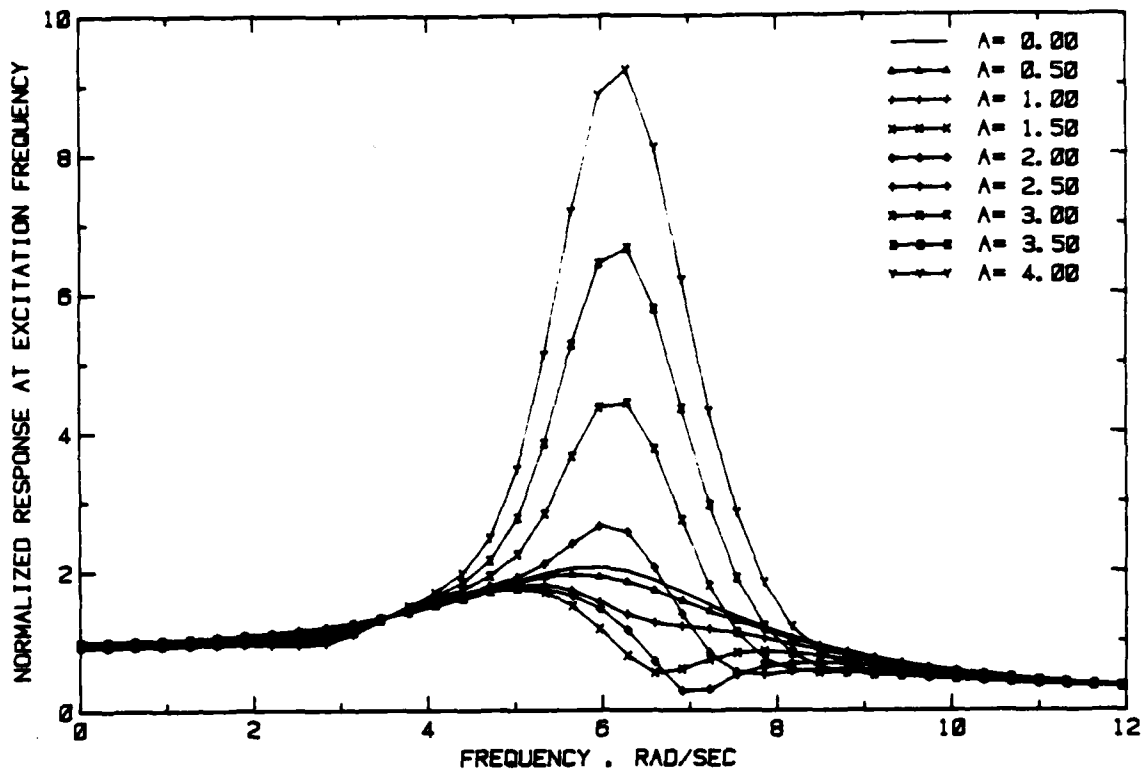


FIGURE 2 NORMALIZED RESPONSE OF THE SIMULATED SYSTEM AT THE EXCITATION FREQUENCY TO VARIOUS EXCITATION AMPLITUDES

Two interim conclusions arise. First, the simulated system may be reasonably representative of some nonlinear seakeeping situations so long as the magnitude of excitation amplitude is two or less. Second, the cubic model seems capable of reflecting far more complicated qualitative behavior than had been imagined at the outset.

## SIMULATED IMPULSE RESPONSES

The next step in the simulation was to invert the frequency domain simulation into the time domain; that is, to derive digital linear, quadratic and cubic impulse response functions. The time domain operation intended was to carry out a discrete version of Equation 5 which may be written as follows:

$$Y(t) \rightarrow Y(n) = Y1(n) + Y2(n) + Y3(n) \quad (14)$$

where:

$$Y1(n) = \sum_j g_j^1 X(n - j) \quad (15)$$

$$Y2(n) = \sum_j \sum_k g_{jk}^2 X(n - j) X(n - k) \quad (16)$$

$$Y3(n) = \sum_j \sum_k \sum_l g_{jkl}^3 X(n - j) X(n - k) X(n - l) \quad (17)$$

where in terms of Equation 5:

$$n = t/\Delta t$$

$$j = t_1/\Delta t$$

$$k = t_2/\Delta t$$

$$l = t_3/\Delta t$$

$\Delta t$  = a sampling interval

$Y(n) = Y(n\Delta t)$  = the sampled response

$X(n) = X(n\Delta t)$  = the sampled excitation

and the digital impulse response functions are:

$$g_j^1 = g_1(j\Delta t) \cdot \Delta t \quad (18)$$

$$g_{jk}^2 = g_2(j\Delta t, k\Delta t) \cdot \Delta t^2 \quad (19)$$

$$g_{jkl}^3 = g_3(j\Delta t, k\Delta t, l\Delta t) \cdot \Delta t^3 \quad (20)$$

(for integer j, k and l).

The domain of the summations in Equations 15 through 17 is over non-zero values of the digital impulse response functions. The sampling interval must be chosen small enough that the implied trapezoidal integrations are reasonable, and for the system defined in the previous section a sampling interval of  $0.0625 = \Delta t$  was chosen.

Computation of the impulse response functions, as in Reference 15, amounts to carrying out numerically the applicable Fourier transform, (Equation 3) for each of the frequency response functions for a range of  $j$ ,  $k$  and  $l$  sufficient to allow eventual truncation of the function.

The required numerical operations were carried out with the Fast Fourier Transform. In particular let:

$$\omega_1 = \frac{2\pi}{\Delta t} \frac{p}{N}$$

$$\omega_2 = \frac{2\pi}{\Delta t} \frac{q}{N}$$

$$\omega_3 = \frac{2\pi}{\Delta t} \frac{r}{N}$$

and assume trapezoidal integration of Equation 3, with integer values of  $p$ ,  $q$  and  $r$  within the following ranges:

$$-N/2 \leq p \leq N/2$$

$$-N/2 \leq q \leq N/2$$

$$-N/2 \leq r \leq N/2$$

Then:

$$g_j^1 = \frac{1}{N} \sum_p G_1(2\pi p/\Delta t N) \text{Exp}(i2\pi j p/N) \quad (21)$$

$$g_{jk}^2 = \frac{1}{N^2} \sum_p \sum_q G_2(2\pi p/\Delta t N, 2\pi q/\Delta t N) \text{Exp}\{i2\pi(jp+kq)/N\} \quad (22)$$

$$g_{jkl}^3 = \frac{1}{N^3} \sum_p \sum_q \sum_r G_3(2\pi p/\Delta t N, 2\pi q/\Delta t N, 2\pi r/\Delta t N) \text{Exp}\{i2\pi(jp+kq+lr)/N\} \quad (23)$$

In these equations numerical values of  $G_1(\omega)$ ,  $G_2(\omega_1, \omega_2)$  and  $G_3(\omega_1, \omega_2, \omega_3)$  were computed in accordance with Equations 10 through 13 and the values of the coefficients of Equation 9 which were given in a previous section.

Equation 21 is exactly what the inverse Fast Fourier Transform does, apart from the leading factor of  $1/N$ , and that values of  $G_1(-\omega)$  must appear as if aliased in the second half of the complex  $N$  point FFT frequency domain array. An additional numerical complication is that the inverse FFT yields a "circular" time function which corresponds properly to positive and negative values of time only if the frequency function presented to it is zero for  $N/4 < |p| < N/2$ . With the provision discussed previously that  $G_1(\omega) = 0$  for  $|\omega| > 8\pi$ , and the value of  $\Delta t$  selected, this requirement is satisfied for  $N = 128$ , which was the value used throughout the computations. Once the inverse FFT is performed  $g_j^1$  is defined for  $(-N/2 + 1) \leq j \leq N/2$ . The value for  $j = -N/2$  is not defined, but the omission is not crucial since if the computation parameters have been selected properly the function must be negligible at the ends of the  $j$  range.

The computation of Equation 22 is equivalent to first doing Equation 21  $N$  times for constant  $q$ ,  $\{(-N/2 + 1) \leq q \leq N/2\}$ . This yields a partial transform of  $G_2(\omega_1, \omega_2)$  which is a function of  $j$  and  $q$  ( $t_1$  and  $\omega_2$ ), and  $N$  additional inverse transforms with respect to  $q(\omega_2)$  complete the computation.

The computation of Equation 23 is equivalent to doing Equation 22  $N$  times for the range of  $r$ , which yields a mixed function of  $j$ ,  $k$  and  $r$  ( $t_1$ ,  $t_2$ , and  $\omega_3$ ), and  $N^2$  inverse transforms with respect to  $r(\omega_3)$  complete the work. It should be noted in this connection that with  $N = 128$  the computer memory requirements for Equations 21 and 22 are quite modest. To accomplish Equation 23 with all elements in memory at once requires of the order of four million words of memory so that in the present instance the computation of Equation 23 was made in stages with storage of intermediate results.

As a practical matter minimization of the necessary range of  $j$ ,  $k$  and  $l$  is advantageous in the application of the discrete impulse responses, Equations 15 through 17. The results of the computations of Equations 21, 22 and 23 were, in all three cases, quite small relative to the maximum for negative values of  $j$ ,  $k$  and  $l$ . This is the result expected from the form of Equation 9. Since the coefficients are

fixed constants, the system should be realizable in real time. This implies that  $g_1(t_1)$ ,  $g_2(t_1, t_2)$  and  $g_3(t_1, t_2, t_3)$  should be exactly zero if any time argument is negative, because negative time arguments imply that the "future" must be known in order to predict the "present". The fact that the values of the computed impulse responses were negligible but not exactly zero is probably attributable to the truncation of  $G_1(\omega)$  described previously and to rounding error in the computations.

Truncation of the computed values of  $g_j^1$  for negative  $j$  resulted in a 65 element kernel for use in Equation 15. Figure 3 indicates the shape of this kernel. The horizontal scale is noted in terms of time ( $t_1 = j\Delta t$ ). The simulated linear subsystem appears to have a memory of about 3 seconds. Convolution of this kernel with cosinusoidal input and harmonic analysis of results yielded correspondence with the analytical simulation, Equation 10, to about 3 significant figures.

Truncation of the computed values of the quadratic kernel,  $g_{jk}^2$ , was also carried out for negative values of the indices. This resulted in a 65 x 65 element kernel ( $j, k = 0 \dots 64$ ). Convolution of this kernel with cosinusoidal input and harmonic analysis of results also yielded correspondence to three significant figures with the analytical simulation, Equation 11, for  $G_2(\omega, \omega)$ , and  $G_2(\omega, -\omega)$ . Figure 4 is an "isometric" picture of the significant part of the quadratic kernel. The intersections of the lines denote the actual values of the kernel, and the values for  $j$  and  $k$  greater than 49 have been omitted from the picture because they are very small. The "horizontal" scales are given in terms of time ( $t_1 = j\Delta t$  and  $t_2 = k\Delta t$ ), the point 0,0 being at the "near" corner. Though the horizontal rotation of the surface was made slightly beyond 45 degrees to improve the appearance, the right to left symmetry (exact in the numerical work) is apparent. The quadratic sub-system also has a memory of about 3 seconds.

Because the third term of the discrete time domain prediction Equation 17 involves on the order of  $3N^3$  multiplications per response point it was of considerable practical importance to truncate  $g_{jkl}^3$  as much as reasonably possible. Omitting the small values computed for negative values of  $j$ ,  $k$  and  $l$  results in a 65 x 65 x 65 matrix for  $g_{jkl}^3$ .

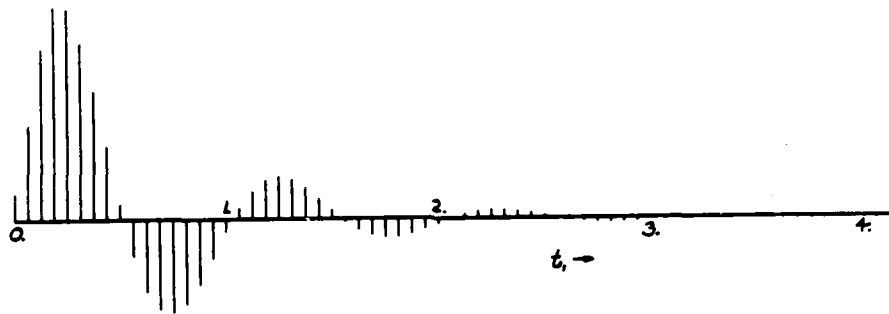


FIGURE 3 TRUNCATED LINEAR DISCRETE KERNEL,  $g_j^1$

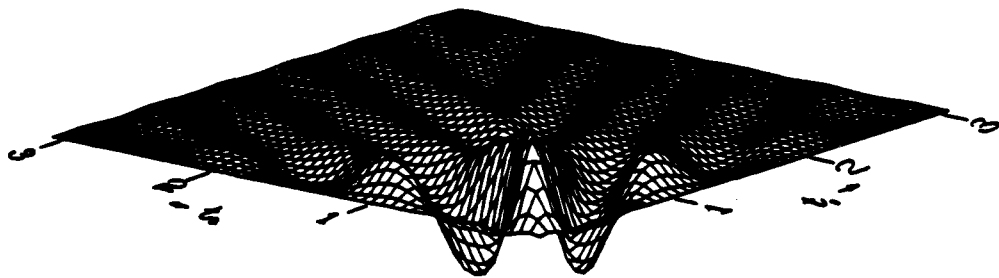


FIGURE 4 TRUNCATED QUADRATIC DISCRETE KERNEL,  $g_{jk}^2$

Examination of the computed values of this discrete kernel for large values of the indices suggested that it would be reasonable to truncate the kernel at  $j, k$  and  $l$  of 49 so that the final truncated kernel became a  $50 \times 50 \times 50$  matrix ( $j, k, l = 0 \dots 49$ ). Convolution of this truncated kernel with cosinusoidal input, and analysis per Equation 7b, yielded estimates of  $G_3(\omega, \omega, -\omega)$  and  $G_3(\omega, \omega, \omega)$  which compared with the analytical values from Equation 12 to between 1 and 2 significant figures. This was less precision than was desired and it was suspected that the error was due to the truncation. However, a  $65 \times 65 \times 65$  kernel requires more than twice the number of multiplications in Equation 17 as a  $50 \times 50 \times 50$ . The less than desired precision was accepted for the present exploratory study in return for a significant economy.

It was of considerable interest to see what a cubic impulse response function looks like. The function,  $g_{jkl}^3$ , is four-dimensional so that the best approach appeared to be to look at the three dimensional functions which can be formed if one of the three time delay arguments is held constant. Figure 5 shows nine of the 50 possible surfaces which may be examined by holding  $l(t_3)$  in  $g_{jkl}^3$  constant. The quasi-isometric projection is the same for each surface and is almost the same as that used in Figure 4 for the picture of the quadratic frequency response function. The "vertical" scales in each surface are the same. The "horizontal" scales in each case are annotated in terms of time delays  $t_1$  and  $t_2$ , and the constant value of  $t_3$  is noted to the right of each surface. The surface for  $t_3 = 0$  is essentially flat to the resolution shown, as is that for  $t_3 = 3.0625$  ( $l = 49$ ). Between  $t_3 = 2$  and 3 the "ripples" shown in the surface at the top of the figure gradually die out, so that the surfaces shown include the significant parts of the cubic impulse response. Since by assumption:

$$g_3(t_2, t_1, t_3) = g_3(t_1, t_2, t_3)$$

there is exact right to left symmetry in each of the surfaces. The numerical results show the required symmetry in the  $t_3$  direction as well, so that the same pictures would have been obtained had  $t_1$  or  $t_2$  been held constant and the surfaces drawn as functions of the remaining two time delays. It appears that the cubic sub-system has about a 3 second memory.

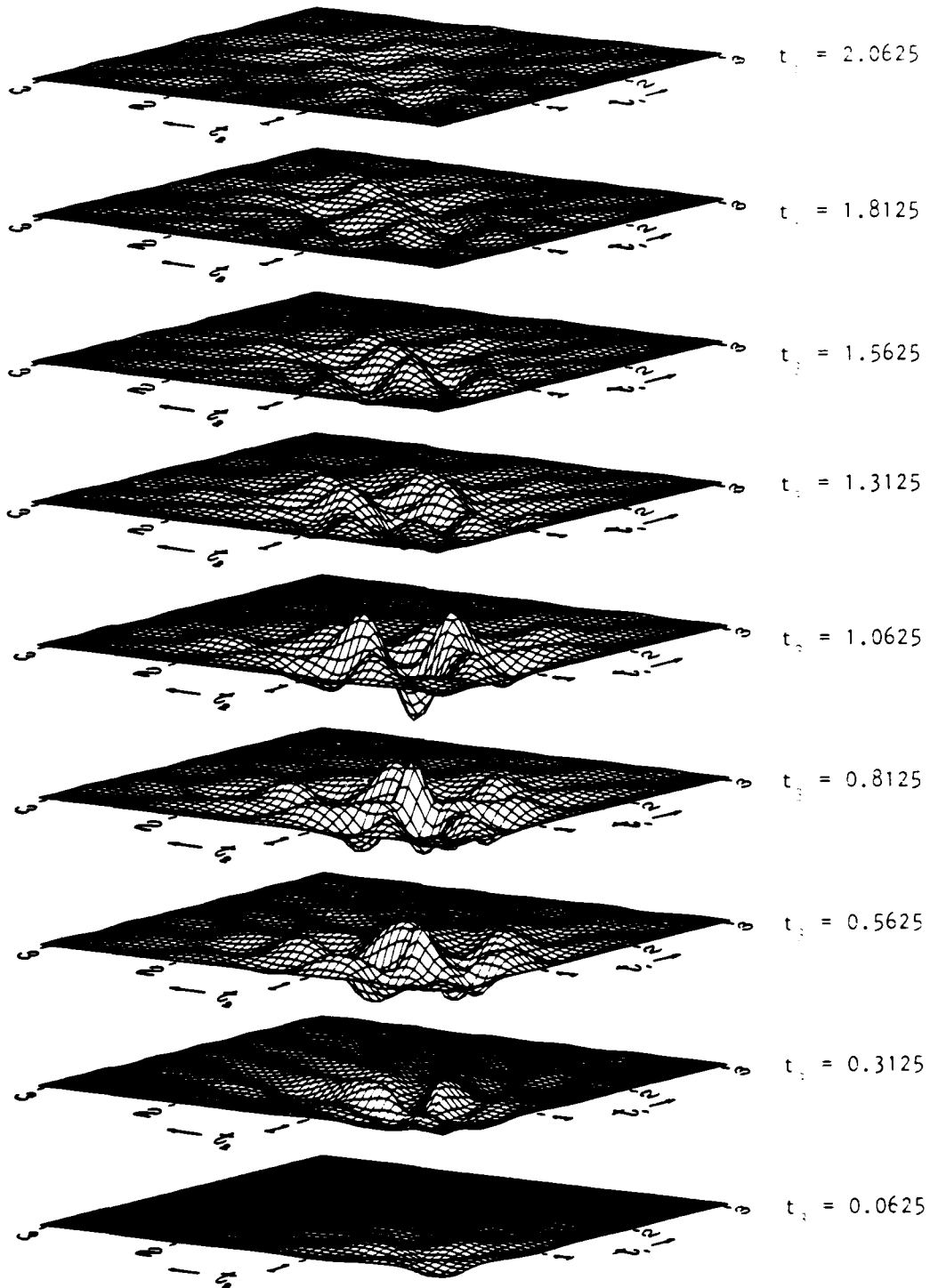


FIGURE 5 PORTIONS OF THE TRUNCATED CUBIC DISCRETE KERNEL,  $q_{jk}^3$

Qualitatively, there appears to be no feature of any of the surfaces shown in Figure 5 which are different than might be expected in a quadratic impulse response.

## TIME DOMAIN COMPUTATIONS: PRACTICAL MATTERS

As is easily appreciated, direct implementation of the time domain computation of Equation 14 with a (50 x 50 x 50) cubic kernel is relatively expensive, and is in fact wasteful of time and computer memory because of the symmetries of the impulse functions. (The convolutions mentioned in the last section were carried out with the methods to be described.)

There is nothing which can be done to speed up the linear part of the computation ( $Y1(n)$ , Equation 15) and in practice it is implemented as-is. Some re-organization, and the two-fold symmetry of the quadratic frequency response function,  $g_{jk}^2$ , allows the number of multiply-add operations in Equation 16 to be reduced by a factor of something more than two. If the limits of the  $j$  and  $k$  summations in Equation 16 are defined as:

$$\begin{aligned} p &\leq j \leq r \\ p &\leq k \leq r \end{aligned}$$

the Equation 16 may be re-written as:

$$\begin{aligned} Y2(n) &= g_{rr}^2 X^2(n-r) \\ &+ \sum_{j=p}^{r-1} X(n-j) \left[ g_{jj}^2 X(n-j) + \sum_{k=j+1}^r 2g_{jk}^2 X(n-k) \right] \end{aligned} \quad (24)$$

In practice it is advantageous to "triangularize" the quadratic kernel for use in Equation 24. This just takes the form of creating a one dimensional array of values of  $g_{jk}^2$  in the order required by the details of the formula. Equation 24, and absorbing the factor of two in each of the elements where  $j \neq k$ .

It is clearly most important to take advantage of the six-fold symmetry of  $g_{jkl}^3$  in Equation 17:

$$\begin{aligned} g_{jkl}^3 &= g_{j\lambda k}^3 \\ &= g_{kjl}^3 \\ &= g_{k\lambda j}^3 \\ &= g_{\lambda jk}^3 \\ &= g_{\lambda kj}^3 \end{aligned}$$

As in the quadratic case the limits on the summations in Equation 17 may be defined as:

$$\begin{aligned} p &\leq j \leq r \\ p &\leq k \leq r \\ p &\leq \ell \leq r \end{aligned}$$

With these conventions Equation 17 may be re-written as:

$$\begin{aligned} Y_3(n) = & X^2(n-p) \left[ g_{ppp}^3 X(n-p) + 3g_{pp,p+1}^3 X(n-p-1) \right] \\ & + X(n-p-1) \left[ X(n-p-1) \left[ g_{p+1,p+1,p+1}^3 X(n-p-1) + 3g_{p,p+1,p+1}^3 X(n-p) \right] \right] \\ & + \sum_{j=p+2}^r X(n-j) \left[ X(n-j) \left[ g_{jjj}^3 X(n-j) + \sum_{k=p}^{j-1} 3g_{jjk}^3 X(n-k) \right] \right. \\ & \left. + \sum_{k=p}^{j-1} 3g_{jkk}^3 X^2(n-k) \right. \\ & \left. + \sum_{k=p+1}^{j-1} X(n-k) \sum_{\ell=p}^{k-1} 6g_{jkl}^3 X(n-\ell) \right] \end{aligned} \quad (25)$$

"Triangularization" of the kernel in this case reduces the size of the kernel by a factor of 6 and allows the factors of 3 and 6 to be absorbed. The scheme is the same as for the quadratic kernel, a one dimensional array of values of  $g_{jkl}^3$  is created in the order required by the details of the formula, Equation 25. This approach, Equation 25, reduces the number of multiply-add operations per response point required for  $Y_3(n)$  with a 50 x 50 x 50 kernel from 375000 for Equation 17 to 24600, a reduction by a factor of 15.

In actual programming account has to be taken of the memory of the system, and the result is that the first valid point of the response to  $X(n)$ ,  $n=1,2,\dots$  is  $Y(1+r)$ , and the excitation must be available for  $p$  points past the last response point computed. In the present instance only the valid range of response and excitation was retained.

## SIMULATION OF RESPONSE TO RANDOM EXCITATION

Within the objectives of the present work it was as important to obtain a qualitative idea of the nature of cubic response to random excitation as it was to generate samples with which to work later on. Accordingly, given the kernels of the simulated system, and the algorithms just described, it remained to generate random excitation sequences and turn on the computer.

For this purpose it was convenient to use a subroutine left over from some previous work, Reference 23\*. What the subroutine does is to generate digital sequences from a pseudo random band passed Gaussian zero mean process. In the routine utilized the numerical band pass filter is configured so that the resulting sequence nominally has the spectral form:

$$U_{xx}(\omega) = 5\sigma_x^2 \omega_0^4 \text{Exp}\{-1.25(\omega_0/\omega)^4\}/\omega^5 \quad (26)$$

where  $U_{xx}(\omega)$  = the single sided spectrum  
 $\sigma_x^2$  = spectrum area  
 = variance  
 $\omega_0$  = modal frequency

and the values of variance and modal frequency may be specified. This spectral form is the same as those of the ITTC two parameter, Pierson-Moskowitz, and Bretschneider wave spectra. The algorithm is not unusual. Random numbers from a uniform distribution are first generated by a standard computer system utility. These numbers are conceptually assumed to represent a Gaussian probability and a numerical approximation is then used to generate zero mean Gaussian deviates with unity variance and a 'white' spectrum. The approach has been checked statistically with very large samples and found to reasonably represent the required zero mean white Gaussian process within 5 standard deviations. The next step is to filter the sequence numerically to shape the signal, and finally to carry out time wise interpolation to generate a sequence with the required sampling interval.

\*23. Dalzell, J.F., "A Note on the Distribution of Maxima of Ship Rolling," Journal of Ship Research, Vol. 17, No. 4, December 1973.

In the present case the sampling interval was fixed at 0.0625 seconds by the previous derivation of the impulse responses. It seemed reasonable for a first attempt to set  $\omega_0 = 2\pi$  so that the peak of the spectrum and the linear resonance would be aligned. For present purposes it was desirable to compute response for various excitation levels, and it made sense to take account of the homogeneity property. In particular, if  $Y1(n)$ ,  $Y2(n)$  and  $Y3(n)$  (Equations 15 through 17) are computed for some nominal level of excitation and stored, then the response to an excitation which is a factor "f" times the nominal is:

$$fY1(n) + f^2Y2(n) + f^3Y3(n)$$

which is to say that once the computation of Equations 15 through 17 is made for one excitation level, Equation 14, the total response, may be evaluated for any number of linearly proportional excitations with trivial extra expense. On this basis it was decided the nominal variance,  $\sigma_x^2$ , of Equation 25 should be 0.0625 so that  $\sigma_x$  is 0.25 and the "significant height" of the basic excitation would be unity.

What remained to be settled was the sample duration. The routine used had provision for 11 widely separated entry points into the underlying pseudo random number sequence. It seemed realistic then to generate 11 samples of a duration similar to that ordinarily achieved in towing tank work. Thus 2100 point (131 second) durations were chosen for each sample. (This choice results in about 150 "wave" encounters, and broadly corresponds to what is often achieved in towing tank experiments at zero ship speed.)

Figures 6a and b indicate the time histories resulting for Sample 1 with the basic excitation level ( $\sigma_x = 0.25$ ). The entire sample is shown in two figures so that individual fluctuations are more visible. At the top of each is the excitation,  $X(t)$ . The three frames in the middle show the three components of the response,  $Y1(t)$ ,  $Y2(t)$  and  $Y3(t)$ . Finally, at the bottom the sum, or total response  $Y(t)$ , Equation 14, is shown. It should be noted that the vertical scales for the response components are different; the scale choice was made so as to show the nature of each component.

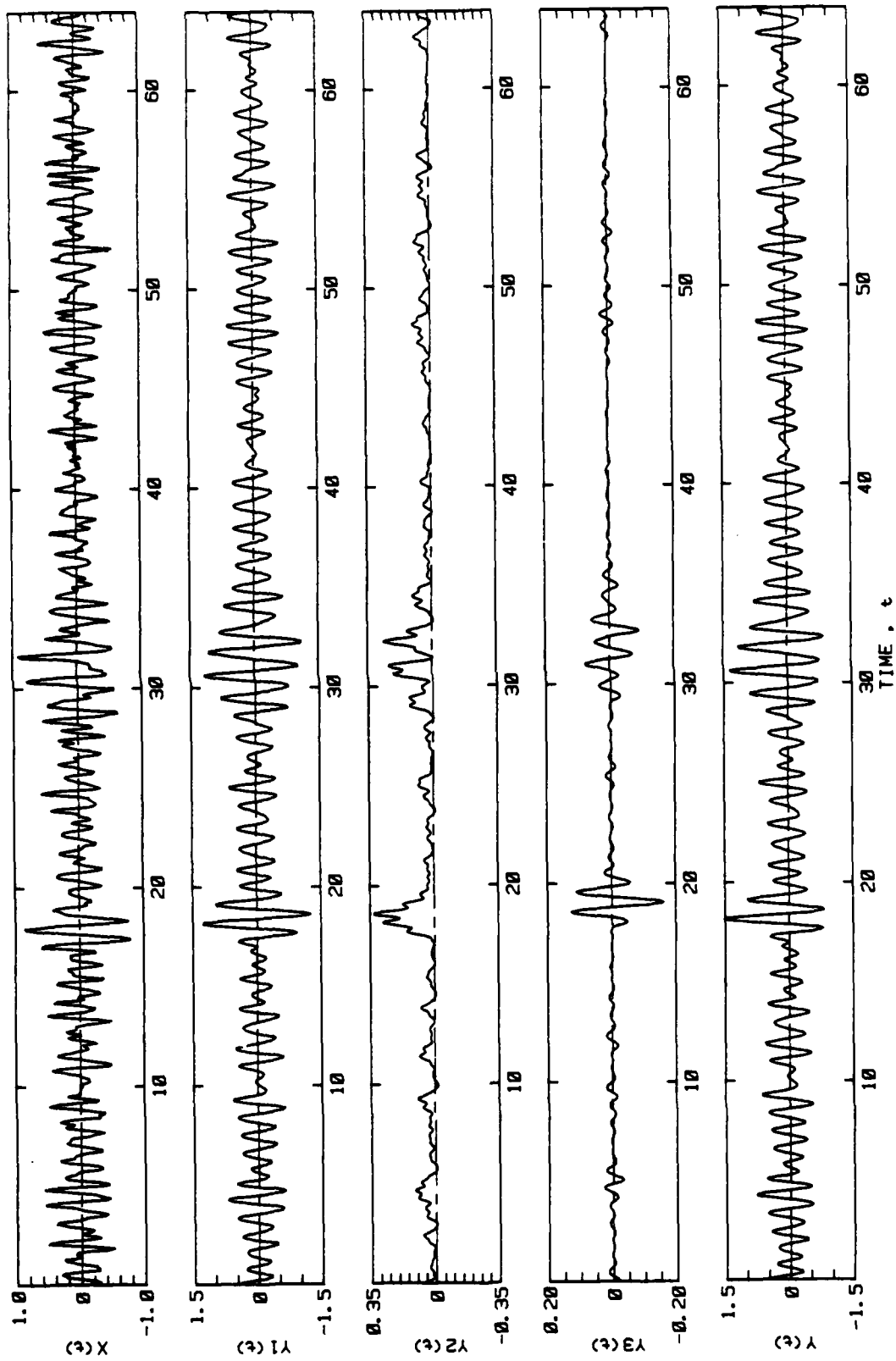


FIGURE 6a SIMULATED TIME HISTORIES OF NONLINEAR RESPONSE  
TO RANDOM EXCITATION: SAMPLE 1,  $\sigma_x = 0.25$

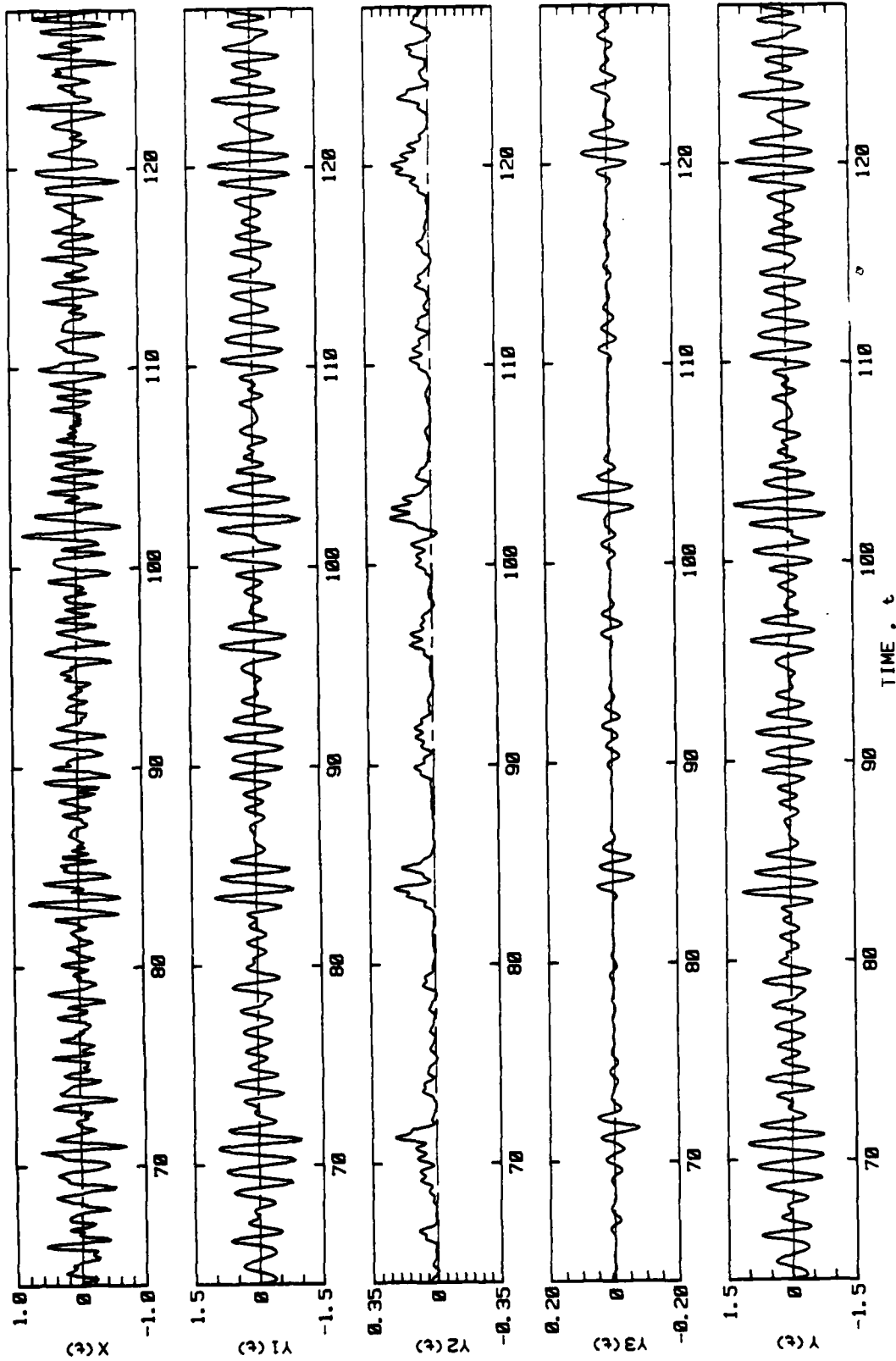


FIGURE 6b SIMULATED TIME HISTORIES OF NONLINEAR RESPONSE  
TO RANDOM EXCITATION: SAMPLE 1,  $\sigma_x = 0.25$

Qualitatively, the linear and quadratic components are exactly as expected. The linear response appears statistically symmetric and contains a narrower band of frequency components than the excitation. The quadratic response is quite asymmetric, includes a non zero mean, and response at very low frequencies as well as a visible high frequency response which is predominately twice the typical linear response frequency.

No ideas about the qualitative nature of the cubic component,  $Y_3(t)$ , were available, and it was this question which occasioned the plotting of time histories. As is clear from Figure 6, the simulated values of the cubic component contain "bursts" of response which appear symmetric and largely to have the same frequency content as the linear response. These bursts of significant cubic response appear to be associated with groups of waves in the excitation, and with significant excursions of the quadratic response,  $Y_2(t)$ . No obvious high frequency components appear in  $Y_3(t)$ . In retrospect, some of this qualitative behavior of the cubic component of response might possibly have been predicted. The simulated cubic frequency response function,  $\hat{G}_3(\omega_1, \omega_2, \omega_3)$ , Equation 12, contains the quadratic frequency response function. Thus some qualitative relationship should result. It was found in the previous numerical evaluations that the cubic response at the third harmonic of excitation frequency was an order of magnitude smaller than the cubic response at the excitation frequency, and a general absence of high frequencies from the cubic response could have been expected on this basis.

It was of interest to see if the qualitative features of the simulated nonlinear response held from sample to sample. To this end a number of the remaining samples were also plotted. Figures 7 and 8 are examples. Sample 4 was found to contain the highest excursion of cubic response of all the eleven samples. This largest excursion of  $Y_3(t)$  is shown at about  $t=5$  seconds in Figure 7. Sample 11 was found generally to have the lowest level of cubic response, and half of this sample is shown in Figure 8. The qualitative nature of the simulated cubic response to random excitation appears to hold throughout the simulated data.

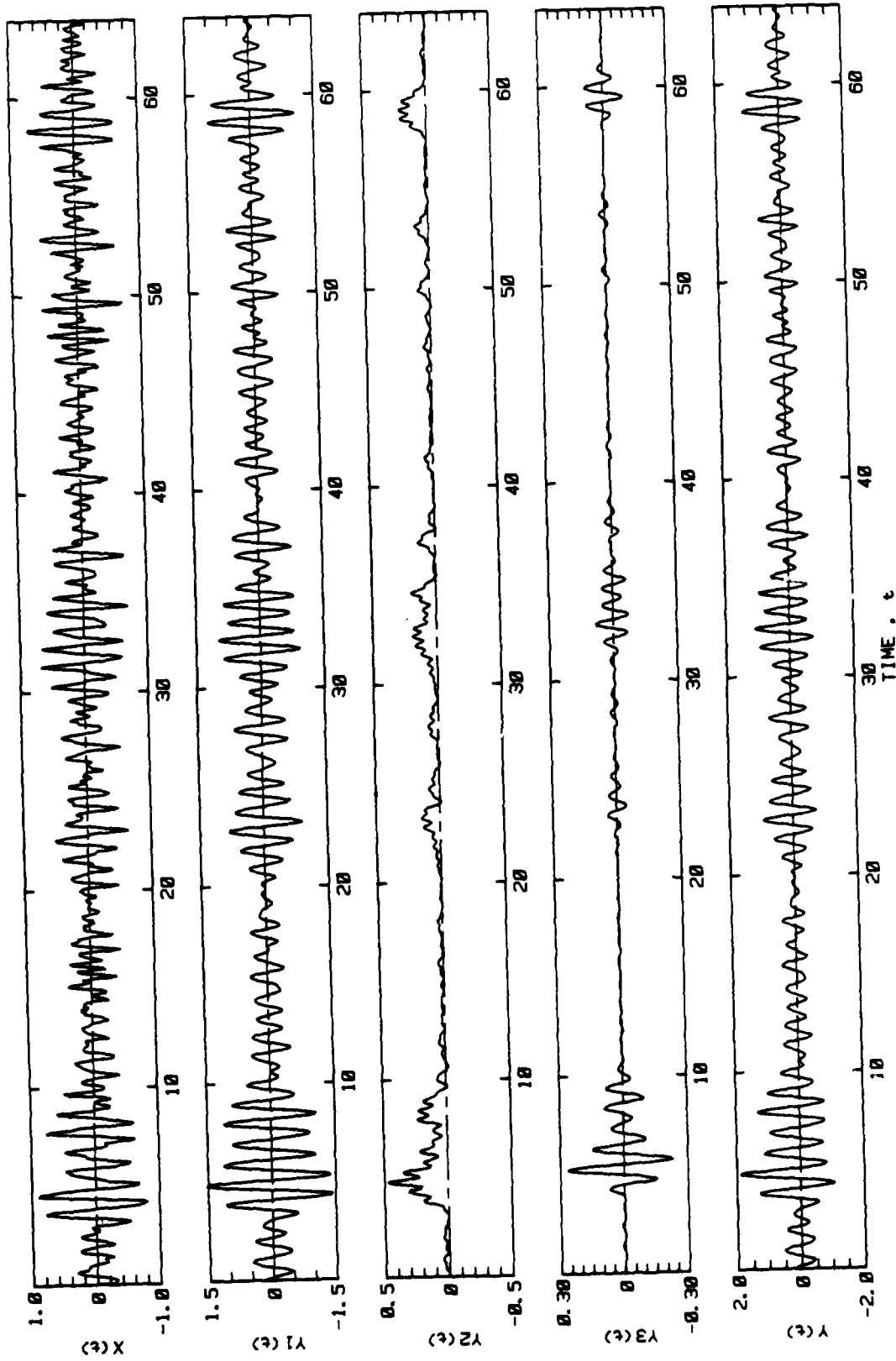


FIGURE 7 SIMULATED TIME HISTORIES OF NONLINEAR RESPONSE  
TO RANDOM EXCITATION: SAMPLE 4,  $\sigma_x = 0.25$

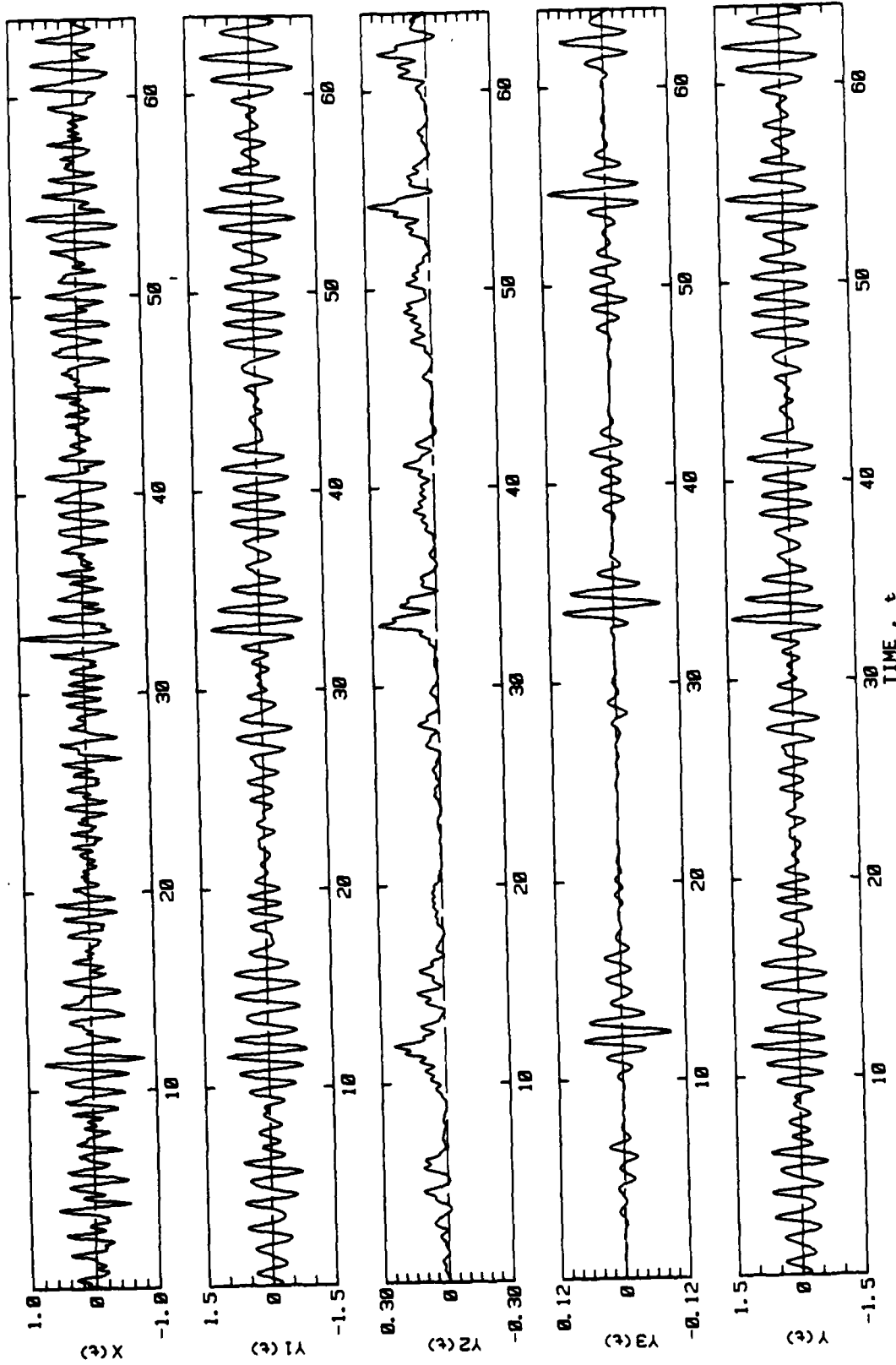


FIGURE 8 SIMULATED TIME HISTORIES OF NONLINEAR RESPONSE  
TO RANDOM EXCITATION: SAMPLE 11,  $\sigma_x = 0.25$

A general comparison of the total response,  $Y(t)$ , in Figures 6 through 8 with the corresponding linear component,  $Y_1(t)$ , indicates almost no qualitative difference. At the basic excitation level the nonlinearities are too small to have much effect. Those quantitative changes which are visible are most easily seen in the first part of Figure 7. There the largest nonlinear responses in the entire simulation produce a non symmetric response and perhaps slightly increase the amplitude of the fluctuations relative to those of the linear component.

It was also of interest to see the qualitative effect upon the total response,  $Y(t)$ , of an increase in the excitation level,  $\sigma_x$ . Figures 9a,b, 10 and 11 indicate this for an excitation four times the nominal ( $\sigma_x = 1.0$ ) for the cases shown in Figures 6 through 8. In accordance with the previous discussion, the synthesis of these results amounts to multiplication of the basic excitation and linear response by 4, multiplication of quadratic response by 16, and multiplication of cubic response by 64 before making the summation for  $Y(t)$ . Thus the time histories in the top four frames of Figure 9a for instance are exactly the same as those in Figure 6a except for a scale change. The qualitative difference is in the bottom frame,  $Y(t)$ . It is clear from Figures 9 through 11 that once the excitation level is high enough there are significant qualitative differences between the linear and the nonlinear response to random excitation, and the differences center about occasional non symmetric large amplitude excursions which change the general appearance of the time history.

Though some of the features of the total simulated response in Figures 9 through 11 may be a bit more extreme than some response histories obtained in towing tank experiments, some of the same behavior is occasionally seen.

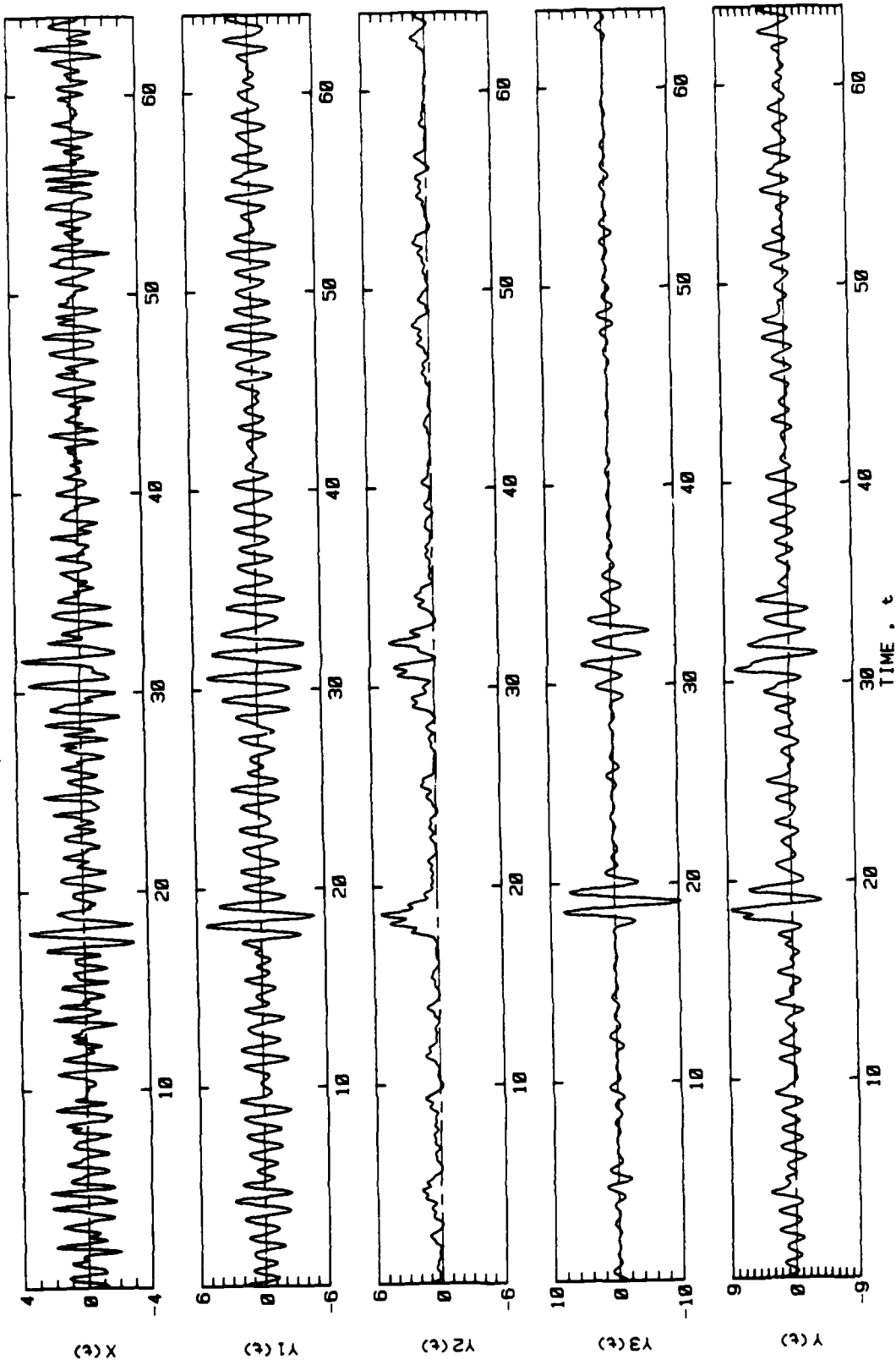


FIGURE 9a SIMULATED TIME HISTORIES OF NONLINEAR RESPONSE  
TO RANDOM EXCITATION: SAMPLE 1,  $\sigma_x = 1.0$

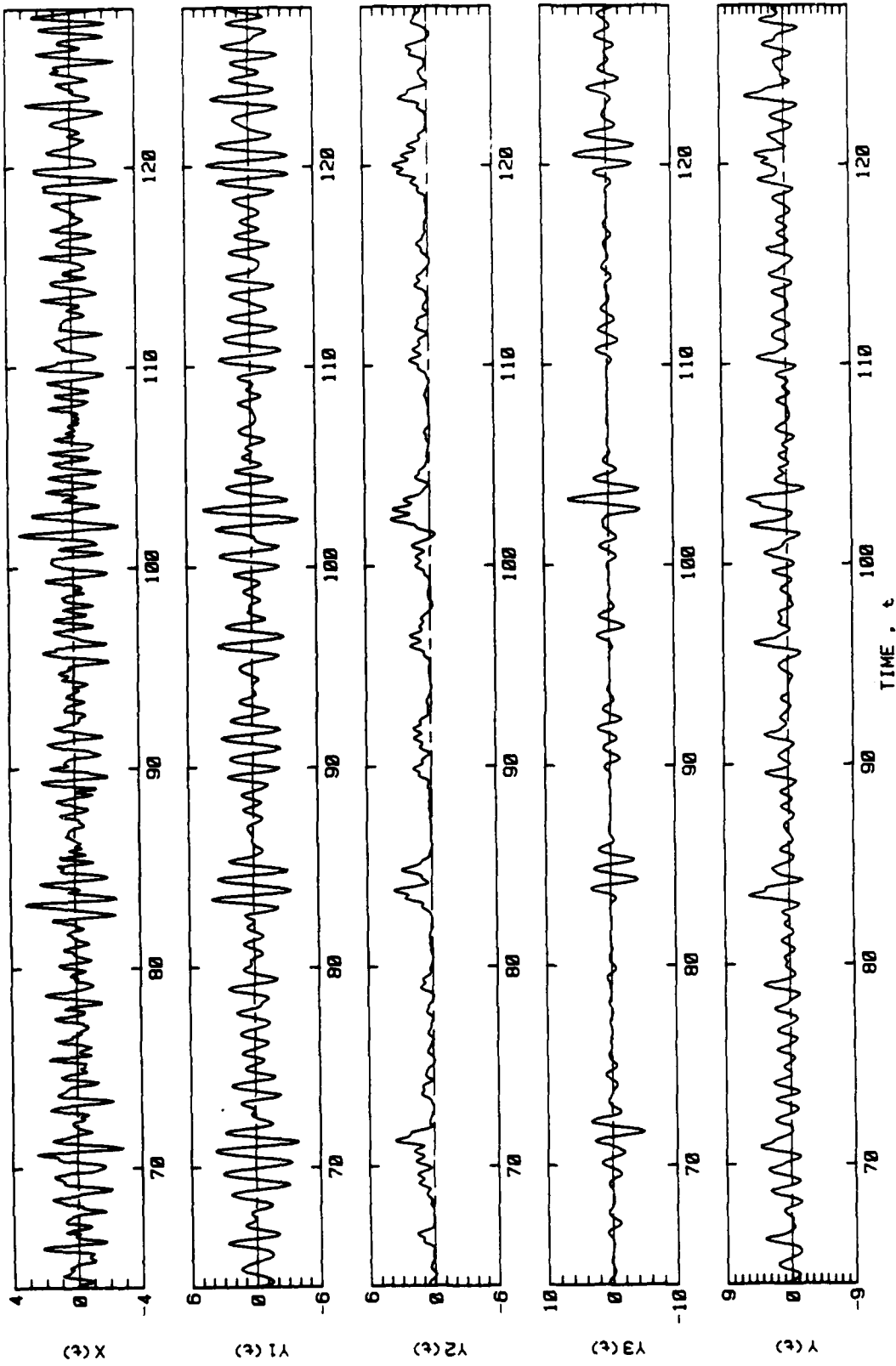


FIGURE 9b SIMULATED TIME HISTORIES OF NONLINEAR RESPONSE  
TO RANDOM EXCITATION: SAMPLE 1,  $\sigma_x = 1.0$

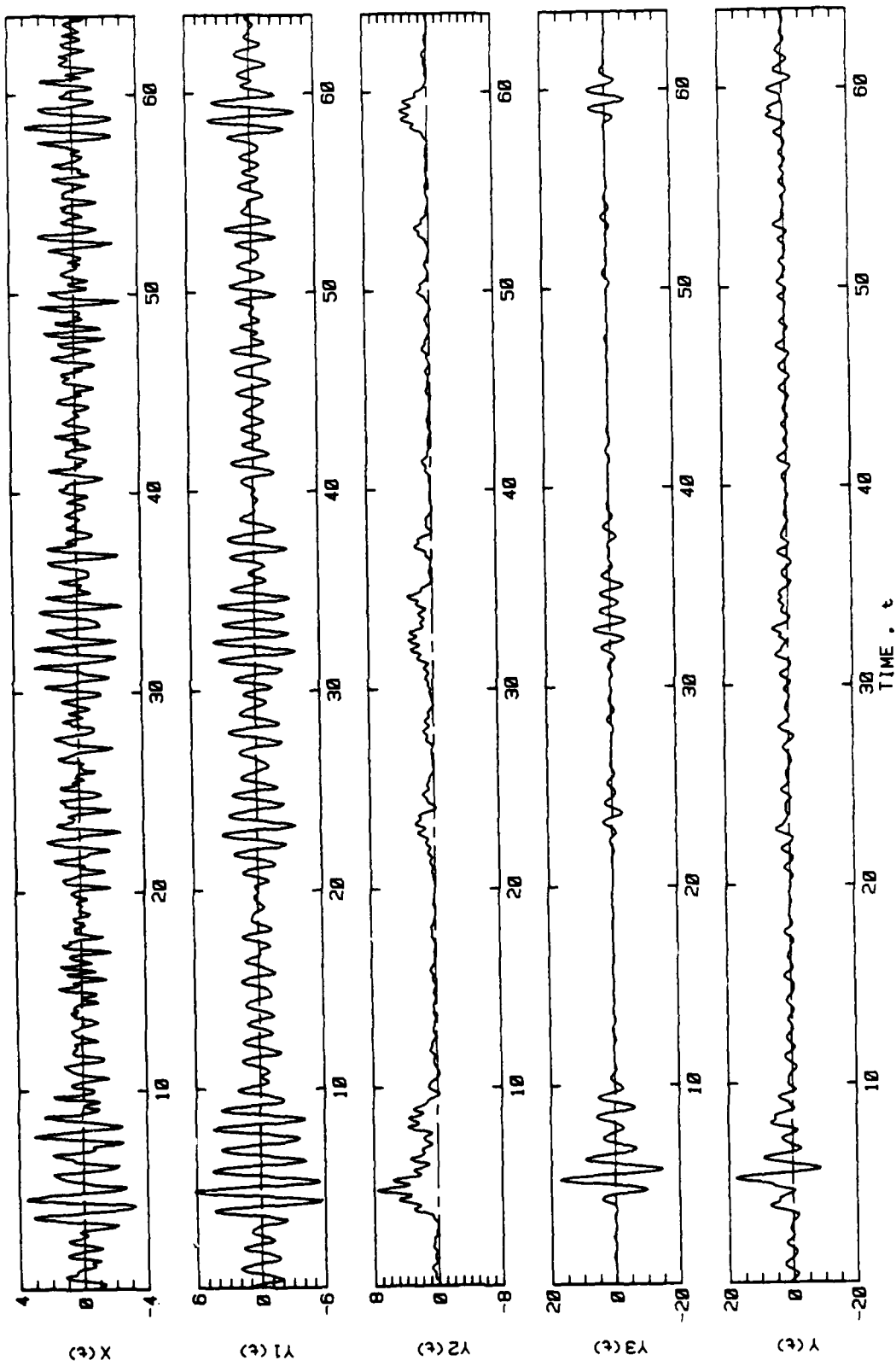


FIGURE 10 SIMULATED TIME HISTORIES OF NONLINEAR RESPONSE TO RANDOM EXCITATION: SAMPLE 4,  $\sigma_x = 1.0$

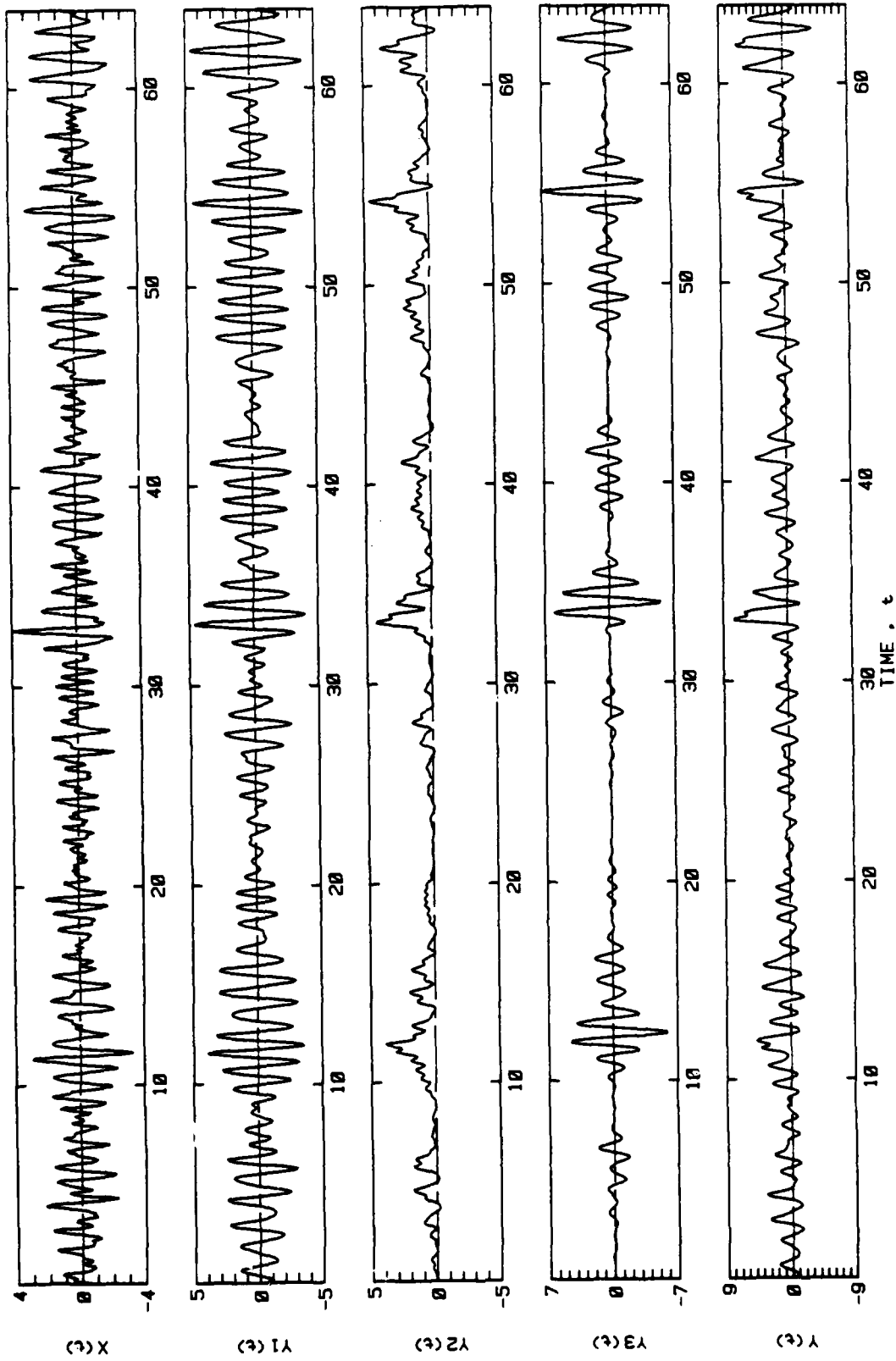


FIGURE 11 SEPARATED TIME HISTORIES OF NONLINEAR RESPONSE  
TO RANDOM EXCITATION: SAMPLE 11,  $\sigma_x = 1.0$

## THE SPECTRUM OF RESPONSE TO RANDOM EXCITATION

Regardless of the possibility of nonlinearities, the scalar spectra of excitation and response are the fundamental state of art approach to the characterization of the random case. The theoretical form of the spectrum for the present model, Equation 5, may be written down from References 4 and 7. For subsequent purposes it is convenient to cite the results first in a particular two-sided form. If,

$$S_{xx}(\omega) = \text{excitation spectrum}$$

$$S_{yy}(\omega) = \text{response spectrum}$$

where both are double sided and normalized so that their integral over frequency is equal to  $(2\pi)$  times variance, then the response spectrum for the linear+quadratic+cubic model may be written in terms of frequency response functions as follows:

$$S_{yy}(\omega) = S_1(\omega) + S_2(\omega) + S_3(\omega) \quad (27)$$

and:

$$S_1(\omega) = S_{xx}(\omega) \left| G_1(\omega) + \frac{3}{2\pi} \int G_3(\omega, v, -v) S_{xx}(v) dv \right|^2 \quad (28)$$

$$S_2(\omega) = \frac{1}{\pi} \int |G_2(\omega-u, u)|^2 S_{xx}(\omega-u) S_{xx}(u) du \quad (29)$$

$$S_3(\omega) = \frac{3}{2\pi^2} \iint |G_3(\omega-v-u, v, u)|^2 S_{xx}(\omega-v-u) S_{xx}(v) S_{xx}(u) dudv \quad (30)$$

By way of comment, if the cubic frequency response function is zero the form of the spectrum is the same as that for the linear plus quadratic system of Reference 15. If both cubic and quadratic frequency response functions are zero, the result is the conventional linear estimate.

In practice, as opposed to theoretical manipulations, the one sided realizable spectrum with area equal to variance is required, and the above equations may be written in terms of one sided spectra by

replacing  $S_{xx}(\omega)$  and  $S_{yy}(\omega)$  by  $-U_{xx}(\omega)$  and  $-U_{yy}(\omega)$  where

$U_{xx}(\omega)$  = the single sided excitation spectrum

$U_{yy}(\omega)$  = the single sided response spectrum

Carrying this and some simple variable changes out results in expressions for the single sided spectra which are analogous to Equations 27 through 30:

$$U_{yy}(\omega) = U1(\omega) + U2(\omega) + U3(\omega) \quad (31)$$

where ( $\omega > 0$ ) and:

$$U1(\omega) = U_{xx}(\omega) \left| G_1(\omega) + 3 \int_0^{\infty} G_3(\omega, v, -v) U_{xx}(v) dv \right|^2 \quad (32)$$

$$U2(\omega) = \int_0^{\infty} G_2\left\{(\omega-v)/2, (\omega+v)/2\right\}^2 U_{xx}(|\omega-v|/2) U_{xx}(|\omega+v|/2) dv \quad (33)$$

$$U3(\omega) = 1.5 \iiint |G_3(\omega-v-u, v, u)|^2 U_{xx}(|\omega-v-u|) U_{xx}(|v|) U_{xx}(|u|) dudv \quad (34)$$

Implicit in Equation 34 is a failure to find a change of variables which would allow reduction of the range of integration. Given the excitation spectrum and expressions for the frequency response functions, Equations 32 through 34 are computable, though Equation 34 is tedious. If, as in the present case, there is interest in response spectra for excitation which is linearly proportional to some nominal excitation, the integrations in Equations 32, 33 and 34 need only be done once. (Once the integrations are performed for a given  $U_{xx}(\omega)$ , the integrals for an excitation a factor "f" times the original are the initial results times  $(f^{2k})$  where k is the number of times  $U_{xx}(\omega)$  appears in the integrand.)

It was of interest both to see if all the above works and to obtain some idea of the relative influence of the various terms. Thus it was decided to compose simulated time histories for various levels of excitation, carry out conventional spectral analyses, and finally do the computations implied in Equations 31 through 34 for comparison.

The first step in this operation was to produce time histories of  $X(t)$  and  $Y(t)$  for excitations 1/2, 1, 2, 3 and 4 times the nominal excitation specified in the last section. As explained previously, given the stored time history components  $Y_1(t)$ ,  $Y_2(t)$  and  $Y_3(t)$  for the nominal excitation, the production of  $X(t)$  and  $Y(t)$  for each excitation level is a trivial exercise. Once it is done, the resulting time series appear more or less like any samples of random input and output, and conventional data reduction techniques can be employed.

Spectrum analysis of each time history was first carried out by the conventional Fast Fourier Transform frequency smoothing technique noted in Reference 24\*. Each time series was truncated from 2100 to 2048 points, corrected to zero mean, tapered with the Tukey 10% cosine taper and directly transformed with the FFT. The raw spectral estimates resulting were averaged in groups of 13 at intervals of 7 to result in spectral estimates with 26 degrees of freedom and a frequency resolution of 0.344 rad/sec. For each excitation level there were 11 such spectra resulting from this operation on excitation and response. Since each time history is a sample from a stationary random process it was considered reasonable to also carry out ensemble smoothing over the 11 samples for each excitation. Thus the final result for each of the five excitations was a single smoothed "observed" excitation spectrum and a single "observed" response spectrum. Each of these spectra had 286 degrees of freedom per spectral estimate, which implies 90% confidence bounds on the estimates of +15% and -12%. Total degrees of freedom for the excitation spectra were in excess of 3000, which implies 90% confidence bounds on variance of  $\pm 4\%$ , and in fact the estimated variance was within 2% of the theoretical value specified in the original time domain simulation. Total degrees of freedom for the "observed" response varied between 1500 and 2500, which would result in confidence bounds on variance of  $\pm 5\%$  if the response could be considered Gaussian. Table 4 summarizes the "observed" standard deviations from the data reduction procedure. It should be noted that the "observed" values of

---

\*24. Bendat, J.S. and Piersol, A.G., "Random Data: Analysis and Measurement Procedures," John Wiley & Sons, 1971.

TABLE 4

"OBSERVED" STANDARD DEVIATIONS OF EXCITATION  
AND RESPONSE FOR VARIOUS NOMINAL EXCITATION LEVELS

Factor on Nominal Excitation	0.5	1.0	2.0	3.0	4.0
Nominal $\sigma_x$	0.125	0.25	0.50	0.75	1.00
"Observed" $\sigma_x$	0.124	0.248	0.496	0.744	0.992
"Observed" $\sigma_y$	0.181	0.356	0.673	0.971	1.396
$\sigma_y/\sigma_x$	1.46	1.44	1.36	1.30	1.41

standard deviation,  $\sigma_x$ , march upward exactly as expected--the operations carried out on the excitation time histories can only result in an increase in standard deviation proportional to the assumed factor on nominal excitation. The "observed" response standard deviations are not exactly proportional to the assumed factor on excitation as must be expected for nonlinear systems.

The next step was to carry out the "prediction" operations of Equation 31 through 34. The frequency response functions for the simulated system, Equations 10 through 12, had been programmed for earlier operations to that numerical values for the functions could be obtained easily. Apart from carrying out the operations, the only other question was whether to use the theoretical expression for  $U_{xx}(\omega)$ , Equation 26, or the "observed" excitation spectrum from the data reduction procedure. It was guessed that use of the "observed" excitation spectrum might wash-out some of the residual effects of statistical variability and the results of the data reduction were used as the excitation in the evaluation of Equations 31 through 34 for the five cases of interest.

Figures 12 through 16 summarize the results of the comparison. Each figure has four frames with frequency the abscissa and spectral density the ordinate. The "observed" excitation spectrum is shown in the uppermost frame, and the "observed" response spectrum in the lower most, both plotted as boxed points connected by straight lines. The "predicted" response spectrum, Equation 31, is overplotted in the lower frame. The middle frames indicate the  $U1(\omega)$ ,  $U2(\omega)$  and  $U3(\omega)$  components of the prediction, Equations 32 through 34. Finally, as an aid in interpretation, the purely linear estimate of the spectrum is indicated. This is just what would be obtained if both quadratic and cubic nonlinearities were ignored, or:

$$U_{xx}(\omega) = |G_1(\omega)|^2$$

In Figure 12, for the lowest excitation level, it is clear that the nonlinearities would be of no practical importance.  $U2(\omega)$  and  $U3(\omega)$  are invisible and the influence of the cubic nonlinearity upon  $U1(\omega)$  is very slight. The agreement between observed and predicted response spectra

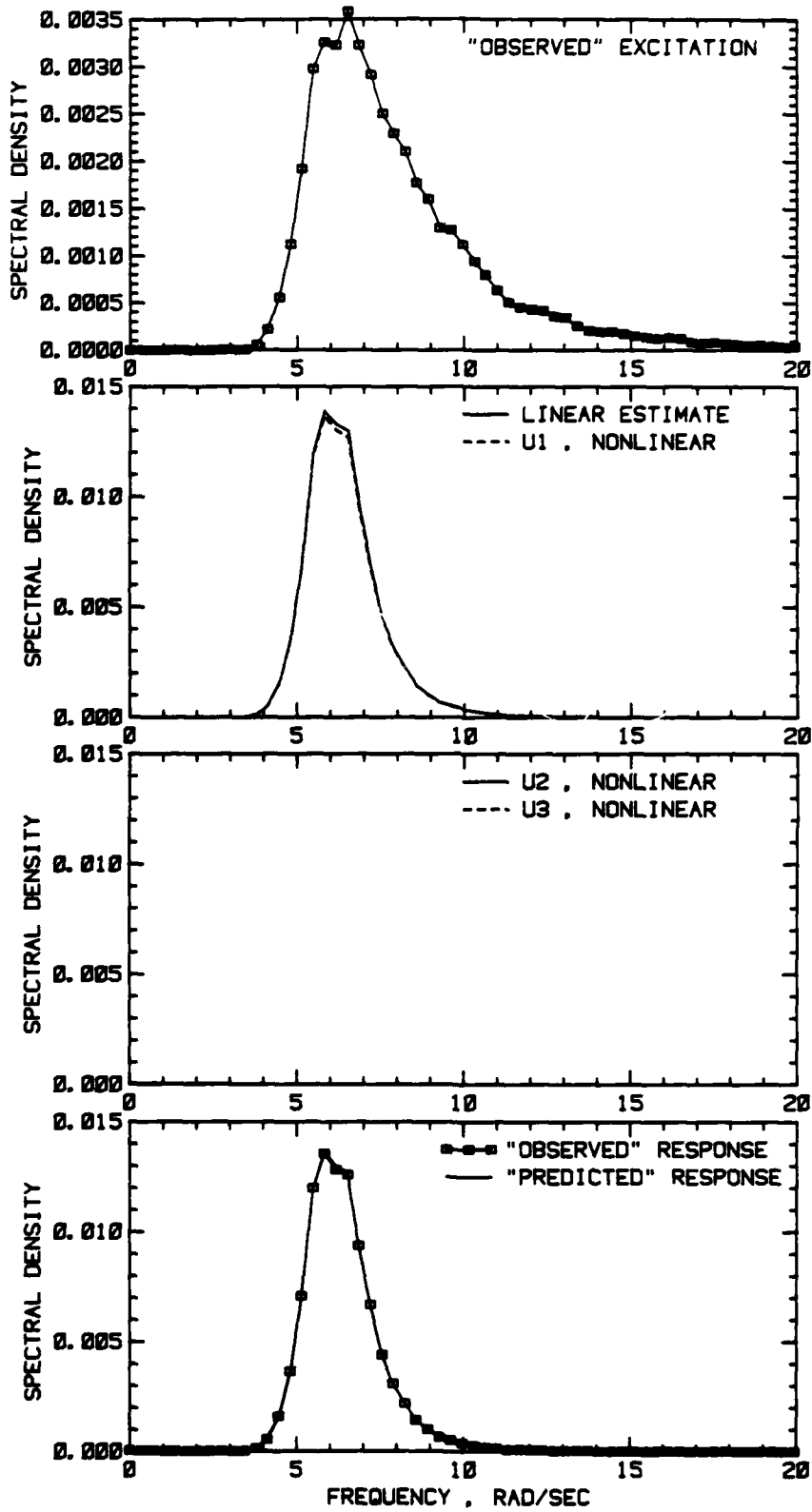


FIGURE 12 OBSERVED AND PREDICTED SPECTRA OF RESPONSE OF THE SIMULATED SYSTEM: NOMINAL  $\sigma_x = 0.125$

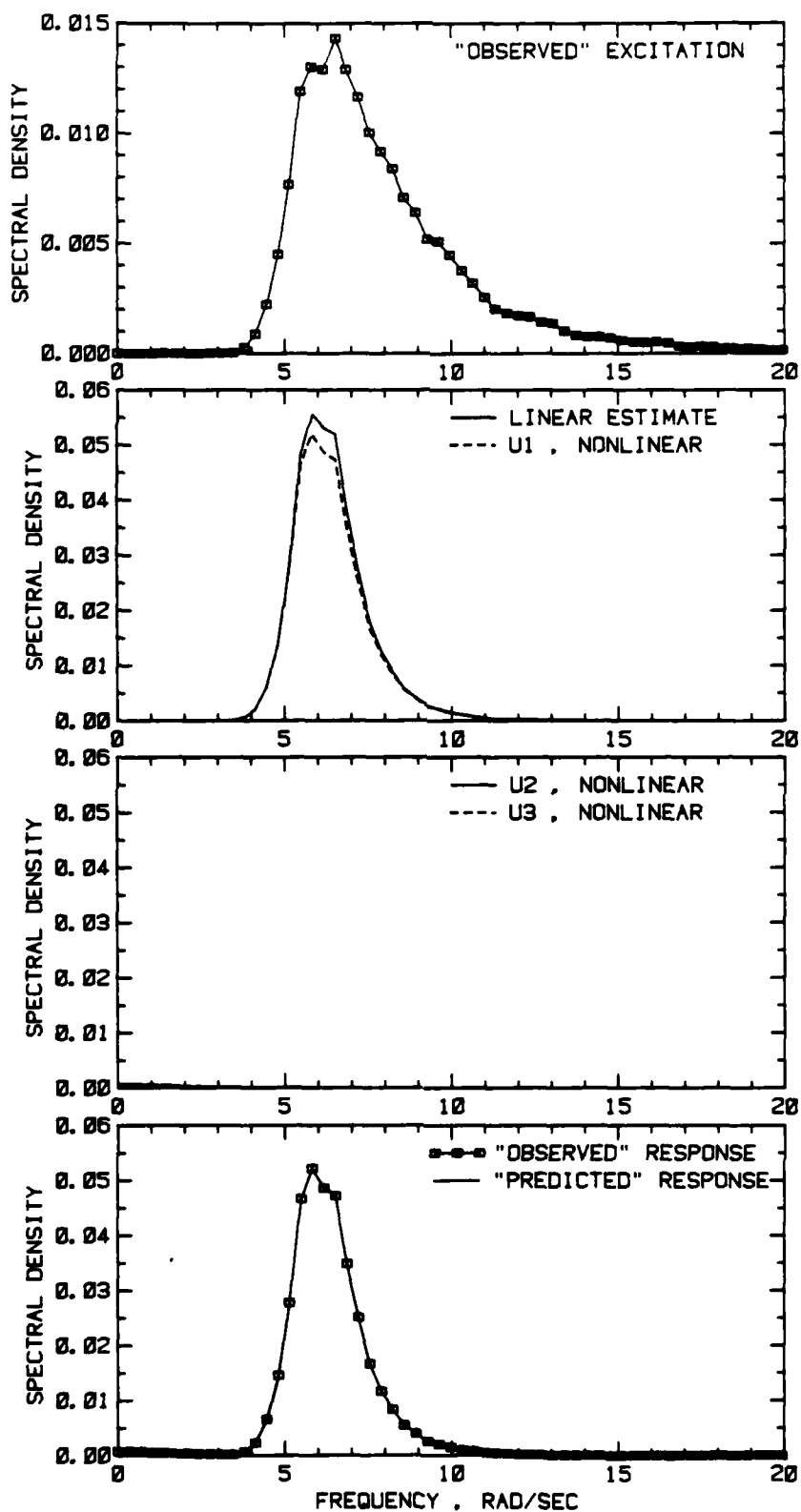


FIGURE 13 OBSERVED AND PREDICTED SPECTRA OF RESPONSE OF THE SIMULATED SYSTEM: NOMINAL  $\sigma_x = 0.25$

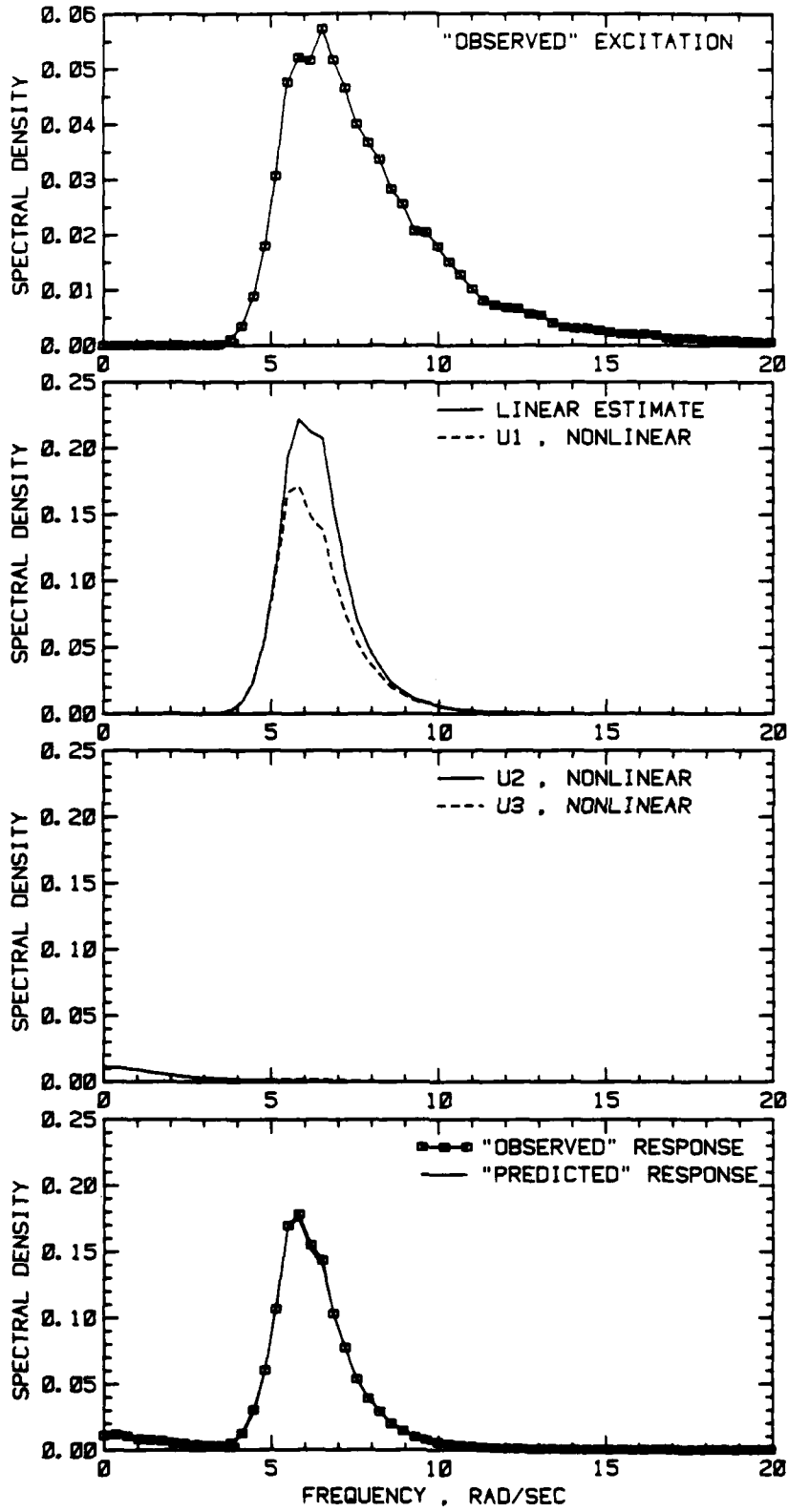


FIGURE 14 OBSERVED AND PREDICTED SPECTRA OF RESPONSE OF THE SIMULATED SYSTEM: NOMINAL  $\sigma_x = 0.5$

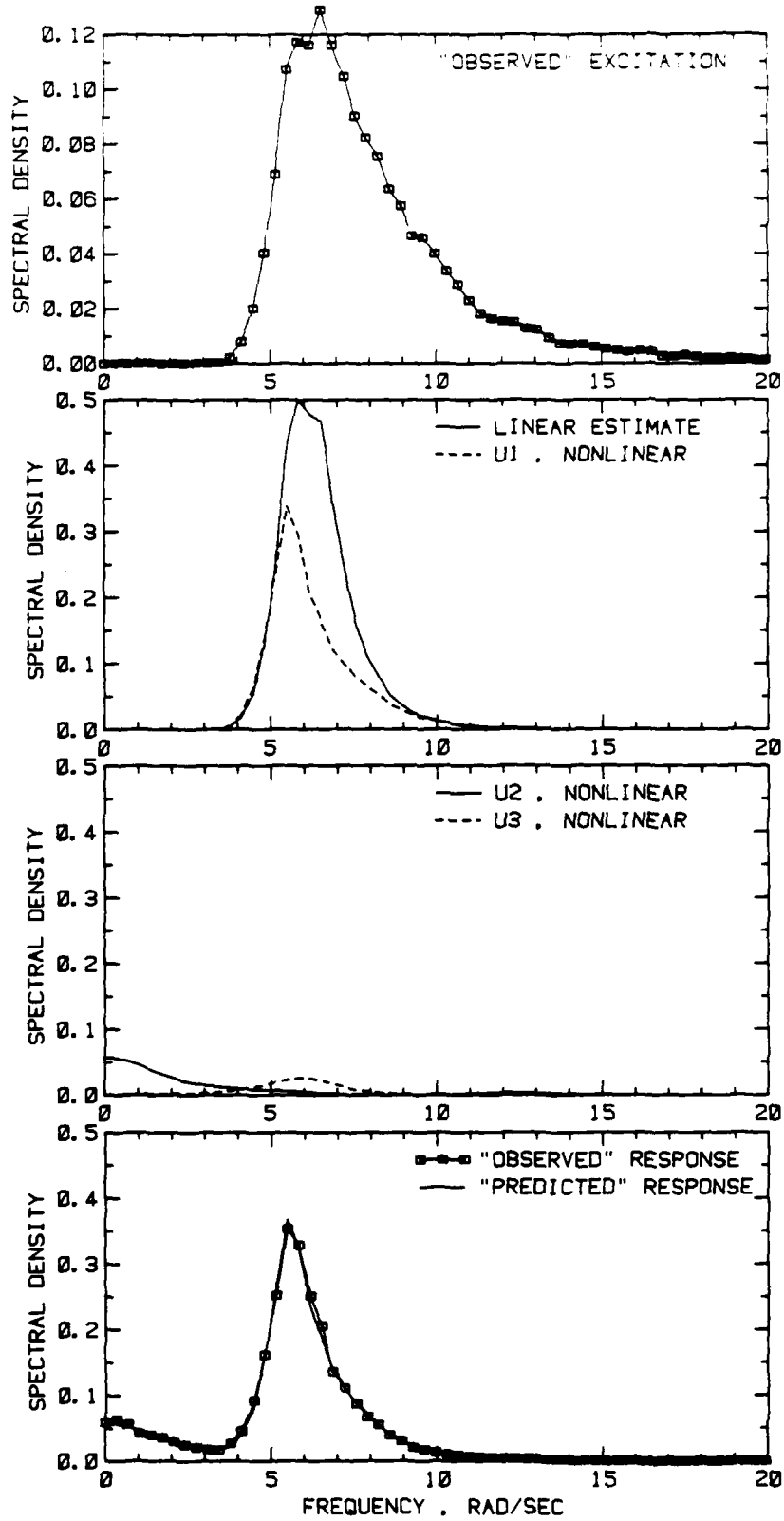


FIGURE 15 OBSERVED AND PREDICTED SPECTRA OF RESPONSE OF THE SIMULATED SYSTEM: NOMINAL  $\sigma_x = 0.75$

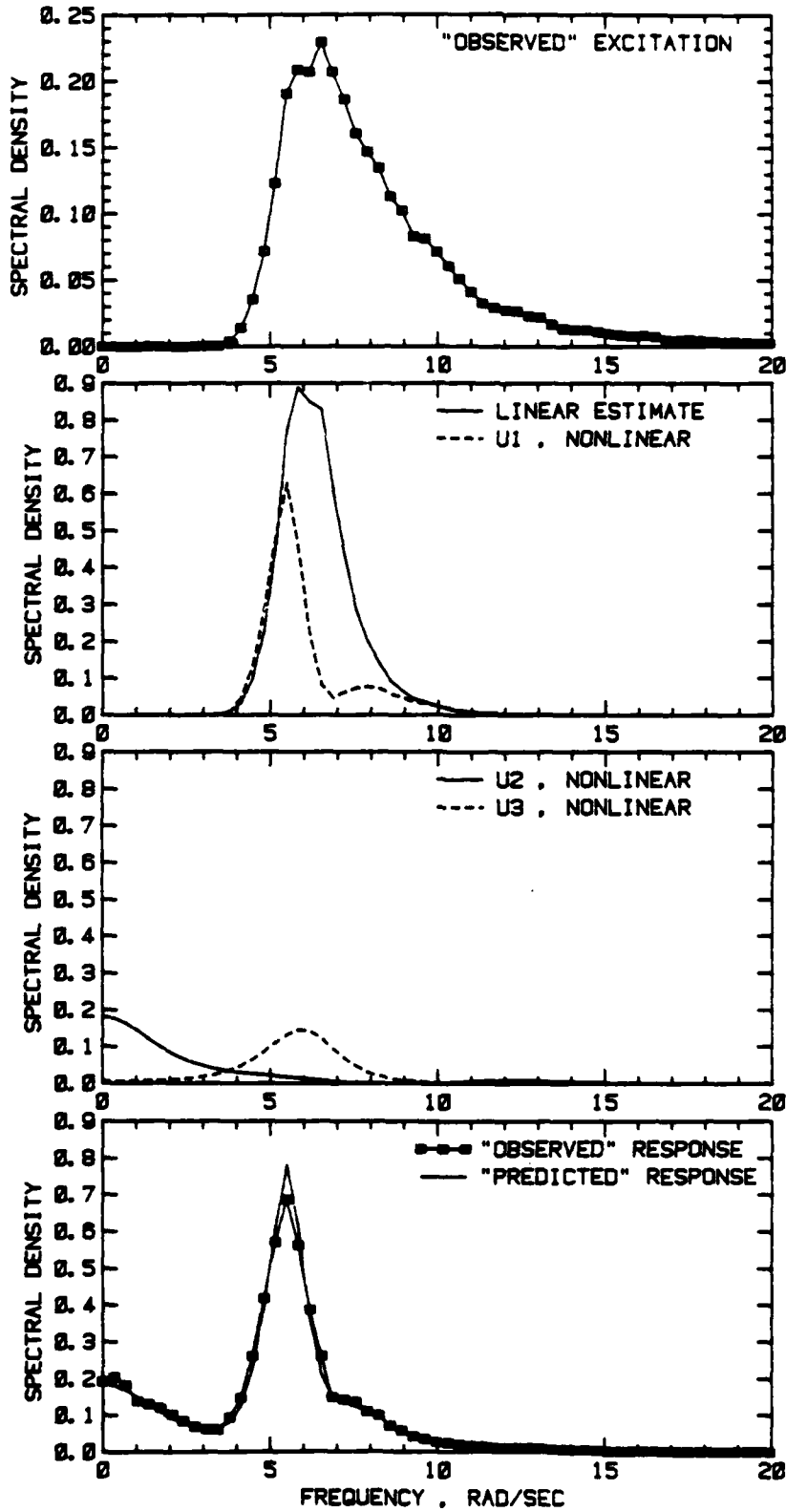


FIGURE 16 OBSERVED AND PREDICTED SPECTRA OF RESPONSE OF THE SIMULATED SYSTEM: NOMINAL  $\sigma_x = 1.0$

is almost embarrassingly good. Very much the same situation appears in Figure 13 for the nominal excitation,  $\sigma_x = 0.25$ . The very low frequency response spectral density due to quadratic interactions,  $U2(\omega)$ , just starts to appear, and the influence of the cubic nonlinearity on  $U1(\omega)$  is slightly greater than in Figure 12.

In Figure 14 the influence of the  $U3(\omega)$  component, Equation 34, just starts to appear. Figures 15 and 16 for  $\sigma_x = 0.75$  and 1.0 indicate the form of the contributions to the spectrum of all three components. The nonlinear part of  $U1(\omega)$ , Equation 32, can significantly change what might be expected from purely linear considerations.  $U2(\omega)$ , the quadratic part, makes a contribution to very low frequency response, perhaps to frequencies in the excitation range, and contributes some high frequency response at frequencies about a factor of 2 above the excitation peak.  $U3(\omega)$ , the pure cubic part, is only significant at the highest excitation level, and makes a contribution in the range of the peak of the spectrum.

It is impossible to generalize, but if the simulated system is representative, it may be that in many practical seakeeping problems only the first component of the spectrum,  $U1(\omega)$ , will be of importance.

One of the most common operations in analysis of random wave experiments is to estimate the modulus of the linear frequency response function by taking the square root of the ratio of observed response and excitation spectra:

$$|G_1(\omega)|_{\text{estimated}} = \left[ U_{yy}(\omega) / U_{xx}(\omega) \right]^{\frac{1}{2}}$$

This operation was performed using the "observed" response and excitation spectra just presented. The results are shown in Figure 17. In accordance with usual practice no results are given for frequencies where the excitation spectrum was less than 10% of its peak.

The equivalent linear response appears to vary systematically with excitation level  $\sigma_x$ . As excitation level increases the results deviate more and more from the form of the simulated linear response

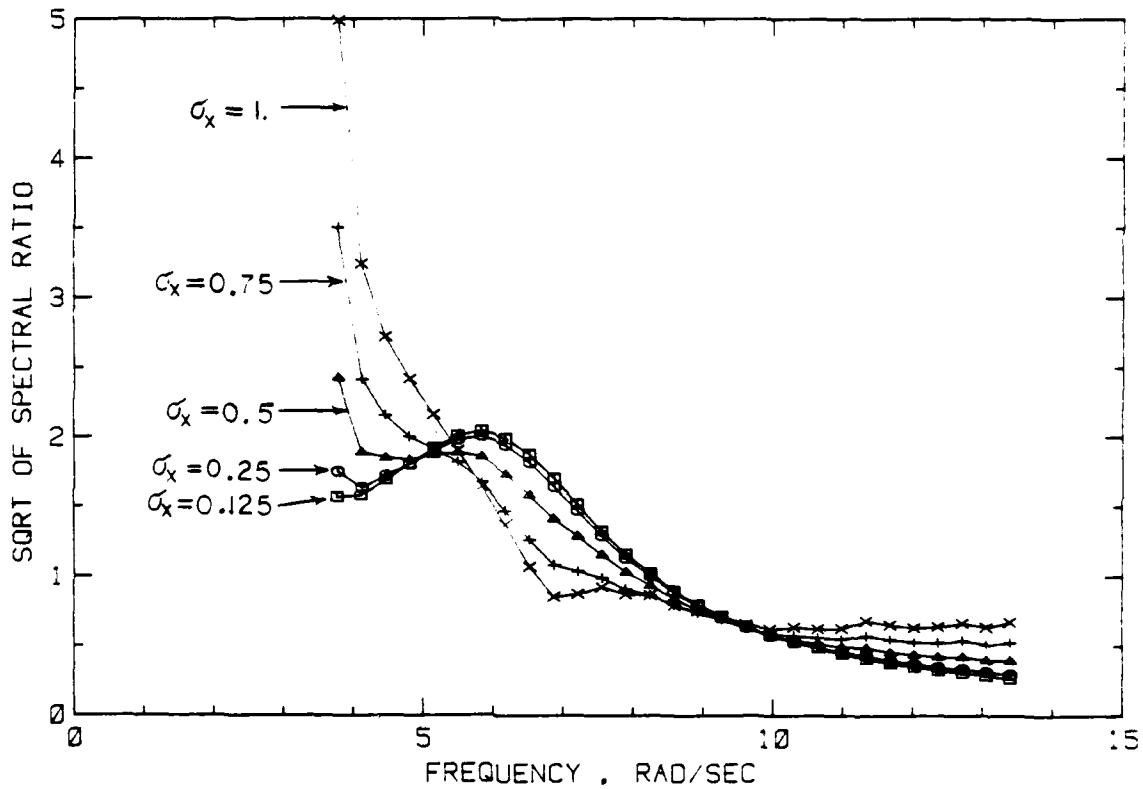


FIGURE 17 EQUIVALENT LINEAR RESPONSE DERIVED FROM THE SPECTRAL ANALYSES OF EXCITATION AND RESPONSE

function, until finally there is no resemblance. The changes at the ends of the frequency range shown in Figure 17 are clearly due to quadratic response ( $U_2(\omega)$ ). The changes in midrange resemble those noted in Figure 1 for the influence of the cubic nonlinearity on the response to single tone excitation.

As in the discussion of the qualitative features of the response to random excitation of the simulated cubic system, the response spectra for excitations of  $\sigma_x = 0.75$  and 1.0 deviate from linear expectations by amounts which might be considered extreme by comparison with towing tank experiments. However, the magnitudes of nonlinear distortion for values of  $\sigma_x$  up to 0.5 is in line with what has been occasionally experienced. It thus appeared that the simulation was reasonably realistic.

## IDENTIFICATION THEORY FOR THE RANDOM CASE

It is clear from the preceding section that the ordinary scalar spectrum analyses of random excitation and response provides no means of identification of frequency response functions. What scalar spectrum analysis can provide is an indication if nonlinearities are serious or not in the case where data is available for a range of excitation levels. The problem of interest here is whether or not the three postulated frequency response functions arising from the basic model, Equation 5, may be identified from samples of random excitation and response.

To begin, the assumptions about the excitation previously noted should be re-stated. It is accepted that the excitation is strictly stationary with bounded moments of all orders. For present purposes the conventional further assumptions about a wave process will also be made; that is, the excitation will be assumed to be an ergodic Gaussian zero mean process. The autocorrelation function of the excitation will be denoted:

$$R_{xx}(\tau) = \overline{X(t) X(t-\tau)} \quad (35)$$

where the overbar denotes the temporal mean, and by assumption the statistical expectation. The two sided spectrum of the excitation will be defined as:

$$S_{xx}(\omega) = \int R_{xx}(\tau) \text{Exp}(-i\omega\tau) d\tau \quad (36)$$

where, as before, the integral of the spectrum is  $2\pi$  times the variance,  $R_{xx}(0)$ . Given the Gaussian zero mean assumption, all the expectations of higher order products are either zero or are defined in terms of  $R_{xx}(\tau)$ , Equation 35. Appendix A summarizes the expectations of up to sixth order products from Reference 25\*.

The general analytical approach in the present section of the report will be to hypothesize certain statistical time domain moments

---

\*25. Laning, J.H., and Battin, R.H., "Random Processes in Automatic Control", McGraw-Hill, 1956.

of response and excitation, and then invert the resulting expressions to the frequency domain. In this operation frequent use is made of an n-dimensional form of Parseval's formula as given in Reference 4. For convenience this formula is given in Appendix B.

The first response moment of interest of the cubic model, Equation 5, is just the temporal mean. Taking the temporal mean of Equation 5:

$$\begin{aligned}
 \overline{Y(t)} &= \int g_1(t_1) \overline{X(t - t_1)} dt_1 \\
 &+ \iint g_2(t_1, t_2) R_{XX}(t_1 - t_2) dt_1 dt_2 \\
 &+ \iiint g_3(t_1, t_2, t_3) \overline{X(t - t_1) X(t - t_2) X(t - t_3)} dt_1 dt_2 dt_3 \\
 &= \iint g_2(t_1, t_2) R_{XX}(t_1 - t_2) dt_1 dt_2 \\
 &= \frac{1}{2\pi} \int G_2(\omega, -\omega) S_{XX}(\omega) d\omega \quad (37)
 \end{aligned}$$

where the derivation follows that of References 8, 14, and 15. It may be noted that this result for the cubic model is exactly the same as that for the quadratic model, Reference 15, because the odd order temporal means are zero for the assumed Gaussian excitation process.

Because cross-spectral analysis is a very common technique in the analysis of linear random processes, it is of interest to look at the cross spectrum between excitation and the nonlinear response model. The two sided cross spectrum may be defined as:

$$S_{YX}(\omega) = \int R_{YX}(\tau) \text{Exp}(-i\omega\tau) d\tau \quad (38)$$

where the cross correlation function between  $X(t)$  and  $Y(t)$  is defined:

$$R_{YX}(\tau) = \overline{[Y(t) - \overline{Y(t)}] X(t + \tau)} \quad (39)$$

Substituting the model for  $Y(t)$ , Equation 5, into Equation 39, eliminating temporal means of odd products of Gaussian variables, applying

the expression for fourth order expected values, Appendix A, and taking advantage of the symmetry of the impulse functions results in a further expression for the cross correlation:

$$R_{yx}(\tau) = \int g_1(t_1) R_{xx}(\tau + t_1) dt_1 + 3 \iiint g_3(t_1, t_2, t_3) R_{xx}(t_1 - t_2) R_{xx}(\tau + t_3) dt_1 dt_2 dt_3 \quad (40)$$

Now substituting Equation 40 into Equation 38, and applying the n-dimensional Parseval formula, Appendix B, results in the following expression for the cross spectrum:

$$S_{yx}(\omega) = S_{xx}(\omega) \left[ G_1(\omega) + \frac{3}{\pi} \int_0^{\infty} G_3(\omega, v, -v) S_{xx}(v) dv \right] \quad (41)$$

Just as in the linear+quadratic case, Reference 14, the quadratic contributions drop out. The result in Equation 41 is similar to the first (and possibly most important) component of the scalar spectrum,  $S_1(\omega)$ , Equation 28.

The ordinary coherency between excitation and response is defined as:

$$\gamma_{yx}^2(\omega) = |S_{yx}(\omega)|^2 / \{S_{yy}(\omega) S_{xx}(\omega)\} \quad (42)$$

Now substituting Equation 27 and Equation 41 into Equation 42, and noting Equation 28, the theoretical expression for the coherence becomes:

$$\gamma_{yx}^2(\omega) = \frac{1}{1 + \frac{S_2(\omega) + S_3(\omega)}{S_1(\omega)}} \quad (43)$$

where  $S_1(\omega)$ ,  $S_2(\omega)$  and  $S_3(\omega)$  are defined in Equation 28 through 30. Clearly, the theoretical coherence cannot be exactly unity as in the fully linear case. However it will approach unity as the excitation level decreases. In the discussion of the spectra of the simulated process of the last section it was noted that at intermediate levels of

excitation  $S_2(\omega)$  and  $S_3(\omega)$  may be negligible in comparison with  $S_1(\omega)$  while at the same time  $S_1(\omega)$  does not correspond to the linear (negligible excitation) case. Relative to the interpretation of actual data, this suggests that there may be situations where the sample coherency may appear reasonable at many excitation levels (suggesting a linear response), yet the apparent frequency response,  $S_{yx}(\omega)/S_{xx}(\omega)$ , varies with excitation level (suggesting a nonlinear response). Something like this can be inferred from some of the results in Reference 26\*, though effects of short samples therein makes the conclusion tenuous.

It is clear from the theoretical form of the cross spectrum, Equation 41, that if the system of interest has a significant cubic response, the identification of the linear frequency response function,  $G_1(\omega)$ , by conventional cross spectrum analyses would require a very large number of independent experiments at various excitation levels. For example, if it was thought reasonable to discretize the integral in Equation 41, and if  $S_{xx}(\omega)$  could be represented by 20 discrete values, Equation 41 might be written as an algebraic equation in 21 complex unknowns for each value of  $\omega$ , and reasonable results might perhaps be obtained with data from  $40^+$  independent experiments. Clearly, Equation 41 is unsatisfactory as a basis for identification of the linear function unless an approach for  $G_3(\omega, \nu, -\nu)$  can be found.

In previous work with the linear+quadratic model an identification technique called cross-bi-spectral analysis was used to identify quadratic frequency response functions. The cross-bi-spectrum may be defined as follows:

$$S_{yxx}(\omega_1, \omega_2) = \iint R_{yxx}(t_4, t_5) \text{Exp}(-i\omega_1 t_4 - i\omega_2 t_5) dt_4 dt_5 \quad (44)$$

where the third order correlation function  $R_{yxx}(t_4, t_5)$  is written:

$$R_{yxx}(t_4, t_5) = \frac{\{Y(t) - \bar{Y}(t)\} X(t - t_4) X(t - t_5)}{\quad} \quad (45)$$

\*26. Dalzell, J.F., "Some Further Experiments on the Application of Linear Superposition Techniques to the Responses of a Destroyer Model in Extreme Irregular Long-Crested Head Seas," Davidson Laboratory Report 918, September 1962.

It should be noted that this definition corresponds to that of Reference 10, and that the definitions given in References 14 and 15 are for a "modified" cross-bi-spectrum which is defined in terms of sum and difference frequencies ( $\omega_1 + \omega_2$ ) and ( $\omega_1 - \omega_2$ ). (The "modified" cross-bi-spectrum has some computational advantage.)

When the basic model for the response,  $Y(t)$ , is substituted into Equation 45 there results:

$$\begin{aligned}
 R_{yxx}(t_4, t_5) = & \int g_1(t_1) \overline{X(t-t_1) X(t-t_4) X(t-t_5)} dt_1 \\
 & + \iint g_2(t_1, t_2) \overline{X(t-t_1) X(t-t_2) X(t-t_4) X(t-t_5)} dt_1 dt_2 \\
 & + \iiint g_3(t_1, t_2, t_3) \cdot \\
 & \left. \overline{X(t-t_1) X(t-t_2) X(t-t_3) X(t-t_4) X(t-t_5)} \right) dt_1 dt_2 dt_3 \\
 & - \overline{Y(t)} R_{xx}(t_4 - t_5) \tag{46}
 \end{aligned}$$

Under the assumptions given for the excitation the expectations of products of an odd number of excitation variables are zero, Appendix A. Thus the terms involving linear and cubic impulse response functions drop out, and the quadratic impulse response is isolated.

Applying the expressions for the fourth order expectation, Appendix A, and noting Equation 37, Equation 46 becomes:

$$R_{yxx}(t_4, t_5) = 2 \iint g_2(t_1, t_2) R_{xx}(t_1 - t_4) R_{xx}(t_2 - t_5) dt_1 dt_2 \tag{47}$$

Finally, applying the Parseval formula, Appendix B to Equation 47, and noting the definition of the cross-bi-spectrum, Equation 44:

$$S_{yxx}(\omega_1, \omega_2) = 2G_2(\omega_1, \omega_2) S_{xx}(\omega_1) S_{xx}(\omega_2) \tag{48}$$

From this result an estimator for the quadratic frequency response function becomes:

$$\tilde{G}_2(\omega_1, \omega_2) = \frac{S_{yxx}(\omega_1, \omega_2)}{2 S_{xx}(\omega_1) S_{xx}(\omega_2)} \tag{49}$$

This estimator is analogous to that of References 14 and 15. The important point relative to the present investigation is that, with the Gaussian assumption on the excitation, cross-bi-spectral analysis isolates the quadratic frequency response whether or not a cubic non-linearity is present.

Now if a third order correlation function  $R_{x^2_{xx}}(t_1, t_2)$  is formed by replacing the response in Equation 45 by the square of the excitation:

$$R_{x^2_{xx}}(t_1, t_2) = \overline{\{X^2(t) - \bar{X}^2(t)\} X(t - t_1) X(t - t_2)} \quad (50)$$

and the double Fourier transform is taken as in Equation 44, there results the cross-bi-spectrum between excitation and excitation squared:

$$\begin{aligned} S_{x^2_{xx}}(\omega_1, \omega_2) &= \iint R_{x^2_{xx}}(t_1, t_2) \text{Exp}(-i\omega_1 t_1 - i\omega_2 t_2) dt_1 dt_2 \\ &= 2 S_{xx}(\omega_1) S_{xx}(\omega_2) \end{aligned} \quad (51)$$

where the derivation follows that in Reference 15. Accordingly an alternate identification technique may be written:

$$\tilde{G}_2(\omega_1, \omega_2) = \frac{S_{yxx}(\omega_1, \omega_2)}{S_{x^2_{xx}}(\omega_1, \omega_2)} \quad (52)$$

Thus the quadratic frequency response function may in principle be estimated by the ratio of cross-bi-spectra, and this approach was noted in Reference 15 as resulting in improved estimates.

The theoretical approaches to the reduction of random data which have just been discussed have been available for some time. The next logical step in the present work was to look for an approach with which there might be hope of isolating the cubic frequency response function, or at least parts of it. It seemed reasonable to proceed by analogy with cross and cross-bi-spectral theory and postulate a fourth order correlation function of the form:

$$\overline{Y(t) X(t - t_4) X(t - t_5) X(t - t_6)}$$

It should be clear from a comparison of this form with Equations 45 and 46 that the quadratic contributions to such a correlation will drop out and the linear and cubic parts will stay. Substituting the model, Equation 5, into the postulated form, expanding the expected values in accordance with Appendix A, and taking advantage of symmetry results in the following:

$$\begin{aligned}
 \overline{Y(t) X(t - t_4) X(t - t_5) X(t - t_6)} = & \\
 = \int g_1(t_1) & \left[ R_{xx}(t_1 - t_4) R_{xx}(t_5 - t_6) \right. \\
 & + R_{xx}(t_1 - t_5) R_{xx}(t_4 - t_6) \\
 & \left. + R_{xx}(t_1 - t_6) R_{xx}(t_4 - t_5) \right] dt_1 \\
 + \iiint g_3(t_1, t_2, t_3) & \left[ R_{xx}(t_1 - t_2) R_{xx}(t_3 - t_4) R_{xx}(t_5 - t_6) \right. \\
 & + R_{xx}(t_1 - t_3) R_{xx}(t_2 - t_4) R_{xx}(t_5 - t_6) \\
 & + R_{xx}(t_2 - t_3) R_{xx}(t_1 - t_4) R_{xx}(t_5 - t_6) \\
 & + R_{xx}(t_1 - t_2) R_{xx}(t_3 - t_5) R_{xx}(t_4 - t_6) \\
 & + R_{xx}(t_1 - t_3) R_{xx}(t_2 - t_5) R_{xx}(t_4 - t_6) \\
 & + R_{xx}(t_2 - t_3) R_{xx}(t_1 - t_5) R_{xx}(t_4 - t_6) \\
 & + R_{xx}(t_1 - t_2) R_{xx}(t_3 - t_6) R_{xx}(t_4 - t_5) \\
 & + R_{xx}(t_1 - t_3) R_{xx}(t_2 - t_6) R_{xx}(t_4 - t_5) \\
 & \left. + R_{xx}(t_2 - t_3) R_{xx}(t_1 - t_6) R_{xx}(t_4 - t_5) \right] dt_1 dt_2 dt_3 \\
 + 6 \iiint g_3(t_1, t_2, t_3) & R_{xx}(t_1 - t_4) R_{xx}(t_2 - t_5) R_{xx}(t_3 - t_6) dt_1 dt_2 dt_3 \\
 & (53)
 \end{aligned}$$

The problem with the expression, Equation 53, is that it contains a linear contribution just as in the cross spectrum, Equation 40. An

apparently workable approach to this problem is provided by Reference 4 in a treatment of partially orthonormal functional expansions. By this means a fourth order correlation function was postulated as follows:

$$R_{YXXX}(t_4, t_5, t_6) = E \left\{ \left[ \overline{Y(t) - \overline{Y(t)}} \right] \left[ \overline{X(t - t_4) X(t - t_5) X(t - t_6)} \right. \right. \\ \left. \left. - X(t - t_4) \overline{X(t - t_5) X(t - t_6)} \right. \right. \\ \left. \left. - X(t - t_5) \overline{X(t - t_4) X(t - t_6)} \right. \right. \\ \left. \left. - X(t - t_6) \overline{X(t - t_4) X(t - t_5)} \right] \right\} \quad (54)$$

where the expectation operator implies that temporal means are to be taken. Now expanding Equation 54 and eliminating terms involving the expectations:

$$\overline{X(t - t_j)} \quad \text{and} \quad \overline{X(t - t_4) X(t - t_5) X(t - t_6)}$$

according to the Gaussian zero mean assumption:

$$R_{YXXX}(t_4, t_5, t_6) = \overline{Y(t) X(t - t_4) X(t - t_5) X(t - t_6)} \\ - R_{XX}(t_4 - t_6) \overline{Y(t) X(t - t_5)} \\ - R_{XX}(t_5 - t_6) \overline{Y(t) X(t - t_4)} \\ - R_{XX}(t_4 - t_5) \overline{Y(t) X(t - t_6)} \quad (55)$$

Now considering terms of the form of the last three terms of Equation 55:

$$R_{XX}(t_j - t_k) \overline{Y(t) X(t - t_l)} \\ = \int g_1(t_1) R_{XX}(t_1 - t_l) R_{XX}(t_j - t_k) dt_1 \\ + \iiint g_3(t_1, t_2, t_3) \left[ R_{XX}(t_1 - t_2) R_{XX}(t_3 - t_l) R_{XX}(t_j - t_k) \right. \\ \left. + R_{XX}(t_1 - t_3) R_{XX}(t_2 - t_l) R_{XX}(t_j - t_k) \right. \\ \left. + R_{XX}(t_2 - t_3) R_{XX}(t_1 - t_l) R_{XX}(t_j - t_k) \right] dt_1 dt_2 dt_3 \quad (56)$$

where as before, the model, Equation 5, has been substituted and the expected values expanded. Comparing Equations 55 and 56 with Equation 53 it may be seen that the effect of the last three terms of Equation 55 is to cancel out the first two integrals in the expression for  $\overline{Y(t) X(t - t_4) X(t - t_5) X(t - t_6)}$ , Equation 53. Thus the postulated fourth order correlation function comes down to:

$$R_{yxxx}(t_4, t_5, t_6) = 6 \iiint g_3(t_1, t_2, t_3) \cdot R_{xx}(t_1 - t_4) R_{xx}(t_2 - t_5) R_{xx}(t_3 - t_6) dt_1 dt_2 dt_3 \quad (57)$$

Now applying the Parseval formula, Appendix B, to Equation 57:

$$R_{yxxx}(t_4, t_5, t_6) = \frac{6}{(2\pi)^3} \iiint G_3(\omega_1, \omega_2, \omega_3) S_{xx}(\omega_1) S_{xx}(\omega_2) S_{xx}(\omega_3) \cdot \text{Exp}\{i(\omega_1 t_4 + \omega_2 t_5 + \omega_3 t_6)\} d\omega_1 d\omega_2 d\omega_3 \quad (58)$$

Equation 58 is in the form of a triple Fourier transform of a function of frequency. Inverting, the cross-tri-spectrum will be defined as:

$$S_{yxxx}(\omega_1, \omega_2, \omega_3) = 6 G_3(\omega_1, \omega_2, \omega_3) S_{xx}(\omega_1) S_{xx}(\omega_2) S_{xx}(\omega_3) \\ = \iiint R_{yxxx}(t_4, t_5, t_6) \text{Exp}(i\omega_1 t_4 - i\omega_2 t_5 - i\omega_3 t_6) dt_4 dt_5 dt_6 \quad (59)$$

Thus, if the cross-tri-spectrum can be evaluated, an estimate for the cubic frequency response function becomes:

$$\tilde{G}_3(\omega_1, \omega_2, \omega_3) = \frac{S_{yxxx}(\omega_1, \omega_2, \omega_3)}{6 S_{xx}(\omega_1) S_{xx}(\omega_2) S_{xx}(\omega_3)} \quad (60)$$

This estimator is clearly analogous to that for the quadratic response, Equation 49. As in the case of the cross-bi-spectrum, the cross-tri-spectrum cannot be appreciable unless the excitation spectrum is appreciable at all three frequencies.

By analogy with the development of Equations 50 through 52, a special fourth order correlation function may be formed by replacing the response,  $Y(t)$ , in Equation 54 with the cube of excitation:

$$R_{x^3xxx}(t_1, t_2, t_3) = E \left[ \left[ X^3(t) - \overline{X^3(t)} \right] \left[ X(t-t_1) X(t-t_2) X(t-t_3) - X(t-t_1) \overline{X(t-t_2) X(t-t_3)} - X(t-t_2) \overline{X(t-t_1) X(t-t_3)} - X(t-t_3) \overline{X(t-t_2) X(t-t_1)} \right] \right] \quad (61)$$

Taking the triple Fourier transform and reducing:

$$\begin{aligned} S_{x^3xxx}(\omega_1, \omega_2, \omega_3) &= \iiint R_{x^3xxx}(t_1, t_2, t_3) \cdot \\ &\quad \text{Exp}(-i\omega_1 t_1 - i\omega_2 t_2 - i\omega_3 t_3) dt_1 dt_2 dt_3 \\ &= 6 S_{xx}(\omega_1) S_{xx}(\omega_2) S_{xx}(\omega_3) \end{aligned} \quad (62)$$

Accordingly, an alternate identification form for the cubic frequency response function becomes:

$$\tilde{G}_3(\omega_1, \omega_2, \omega_3) = \frac{S_{yxxx}(\omega_1, \omega_2, \omega_3)}{S_{x^3xxx}(\omega_1, \omega_2, \omega_3)} \quad (63)$$

Thus, as in the quadratic case, the cubic frequency response function may in principle be estimated by the ratio of cross-tri-spectra.

It may be noted that there is a very significant difference in form between the fourth order correlation,  $R_{yxxx}(t_4, t_5, t_6)$ , Equation 54, and the second and third order correlations,  $R_{yx}(\tau)$  and  $R_{yxx}(t_4, t_5)$ , Equations 39 and 45. This is the presence of the terms of the form:

$$R_{xx}(t_j - t_k) \overline{Y(t) X(t - t_\ell)}$$

which is expanded in Equation 56. When the triple Fourier transform of

Equation 56 is taken and a reduction by means of the Parseval formula, Appendix B is carried out the results are of the form:

$$\Gamma_{jk} S_{xx}(\omega_j) S_{xx}(\omega_k) \cdot \left[ G_1(\omega_j) + \frac{3}{2\pi} \int G_3(v, -v, \omega_j) S_{xx}(v) dv \right]$$

where  $\Gamma_{jk} = 1$  if  $\omega_j = -\omega_k$   
 $= 0$  otherwise.

Thus the triple transform of the fourth order correlation analogous to the second and third order correlations, Equation 53, contains delta functions and the subtractive terms in the correlation function expressed in Equation 54 are for the purpose of canceling them out. With respect to the tri-frequency space in which the cross-tri-spectrum is defined the delta functions lie in the planes:

$$\begin{aligned} \omega_1 &= -\omega_2 \\ \omega_1 &= -\omega_3 \\ \omega_2 &= -\omega_3 \end{aligned}$$

and if they are not removed somehow cross-tri-spectral estimates of the form  $S_{yxxx}(v, -v, \omega)$  will be distorted, perhaps very badly.

If the qualitative results from the simulation are applicable in general, the surface defined by tri frequencies of the form  $(v, -v, \omega)$  would involve the portion of the cubic frequency response function of most practical importance. Accordingly this portion of the function must be dealt with, whatever unpleasant turns the delta functions make in the numerical analysis.

The foregoing was about as far as identification theory could be pushed in the present work. Several similar avenues of approach (other forms of correlation functions) were attempted, but with no better success, and in general the same form of result. Most importantly, no relatively clean approach to the identification of the linear response function could be developed. The conclusion with respect to making further progress was to postulate the following identification strategy:

- a) Cross-bi-spectral analysis for the quadratic frequency response function, Equation 49 or 52.
- b) Cross-tri-spectral analysis for the cubic frequency response function, especially the values of  $\tilde{G}_3(v, -v, \omega)$ , Equation 60 or 63.
- c) Carry out a standard cross-spectral analysis and make an estimate of  $G_1(\omega)$  with a transposed form of Equation 41:

$$\tilde{G}_1(\omega) = \frac{S_{yx}(\omega) - \frac{3}{\pi} \int_0^{\infty} \tilde{G}_3(\omega, v, -v) S_{xx}(v) dv}{S_{xx}(\omega)} \quad (64)$$

where the estimates of  $\tilde{G}_3(v, -v, \omega)$  from step b are used to "correct" the cross spectrum.

## CROSS-TRI-SPECTRAL ESTIMATION

With the tentative strategy just noted the only non-trivial new computational problem was the cross-tri-spectrum, Equation 59. The approach followed in the development of procedures for the cross-bi-spectrum in References 14 and 15 followed the approach in Reference 12 which was in turn analagous to the Tukey autocorrelation approach to scalar and cross spectral estimation. The Fast Fourier Transform approach of Reference 13 was by-passed then because it was initially desired only to probe specialized parts of the cross-bi-spectrum, and because the writer better understood the former approach. In retrospect, the decision was probably unwise. In the event, it was desirable to compute the entire cross-bi-spectrum, an operation which was computationally inefficient with the methods developed in Reference 14.

However, some thought was given to an adaptation of the autocorrelation approach to the cross-tri-spectrum. The attraction of this approach for the cross-bi-spectrum had been that a simple transformation of frequency variables realigned the computation along and normal to the lines of symmetry of the cross-bi-spectrum. The new frequency co-ordinate system was orthogonal and the result was a third moment function which was easier to organize than that indicated in Equation 45. Accordingly, some effort was given over to a search for a frequency transformation for tri-frequency space such that the new frequency axes would lie in the planes of symmetry of the cross-tri-spectrum. A number of simple transformations were found, but none were orthogonal, and thus no approach was found to the minimization of the computational problems that Equations 54 and 59 imply.

There was thus reason to consider the methods of Reference 27<sup>\*\*</sup> more closely than had been the case previously. This reference was the only one known which considers spectra of higher order than the bi-spectrum, and in which some tri-spectral estimates were presented.

---

<sup>\*\*</sup>27. Brillinger, D.R. and Rosenblatt, M., Two Papers: "Asympotic Theory of Estimates of kth Order Spectra," and "Computation and Interpretation of kth Order Spectra," Proceedings of an Advanced Seminar on Spectral Analysis of Time Series, Edited by B. Harris, October 1966, John Wiley & Sons, New York.

The description in Reference 28<sup>\*</sup> of a more recent application of the methods to bi-spectral computations illuminated some parts of the procedure which seemed unclear in the original reference. No explicit mention of cross-bi or cross-tri-spectra is made in Reference 27. However the basic assumptions involve a real, stationary vector process  $(X_a(t); a = 1, \dots)$  in which all moments are assumed to exist. In terms of the present notation it is thus possible to put:

$$X_1(t) = Y(t)$$

$$X_2(t) = X(t)$$

so that the methods of Reference 27 appeared to apply to the present problem, with a minor redefinition of terminology.

The basic idea of the higher order spectral estimates of Reference 27 is that a  $k^{\text{th}}$  order spectral estimate is a weighted smoothing of a  $k^{\text{th}}$  order periodgram over a  $(k-1)^{\text{th}}$  order frequency space. In terms of Reference 27:

Cross and scalar spectra are second order ( $k=2$ )

Cross-bi-spectra are third order ( $k=3$ )

Cross-tri-spectra are fourth order ( $k=4$ )

The adaptation made of the methods of Reference 27 for present purposes will be outlined in the order in which the computations would be carried out. First it is assumed that digital samples  $(N-1)\Delta t$  seconds in length are available for the excitation,  $X(t)$ , and the nonlinear response,  $Y(t)$ . It is common in experimental work that the actual level of zero excitation or response is not known to high precision. Thus correction of time series to zero sample mean (and removal of evident trends) is a normal first step in spectrum analyses and was assumed also to be important in higher order analyses. The response,  $Y(t)$ , in all the correlations of the last section appears in the form of an implied correction to zero sample mean. Accordingly, the first step in the process is to remove trends and correct the response to

\*28. Lii, K.S., Rosenblatt, M., and Van Atta, C., "Bi-spectral Measurements in Turbulence," Journal of Fluid Mechanics, Vol. 77, Part 1, 1976.

zero sample mean so that the resulting time series may be defined:

$$Y(t) - \overline{Y(t)} \rightarrow Y'(n), n = 0 \dots N - 1$$

Similarly, correcting the excitation to zero sample mean defines the series:

$$X(t) \rightarrow X'(n), n = 0 \dots N - 1$$

There are two other simple functions of excitation noted in the last section, the squared excitation less its expectation and the cubed excitation less its expectation. It appeared reasonable in these cases to square and cube  $X'(n)$  for  $n = 0 \dots (N - 1)$  and to correct the resulting series to zero sample mean so that the time series corresponding to the squared and cubed functions of excitation will be defined:

$$X^2(t) - \overline{X^2(t)} \rightarrow W'(n), n = 0 \dots N - 1$$

$$X^3(t) - \overline{X^3(t)} \rightarrow Z'(n), n = 0 \dots N - 1$$

It may be noted that the four operations just described are exactly those which would first be carried out in an implementation of an autocorrelation approach to cross, cross-bi, and cross-tri-spectral analyses.

One of the subsequent steps in the procedure is to perform the direct Fast Fourier Transform on each of the time series defined above. "Tapering" the data to improve the shape of the FFT spectral window and to prevent "leakage" from high to low frequencies and vice versa is fairly conventional in scalar spectrum analysis using the FFT, is recommended in Reference 27, and was assumed to be worthwhile in the present instance. Thus the next step in the procedure was to taper each of the four time series just described with the Tukey 10% cosine taper as described in Reference 24. The effect, on average, of applying this taper function is a "loss" of 12 1/2% of variance. To make an approximate correction for this effect the tapered time series were finally multiplied by 1.069. At this stage in the procedure the four time series may be respresented as follows:

$$\begin{aligned} Y(t) - \overline{Y(t)} &\rightarrow Y(n), n = 0, 1 \dots N - 1 \\ X(t) &\rightarrow X(n), n = 0, 1 \dots N - 1 \\ X^{\cdot}(t) - \overline{X^{\cdot}(t)} &\rightarrow W(n), n = 0, 1 \dots N - 1 \\ X^{\ddot{}}(t) - \overline{X^{\ddot{}}(t)} &\rightarrow Z(n), n = 0, 1 \dots N - 1 \end{aligned}$$

where each time series is corrected to zero sample mean, tapered, and compensated for loss of variance.

The next step in the procedure is to perform the direct Fast Fourier Transform on each series. The FFT algorithm used in the present instance performs the following operations:

$$\overline{Y}(k) = \frac{1}{N} \sum_{n=0}^{N-1} Y(n) \text{Exp}(-i2\pi nk/N) \quad (65)$$

$$\overline{X}(k) = \frac{1}{N} \sum_{n=0}^{N-1} X(n) \text{Exp}(-i2\pi nk/N) \quad (66)$$

$$\overline{W}(k) = \frac{1}{N} \sum_{n=0}^{N-1} W(n) \text{Exp}(-i2\pi nk/N) \quad (67)$$

$$\overline{Z}(k) = \frac{1}{N} \sum_{n=0}^{N-1} Z(n) \text{Exp}(-i2\pi nk/N) \quad (67)$$

where the transforms are defined for:

$$-(\frac{N}{2} - 1) < k < N/2$$

circular frequency is related to the index  $k$  by:

$$\omega = \frac{2\pi k}{N\Delta t}$$

and the transform for negative  $k$  is the complex conjugate of that for positive values:

$$\begin{aligned} \overline{Y}(-k) &= \overline{Y}^*(k) \\ \overline{X}(-k) &= \overline{X}^*(k) \\ \overline{W}(-k) &= \overline{W}^*(k) \\ \overline{Z}(-k) &= \overline{Z}^*(k) \end{aligned}$$

Apart from the sequence of the compensation for variance loss, the operation thus far is exactly that which would be carried out in deriving scalar spectra of  $X(t)$ ,  $Y(t)$ ,  $\dot{X}(t)$  and  $\dot{X}^2(t)$  by the FFT method.

It is necessary next to define the periodograms required by the methods of Reference 27 in present notation. Starting with the second order case, an obvious estimate of the cross correlation function, Equation 39, for an  $N$  point sample may be written:

$$R_{yx}(p) = \frac{1}{N} \sum_{n=D_2} Y(n) X(n+p) \quad (69)$$

where the domain of the summation is:

$$D_2 \rightarrow \left( \begin{array}{l} 0 < n < N - 1 \\ 0 < n - p < N - 1 \end{array} \right)$$

The second order periodogram is the discrete Fourier transform of Equation 69:

$$\begin{aligned} P_{yx}(j) &= \Delta t \sum_{p=-N+1}^{N-1} R_{yx}(p) \text{Exp}(-i2\pi pj/N) \\ &= N\Delta t \sum_{n=D_2} \sum_{p=-N+1}^{N+1} \left[ \frac{1}{N} Y(n) \text{Exp}(+i2\pi nj/N) \right] \\ &\quad \left[ \frac{1}{N} X(n+p) \text{Exp}\{-i2\pi j(n+p)/N\} \right] \\ &= N\Delta t \bar{Y}(-j) \bar{X}(j) \end{aligned} \quad (70)$$

The result, Equation 70, is, apart from notation, the "raw" cross spectrum of Reference 24.

The third order periodogram may be approached similarly by defining an estimate of the third order correlation function of Equation 45 as:

$$R_{yxx}(p,q) = \frac{1}{N} \sum_{n=D_3} Y(n) X(n-p) X(n-q) \quad (71)$$

where the domain  $D_3$  is defined:

$$\left( \begin{array}{l} 0 < n < N - 1 \\ 0 < n - p < N - 1 \\ 0 < n - q < N - 1 \end{array} \right)$$

The corresponding third order periodogram is the double Fourier transform of Equation 71:

$$\begin{aligned} P_{yxx}(j,k) &= (\Delta t)^2 \sum_{p=-N+1}^{N-1} \sum_{q=-N+1}^{N-1} R_{yxx}(p,q) \text{Exp}(-i2\pi pj/N - i2\pi qk/N) \\ &= (N\Delta t)^2 \bar{Y}(j+k) \bar{X}(-j) \bar{X}(-k) \end{aligned} \quad (72)$$

where the derivation is similar to that of the second order case. The third order periodogram corresponding to the squared excitation correlation, Equation 50, may be written by analogy:

$$P_{wxx}(j,k) = (N\Delta t)^2 \bar{W}(j+k) \bar{X}(-j) \bar{X}(-k) \quad (73)$$

Next, the fourth order periodogram is approached by defining a fourth order correlation estimate analogous to the first term of Equation 54:

$$R_{yxxx}(p,q,r) = \frac{1}{N} \sum_{n=D_4} Y(n) X(n-p) X(n-q) X(n-r) \quad (74)$$

where the domain  $D_4$  is defined:

$$D_4 \rightarrow \left( \begin{array}{l} 0 < n < N - 1 \\ 0 < n - p < N - 1 \\ 0 < n - q < N - 1 \\ 0 < n - r < N - 1 \end{array} \right)$$

The corresponding fourth order periodogram is the triple Fourier transform of Equation 74:

$$P_{yxxx}(j,k,\ell) = (\Delta t)^3 \prod_{p=-N+1}^{N+1} \prod_{q=-N+1}^{N+1} \prod_{r=-N+1}^{N+1} R_{yxxx}(p,q,r) \cdot \text{Exp}[-i2\pi pj/N - i2\pi qk/N - i2\pi r\ell/N]$$

$$= (N\Delta t)^3 \bar{Y}(j+k+\ell) \bar{X}(-j) \bar{X}(-k) \bar{X}(-\ell) \quad (75)$$

and the periodogram corresponding to the first term of the cubed excitation correlation, Equation 61, may be written:

$$P_{zxxx}(j,k,\ell) = (N\Delta t)^3 \bar{Z}(j+k+\ell) \bar{X}(-j) \bar{X}(-k) \bar{X}(-\ell) \quad (76)$$

It may be noted that the frequency indices in the final expressions for the periodograms (Equations 70, 72, 73, 75, 76) sum to zero. That is, in Equation 75 for example,

$$(j+k+\ell) + (-j) + (-k) + (-\ell) = 0$$

This is a property required by the definition of the  $k^{\text{th}}$  order periodogram of Reference 27.

It was shown in Reference 27, for the strictly stationary processes presently assumed, that the expected value (or temporal mean) of the  $k^{\text{th}}$  order periodogram equals the  $k^{\text{th}}$  order spectrum, but with an important provision. The provision has to do with the presence of delta functions discussed in the last section. Essentially, as sample length approaches infinity, the periodogram approaches the spectrum except in those particular regions of frequency space where delta functions are expected. However it was suggested that reasonable estimates may be made by a multi-dimensional frequency smoothing operation on the periodograms if the problem regions are avoided.

As in lower order spectrum analyses from finite samples it is possible only to estimate higher order spectral averages of the form:

$$\hat{S}(\omega_1, \omega_2, \dots) = \iiint \dots \int \tilde{W}(\omega_1 - \Omega_1, \omega_2 - \Omega_2, \dots) S(\Omega_1, \Omega_2, \dots) d\Omega_1 d\Omega_2 \dots$$

where the weighting function  $\tilde{W}(\alpha_1, \alpha_2, \dots)$  peaks at frequency vector  $(0, 0, \dots)$ , falls off to zero in every direction, and has the property:

$$1 = \iiint \dots \int \tilde{W}(\alpha_1, \alpha_2, \dots) d\alpha_1 d\alpha_2 \dots$$

No specific guidance is given in Reference 27 as to what the discrete analog of the weighting function ought to be for the higher order case. By analogy with conventional frequency weighting (smoothing) techniques for scalar and cross spectra, Reference 24, a reasonable solution was anticipated if  $\tilde{W}(\alpha_1, \alpha_2, \dots)$  was zero everywhere except within some region:

$$\begin{aligned} -\epsilon < \alpha_1 < \epsilon \\ -\epsilon < \alpha_2 < \epsilon \\ \cdot \\ \cdot \end{aligned}$$

and a constant otherwise (essentially a multiple dimension block average). This was found to be the case in the analysis of Reference 28, and thus encouraged, the block average technique was adopted for the present.

With this decision, the estimating forms for the various cross spectra of present interest could be translated from the basic development of Reference 27. The cross-spectral estimate corresponding to Equation 38 becomes:

$$\hat{S}_{yx}(j) = \frac{N\Delta t}{H} \sum_{h=j-m}^{j+m} \bar{Y}(-h) \bar{X}(h) \phi_1(h) \quad (77)$$

where, as before, circular frequency is defined as:

$$\omega = \frac{2\pi j}{N\Delta t}$$

"m" is the block size parameter corresponding to  $\epsilon$ , "H" equals the number of terms summed, and

$$\phi_1(h) = 0 \quad \text{if } h = 0 \\ = 1 \quad \text{otherwise}$$

The switch function  $\phi_1(h)$  suppresses a delta function at zero frequency. Otherwise, the estimate, Equation 77, is exactly the conventional FFT frequency smoothed cross spectral estimate.

Cross-bi-spectral estimates corresponding to Equations 44 and 48 become:

$$\hat{S}_{yxx}(j,k) = \frac{(N\Delta t)^2}{H} \sum_{f=j-m}^{j+m} \sum_{h=k-m}^{k+m} \bar{Y}(f+h) \bar{X}(-h) \bar{X}(-f) \phi_2(h,f) \quad (78)$$

$$\hat{S}_{x^2xx}(j,k) = \frac{(N\Delta t)^2}{H} \sum_{f=j-m}^{j+m} \sum_{h=k-m}^{k+m} \bar{W}(f+h) \bar{X}(-h) \bar{X}(-f) \phi_2(h,f) \quad (79)$$

The switch function  $\phi_2(h,f)$  is defined:

$$\phi_2(h,f) = 0 \quad \text{if: } h = 0 \\ \quad \quad \quad \text{or: } f = 0 \\ \quad \quad \quad \text{or: } h + f = 0 \\ \phi_2(h,f) = 1 \quad \text{otherwise}$$

In this case it may be noted that the development of Reference 27 predicts delta functions along the line  $j = -k$  in the bi-frequency plane, and the switch function suppresses the periodogram estimates along this line. This is in contrast to the autocorrelation based methods of Reference 14 and 15 with which no such problem appeared to exist.

Finally, cross-tri-spectral estimates corresponding to Equations 59 and 62 become:

$$\hat{S}_{yxxx}(j,k,\ell) = \frac{(N\Delta t)^3}{H} \sum_{e=j-m}^{j+m} \sum_{f=k-m}^{k+m} \sum_{h=\ell-m}^{\ell+m} \bar{Y}(e+f+h) \bar{X}(-e) \bar{X}(-f) \bar{X}(-h) \phi_3(e,f,h) \quad (80)$$

$$\hat{S}_{x^3xxx}(j,k,\ell) = \frac{(N\Delta t)^3}{H} \sum_{e=j-m}^{j+m} \sum_{f=k-m}^{k+m} \sum_{h=\ell-m}^{\ell+m} \bar{Z}(e+f+h)\bar{X}(-e)\bar{X}(-f)\bar{X}(-h) \phi_3(e,f,h) \quad (81)$$

The switch function  $\phi_3(e,f,h)$  is defined:

$$\begin{aligned} \phi_3(e,f,h) = 0 \quad \text{if:} \quad & e = 0 \\ & \text{or: } f = 0 \\ & \text{or: } h = 0 \\ & \text{or: } e+f+h = 0 \\ & \text{or: } e+f = 0 \\ & \text{or: } e+h = 0 \\ & \text{or: } f+h = 0 \\ \phi_3(e,f,h) = 1 \quad & \text{otherwise} \end{aligned}$$

As would be anticipated from the discussion of the last section, the switch function suppresses the delta functions in the periodogram which lie exactly in the planes of the cross-tri-spectrum which may be of considerable practical importance. As previously noted, it was hoped that averaging over  $(2m)$  adjacent periodogram estimates would provide reasonable results in these cases.

As in conventional spectrum analyses it is expected that there is little point in producing estimates of any of the cross spectra for frequencies spaced at intervals less than  $2\pi(2m+1)/N\Delta t$ . The analysis parameter ' $m$ ' controls the extent of frequency smoothing and must be chosen in accordance with the problem at hand and the frequency resolution of the basic Fast Fourier transforms. So long as the minimum frequency increments correspond to  $(2m+1)$  there appears no disadvantage in basic programming suitable for probing the cross-bi and cross-tri-spectra as opposed to a complete computation for all combinations of frequency.

The primary reason for the frequency smoothing operations is to reduce the variance of the estimates. There appears no reason in References 27 and 28 why simple ensemble averaging of estimates should not also be carried out to the extent that multiple independent time domain samples are available.

CROSS-BI-SPECTRAL IDENTIFICATION OF THE QUADRATIC  
FREQUENCY RESPONSE FUNCTION

The last objective of the present work was to attempt the application of the approaches described in the last two sections to the simulated random data. As noted previously, the simulated response data had been produced in such a way that response could easily be computed for various excitation levels. Accordingly, the first decision to be made was what excitation level to employ. It appeared from the analysis of scalar spectra that the response of the simulated system to excitation twice the nominal was in line with nonlinear response which might be observed in towing tank experiments, and this level ( $\sigma_x = 0.5$ ) was selected. (The corresponding scalar spectra are shown in Figure 14.)

For convenience, the initial basic steps noted in the previous section were carried out on each of the eleven samples of excitation and response which were available, and the results were stored for subsequent use. In particular, the processing steps carried out were:

1. Compose the samples to be analyzed by multiplying the nominal excitation series and response component  $Y_1(n)$  by two,  $Y_2(n)$  by 4, and  $Y_3(n)$  by 8. Summing the response components in accordance with Equation 14, there resulted 11 sets of time history of response,  $Y(n)$  and excitation  $X(n)$ .
2. Correct both series to zero sample mean, and derive  $W'(n)$  and  $Z'(n)$  as previously described.
3. Taper each series and correct for variance loss.
4. Perform the direct Fast Fourier Transform on each series, so that  $\bar{X}(k)$ ,  $\bar{Y}(k)$ ,  $\bar{W}(k)$  and  $\bar{Z}(k)$  were available as in Equations 65 through 67.

The first step of the analysis strategy previously noted is to perform cross-bi-spectral analyses to define quadratic response. Since this type of analysis has been done previously, there was no particular

question of feasibility involved. However, in the present instance it was though worthwhile to perform the cross-bi-spectral analysis with the FFT based method to gain some experience and to see if the switch function shown after Equation 79 would adequately cope with the delta functions expected along the line  $\omega_2 = -\omega_1$  in the bi-frequency plane. To this end Equations 78 and 79 were programmed together in order to save some complex multiplications, and applied to the 11 sets of transform data previously described. The block averaging parameter 'm' was set at 4; that is, 81 adjacent values of the third order periodogram were averaged to form the cross-bi-spectral estimate at frequencies  $\omega_1 = j\Delta\omega$ ,  $\omega_2 = k\Delta\omega$  where

$$\Delta\omega = \frac{18\pi}{N\Delta t} = 0.422 \text{ rad/sec}$$

The result was a set of cross-bi-spectral estimates for each of the 11 samples of data, and the final estimates were made by ensemble smoothing; that is, by averaging the 11 sets of cross-bi-spectral estimates.

Qualitatively, the resulting cross-bi-spectral estimates appeared reasonable, and it appeared that the most sensitive way to check the result would be to form an estimate of  $G_2(\omega_1, \omega_2)$  and compare the results with the known theoretical quadratic frequency response function. To this end the quadratic frequency response function was estimated by:

$$\tilde{G}_2(\omega_1, \omega_2) = \frac{\hat{S}_{yxx}(\omega_1, \omega_2)}{\hat{S}_{x^2xx}(\omega_1, \omega_2)}$$

where the cross-bi-spectra were the final ensemble smoothed values. Previous experience with this type of analysis has suggested that such estimates cannot be good outside the range of bi-frequency where the product  $S_{xx}(\omega_1) S_{xx}(\omega_2)$  is appreciable. Inspection of  $\hat{S}_{x^2xx}(\omega_1, \omega_2)$  suggested that only in the range:

$$5 < |\omega_1| < 10$$

$$5 < |\omega_2| < 10$$

would this be reasonably satisfied, and accordingly attention was paid only to this range of bi-frequency. For comparison, theoretical values of  $G_2(\omega_1, \omega_2)$  were computed by means of Equations 11 and 13 for the discrete bi-frequencies of the estimates from the simulated samples.

The resulting comparisons are shown in Figures 18 through 20. Figure 18 involves the modulus of  $G_2(\omega_1, \omega_2)$ , Figure 19 the real part and Figure 20 the imaginary part. These figures are essentially plotted tables. In the region of the bi-frequency plane where both frequencies are positive and the frequencies are between 5 and 10 rad/sec the procedure just described results in a matrix of 121 estimates. Because of the symmetry of the function it suffices to show only the 65 estimates where  $\omega_1 \geq \omega_2$ , and these are plotted at their location in the plane in vertical lettering. Just below each of the estimates the corresponding theoretical value is shown in slanted lettering. Similarly 65 unique estimates of  $G_2(\omega_1, \omega_2)$  result for the case that  $\omega_1$  and  $\omega_2$  differ in sign and these are shown in the lower part of the figures along with the corresponding theoretical values.

In general, the correspondence between theoretical and estimated  $G_2(\omega_1, \omega_2)$  shown in Figures 18 through 20 seems quite good, in fact, better than might have been expected on the basis of past experience with samples of about the same size and the cross correlation approach, References 14 and 15. Signs and magnitudes of real and imaginary parts are in quite reasonable agreement except for the values shown at  $\omega_1, \omega_2 = (9.7, -9.7)$ . In this instance  $S_{X^2_{XX}}(\omega_1, \omega_2)$  is very much smaller than adjacent estimates, and it was suspected that the bad result was largely a matter of division by noise. It is along the line  $\omega_2 = -\omega_1$  in the lower part of the figures where wild disagreement due to the presence of delta functions would be expected. With the exception just noted, percentage differences between estimate and theory along this line do not seem greatly different from those off the line. The net result of the cross-bi-spectral exercise was to suggest that cross-tri-spectral estimation should next be attempted since the switch function in Equations 78 and 79 appeared to be coping with the anticipated problem area.

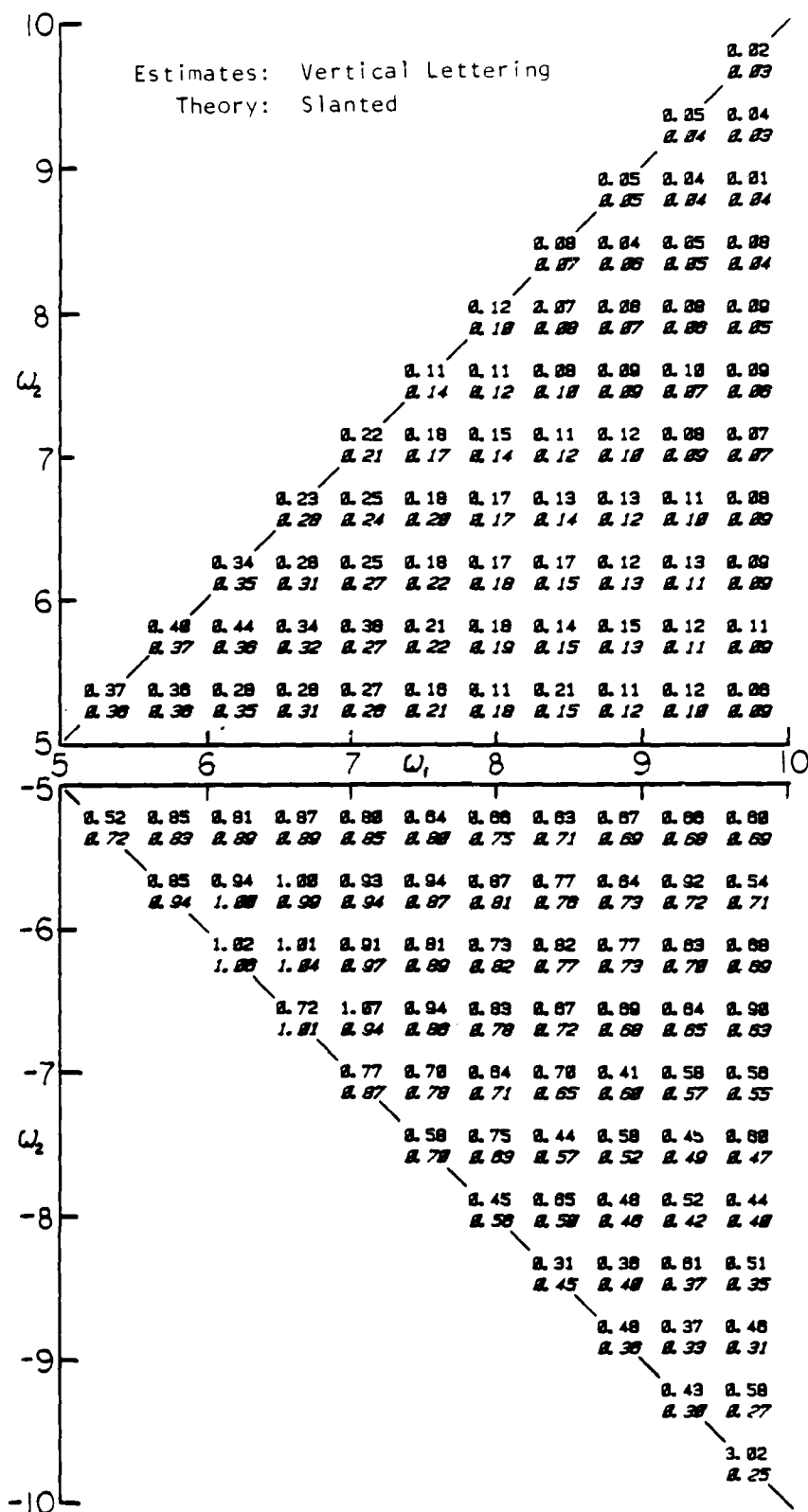


FIGURE 18 COMPARISON OF ESTIMATED AND THEORETICAL MODULUS OF  $G_2(\omega_1, \omega_2)$

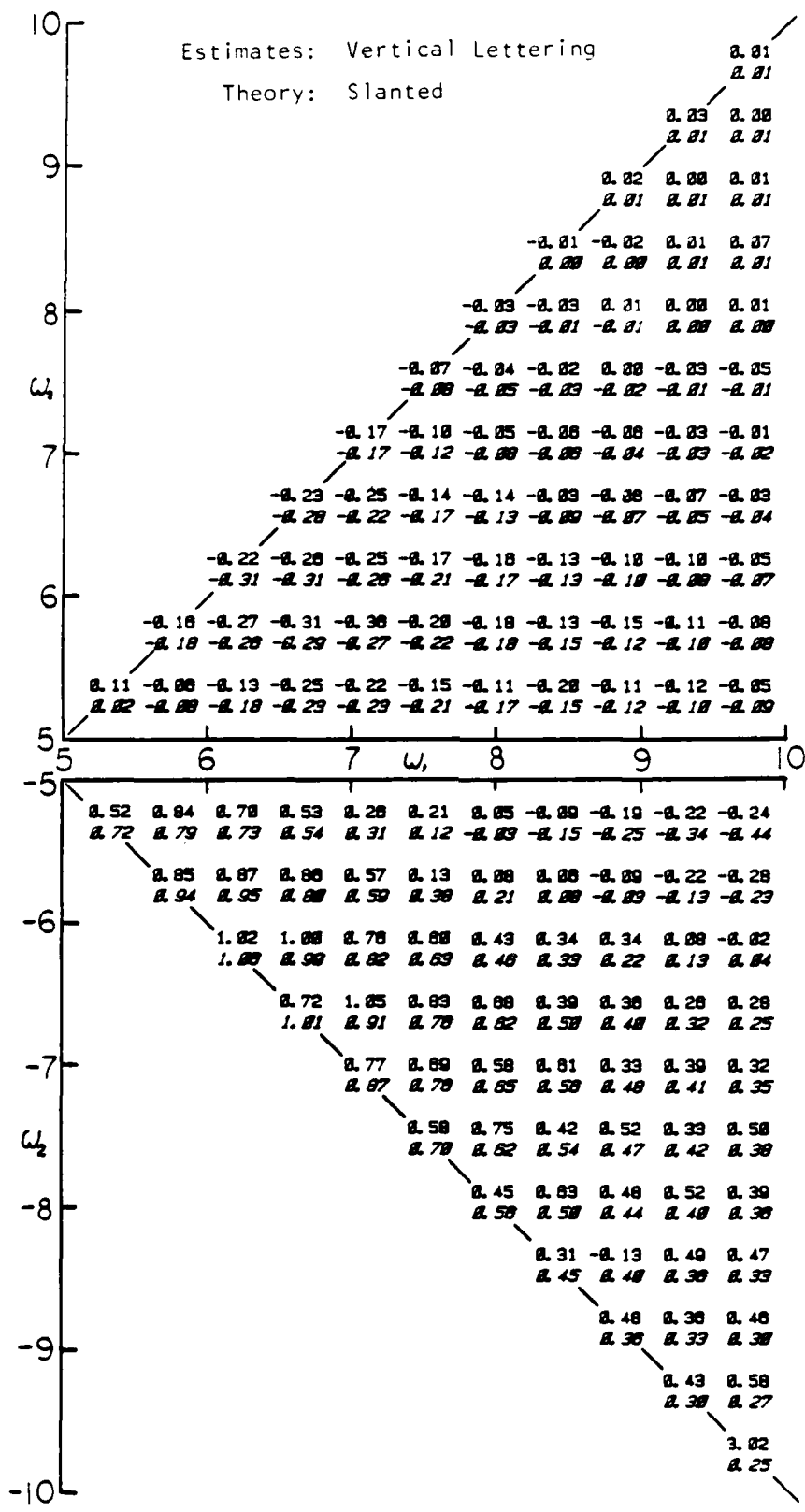


FIGURE 19 COMPARISON OF ESTIMATED AND THEORETICAL REAL PART OF  $G_1(\omega_1, \omega_2)$

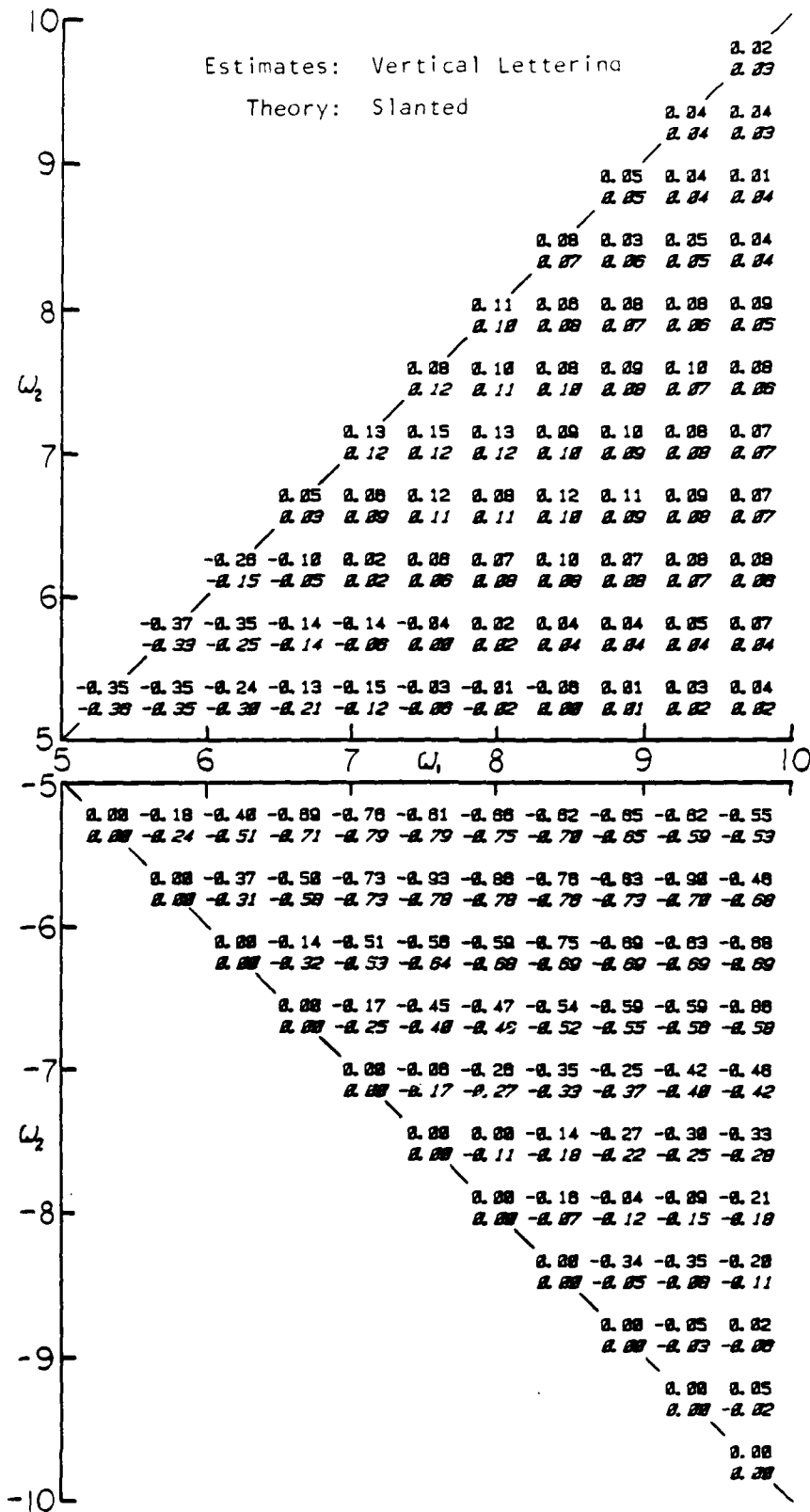


FIGURE 20 COMPARISON OF ESTIMATED AND THEORETICAL IMAGINARY PART OF  $G(\dots)$

## TRIAL CROSS-TRI-SPECTRAL IDENTIFICATIONS

Since the main objective was to identify the cubic frequency response function from simulated data, and the theoretical response function was all that was known, the trial analyses followed the general approach of the last section. That is; the estimates defined by Equations 80 and 81 were programmed together so as to allow computation of the cross-tri-spectral estimates  $\hat{S}_{YXXX}(\omega_1, \omega_2, \omega_3)$  and  $\hat{S}_{X^3XXX}(\omega_1, \omega_2, \omega_3)$ , and then the cubic frequency response function was estimated by:

$$\tilde{G}_3(\omega_1, \omega_2, \omega_3) = \frac{\hat{S}_{YXXX}(\omega_1, \omega_2, \omega_3)}{\hat{S}_{X^3XXX}(\omega_1, \omega_2, \omega_3)}$$

in accordance with Equation 63. Trial computations of theoretical values of  $G_3(\omega_1, \omega_2, \omega_3)$  suggested that the frequency resolution of the analysis should not be coarser than that of the quadratic analysis of the last section and the same block averaging parameters were picked. The block averaging parameter "m" was thus set at 4, and accordingly 729 adjacent estimates of the fourth order periodograms were to be averaged in order to form the cross-tri-spectral estimates at tri-frequencies which would be multiples of  $\Delta\omega = 0.442$ . The same basic transform data ( $\bar{X}(k)$ ,  $\bar{Z}(k)$  and  $\bar{Y}(k)$ ) produced for the cross-bi-spectral analysis was required for the cross-tri-spectral. Thus the starting point for the present analysis was the eleven sets of transforms previously used which correspond to the simulations for  $\sigma_x = 0.5$  (spectra in Figure 14). As in the cross-bi-spectral case, ensemble smoothing was performed over the cross-tri-spectral estimates formed from each of the 11 simulated data records.

It is clear from the basic identification theory that cross-tri-spectral estimates cannot be appreciable outside the range of tri-frequency where the product:

$$S_{XX}(\omega_1) S_{XX}(\omega_2) S_{XX}(\omega_3)$$

is appreciable. Estimates of  $G_3(\omega_1, \omega_2, \omega_3)$  outside this range are apt to be seriously corrupted by noise. Some preliminary computations of

$S_{x^3xxx}(\omega_1, \omega_2, \omega_3)$  and inspection of the excitation spectrum of Figure 14 suggested that only in the range

$$5 < |\omega_1| < 8 \text{ radians/second}$$

$$5 < |\omega_2| < 8$$

$$5 < |\omega_3| < 8$$

would there be hope of reasonable results.

Since an analysis over even a restricted region of tri-frequency space would require appreciable computation time, it was determined to start slowly and first examine some simple cases. The simplest case is just to estimate  $G_3(\omega, \omega, \omega)$ , the third harmonic response function. In this case delta function problems are not of concern. Accordingly, estimates of cross-tri-spectra along the line ( $\omega_1 = \omega_2 = \omega_3 = \omega$ ) were formed from each of the eleven samples, averaged, and from these results estimates of the cubic response function  $G_3(\omega, \omega, \omega)$  were made. The results are shown as circled points in Figure 21. In the figure the real and imaginary parts as well as the modulus of  $G_3(\omega, \omega, \omega)$  are plotted for the restricted range of frequency just noted. The corresponding theoretical values of  $G_3(\omega, \omega, \omega)$  are shown as dashed lines. It will be noted that arrows have been drawn to indicate the direction of the estimates made for a frequency just below 5 rps (the positions of these points are off the plotting field).

It may be noted from Figure 21 that the results of this first cross-tri-spectral identification (circled points) were at least recognizable as an estimate of the theoretical values of the function. Clearly, significant deviations were present. Those at the ends of the frequency range are typical of what can happen when the excitation cross-tri-spectrum gets small. However the deviations in mid range gave rise to the thought that perhaps the sample size (11 records) was too small. There is no theory of sampling variability available for cross-tri-spectral estimation of cubic response functions. (There is none for cross-bi-spectral identification either.)

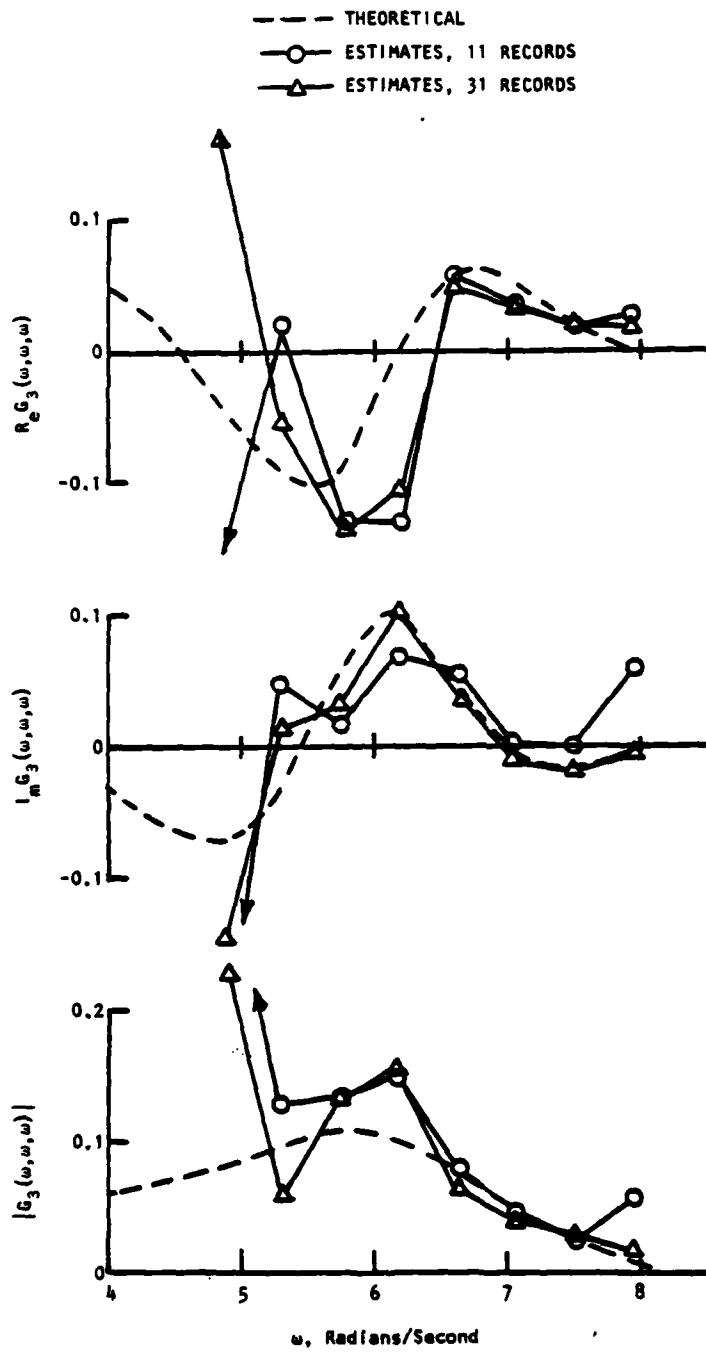


FIGURE 21 COMPARISON OF ESTIMATED AND THEORETICAL VALUES OF THE CUBIC FREQUENCY RESPONSE FUNCTION ALONG THE LINE  $\omega_1 = \omega_2 = \omega_3 = \omega$ .

An obvious next step was to generate significantly more sample and repeat the identification. It was relatively convenient to modify the programs described in conjunction with the basic simulation so that an additional 20 statistically independent time domain sample records of excitation could be generated. Computation of the time domain responses for each of these was carried out as before, with the result that the simulated data set was increased from 11 to 31 records--roughly tripling the available sample. The cross-tri-spectral analysis was repeated with ensemble smoothing over the 31 records, and the results are shown in Figure 21 as triangles.

The results in Figure 21 for 31 records are clearly an improvement over the first analysis. Agreement between estimate and theory is reasonably good at the high end of the frequency range. At the low end of the range the deviations between estimate and theory were reduced, but not by a great deal. The results of varying sample size suggest that the point of diminishing returns may be somewhere between 11 and 31 records so that the idea of generating even more sample was discarded. It has been noted that the third harmonic response of the present system is quite small. In this light the results in Figure 21 might be considered not too bad for a first attempt.

The next set of trial identifications were for the cubic response function along the line:

$$\omega_1 = \omega_2 = \omega$$

$$\omega_3 = -\omega$$

This, according to the speculations previously made may generally be the most practically important part of the cubic frequency response function.  $G_3(\omega, \omega, -\omega)$  expresses cubic nonlinear response at excitation frequency, and is part of the special case,  $G_3(\omega, \nu, -\nu)$ , which must be identified if the linear response function is to be separated. Cross-tri-spectral identification was carried out as before for this case with the results shown in Figure 22. This figure indicates the real and imaginary parts as well as the modulus of estimated and theoretical values of  $G_3(\omega, \omega, -\omega)$ .

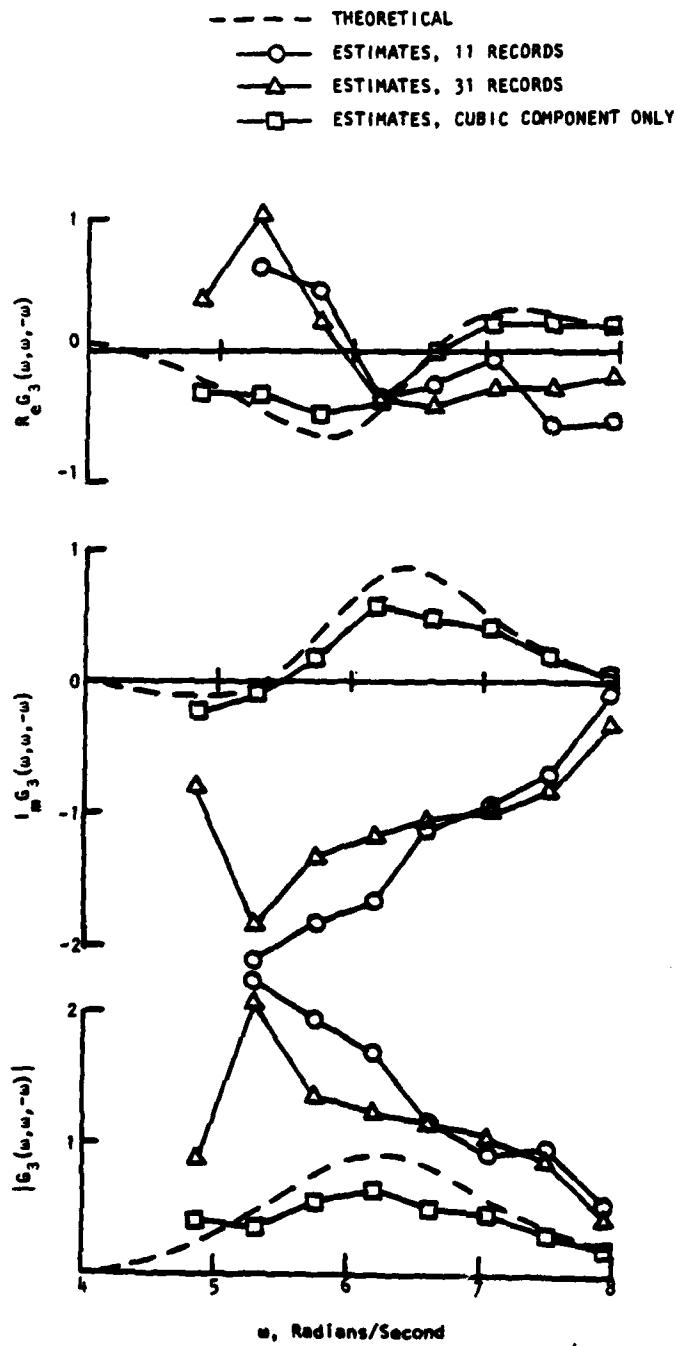


FIGURE 22 COMPARISON OF ESTIMATED AND THEORETICAL  
 VALUES OF THE CUBIC FREQUENCY  
 RESPONSE FUNCTION ALONG THE  
 LINE  $\omega_1 = \omega_2 = \omega; \omega_3 = -\omega$

Ensemble smoothed estimates for 11 and 31 records are shown by circular and triangular symbols. As in the previous trial the differences between estimates for 11 and 31 samples imply that sample size is acceptable.

Comparing the estimates and the theory in Figure 22, it is clear that something is wrong. The magnitude of the estimates are in the ballpark but the signs of the real and imaginary parts are consistently opposite what they should be.

An obvious diagnostic step was to see if the presence of a quadratic component ( $Y_2(n)$ , Equation 14) was upsetting things. To this end new time domain samples with quadratic component suppressed were made up for a few records and the identification repeated. Omitting the quadratic component had little effect on the estimates from the cross-tri-spectral identification. This is of course what is expected from the theory.

Continuing the diagnosis, new time domain samples which contained only the cubic component ( $Y_3$ ) of Equation 14) were constructed and the cross-tri-spectral identification repeated. The results are shown by rectangular symbols in Figure 22. (Ensemble smoothing over all 31 time domain samples was involved.) The estimates of  $G_3(\omega, \omega, -\omega)$  for the case where only the cubic component is involved in the data are quite reasonable relative to the theoretical values.

It is obvious from this evidence that there is a problem with the delta functions, since they will be involved in this case. The theory of Reference 27 says essentially that reasonable results should be obtained for averages near, "but not too near" the delta function tri-frequencies. It was thought possible that the influence of the deltas was spread out over a few more periodogram estimates than those which are exactly on the critical tri-frequencies. Accordingly, the switch functions, Equations 80 and 81, were modified so that periodogram estimates close to but not at the critical points could also be neglected. The modified program was exercised so as to do the identification with

neglect of successively wider bands of periodogram estimates. No essential change in the character of the estimates was noted up to a neglect band which amounted to almost half the delta frequency of the analysis. At this point the scatter of estimates increased radically since far fewer periodogram estimates were being averaged. The conclusion is that the influence of the delta functions "spreads out" considerably from the exact critical tri-frequencies.

Clearly, the presence of the linear component in the data strongly influences the importance of the delta's (see discussion after Equation 63). It appeared that the cross-tri-spectral identification method developed would only yield reasonable results for  $G_3(\omega, \omega, -\omega)$  when the linear component was relatively small; that is, for excitation levels in which the major part of the response was cubic. This is not likely to happen in practical ship seakeeping problems so that the method as developed appears unsatisfactory for  $G_3(\omega, \omega, -\omega)$ . Since  $G_3(\omega, \omega, -\omega)$  is probably the most important part of  $G_3(\omega, \nu, -\nu)$  the method is almost certainly an unsatisfactory approach to the latter case. There seemed no point in proceeding further until a method which was satisfactory for  $G_3(\omega, \omega, -\omega)$  was in hand, since identification of the linear frequency response function depends upon success with the identification of cubic response function of this type.

## CONCLUDING REMARKS

The objectives of the present work were to explore the applicability of the third degree functional polynomial model to nonlinear seakeeping problems, and to attempt the development of analysis approaches by which third degree nonlinearities in the responses of ships in waves might be interpreted and characterized.

It appears that the functional polynomial of third degree (which contains linear, quadratic and cubic terms) may be capable of representing a wide variety of the relatively weak nonlinearities which can be anticipated in the response of ships to waves. Conceptually, the ship dynamics would be represented by a series of frequency response functions--linear, quadratic and cubic. These functions can be interpreted in terms of the responses to the superposition of one, two and three periodic excitations. Thus in principle the functions may be identified by deterministic experiments. It appears that extension of hydrodynamic theory to include cubic nonlinearities may be accomplished at the expense of systematic development to "third order" just as it was found possible to include quadratic nonlinearities with a development to "second order".

Within limits, the functional polynomial model is compatible with the random excitation case. Past work has shown the qualitative and quantitative influence of quadratic nonlinearities upon the response to random excitation. A significant part of the present work was to explore the influence of cubic nonlinearities. This was done by means of a simulation of a relatively arbitrary nonlinear system so that the indications are hardly general. However in many respects the response of the simulated system reflected some types of nonlinear behavior which has been seen in experiment so that some reasonable conjectures can be made. The first is that the most significant aspects of cubic nonlinear time domain response to random waves may be associated with wave groups, just as has been noted in the quadratic case. The second is that the most important influence of cubic nonlinearities on the scalar spectrum of nonlinear response appears to be dependent upon a special portion of the cubic frequency response function. This special portion of the

function involves third degree nonlinear interactions between two frequency components as well as a self interaction involving a single frequency.

It was important in the development of credibility of both the linear and the quadratic functional models as applied to ship response that means be developed of identifying linear and quadratic frequency response functions from samples of random excitation and response. Accordingly, a considerable part of the present work was given over to the development of theoretical identification methods for the cubic response function. The theoretical developments in this direction included the definition of an entity named the cross-tri-spectrum, which is simply related to the cubic frequency response function, and thus in principal to an identification method.

The theoretical development disclosed a complication with cubic systems not present in the linear plus quadratic model. This is that the linear and cubic responses are mixed together in such a way that the results of a conventional cross spectrum identification cannot be simply related to the linear response function. To the extent that it was possible to progress the theory, it appears that in analyzing linear plus cubic systems a portion of the cubic response function must be identified first. The theory also disclosed that the cross-tri-spectrum is not a simple extension of cross and cross-bi-spectral theory. The difference is related to the problem with the cross spectrum. Essentially, unless special provision are made, a cross-tri-spectrum will contain delta functions which are strongly influenced by the linear components of response. Unfortunately, the location of these delta functions corresponds exactly to that of the portion of the cubic frequency response function thought to be of most practical importance.

The last part of the present work was to attempt the cross-tri-spectral identification of the cubic response functions from simulated random excitation and response data. There were two avenues of approach

available for cross-tri-spectral estimation, a correlation function approach thought to be extremely expensive, and a Fast Fourier Transform approach. The FFT approach was opted for and both cross-bi and cross-tri-spectral estimating methods were developed. Identifications of the quadratic frequency response function were reasonably successful with this approach. However when trial identifications of cubic frequency response functions were carried out troubles surfaced immediately. Essentially, the methods developed appear workable for those portions of the cross-tri-spectrum where no delta functions are expected, and for the portions which have delta functions when no linear component of response is present. Thus the FFT methods developed were found unsatisfactory for the portion of the cubic frequency response function of most practical importance, so that there appeared little point in further pursuit of the FFT based cross-tri-spectral analysis method.

## RECOMMENDATIONS

Clearly, the FFT cross-tri-spectral estimating approach attempted in the present work appears a failure in the case of most practical importance. This does not necessarily mean that the basic identification theory is incorrect or unusable, because the FFT approach was selected largely upon economic grounds. If the third degree functional model is to achieve credibility some means of identification from random wave data will be required. The obvious next step in the development of cross-tri-spectral analysis is to go back to the theoretical correlation function approach and to develop numerical estimation methods on that basis.

Most of the qualitative results obtained herein are relative to a simulated system which may or may not be reasonable relative to ship motions problems. An experimental or analytical investigation of the nature of cubic frequency response functions for a realistic ship seakeeping situation is recommended.

The "bottom line" in all seakeeping predictions is usually certain statistics of response maxima, and only when this is possible can a complete theory of seakeeping be claimed. Efforts should thus be made to develop an approach to the probability density function of the maxima of a cubic system.

## REFERENCES

1. St. Denis, M. and Pierson, W.J., "On the Motions of Ships in Confused Seas", SNAME Vol. 61, 1953.
2. Dalzell, J.F., "The Input-output" Approach to Seakeeping Problems: Review and Prospects", T.&R. Symposium S-3, Seakeeping 1953-1973, Society of Naval Architects and Marine Engineers, October 1973.
3. Wiener, N., "Non-linear Problems in Random Theory", The Technology Press of MIT and John Wiley and Sons, Inc., 1958.
4. Barrett, J.F., "The Use of Functionals in the Analysis of Non-Linear Physical Systems", Journal of Electronics and Control, 15, No. 6 December 1963.
5. George, D.A., "Continuous Non-Linear Systems", Doctoral Dissertation, Department of Electrical Engineering, M.I.T., July 1959.
6. Ku, Y.H., and Wolf, A.A., "Volterra-Wiener" Functionals for the Analysis of Non-linear Systems", Journal of the Franklin Institute, 281, No. 1, January 1966.
7. Bedrosian, E. and Rice, S.O., "The Output Properties of Volterra Systems (Non-linear Systems with Memory) Driven by Harmonic and Gaussian Inputs", Proceedings of the IEEE, Vol. 59, No. 12, December 1971.
8. Vassilopoulos, L.A., "The Application of Statistical Theory of Non-linear Systems to Ship Motion Performance in Random Seas", Ship Control Systems Symposium, Annapolis, November 1966.
9. Bishop, R.E.D., Burcher, R.K., and Price, W.G., "The Uses of Functional Analysis in Ship Dynamics", Proceeding, Royal Society of London, A. 332, 1973.
10. Tick, L.J., "The Estimation of the "Transfer Functions" of Quadratic Systems", TECHNOMETRICS, 3, No. 4, 1961.
11. Hasselman, K., "On Non-linear Ship Motions in Irregular Waves", JSR 10, No. 1, 1966.
12. Shaman, Paul, "Bi-Spectral Analysis of Stationary Time Series", Scientific Paper #18, Statistical Laboratory, School of Engineering and Sciences, N.Y.U., January 1964.
13. Rosenblatt, M. and Van Ness, J.W., "Estimates of the Bi-Spectrum of Stationary Random Processes", Technical Report 11, Nonr 562(29)/11, Division of Applied Mathematics, Brown University, Providence, R.I., March, 1964.

14. Dalzell, J.F., "Cross-Bi-Spectral Analysis: Application to Ship Resistance in Waves", Journal of Ship Research, Vol. 18, No. 1, March 1974, pp62-72.
15. Dalzell, J.F., "Application of the Functional Polynomial Model to the Ship Added Resistance Problem", Eleventh Symposium on Naval Hydrodynamics, University College, London, 1976.
16. Dalzell, J.F. and Kim, C.H., "An Analysis of the Quadratic Frequency Response for Added Resistance", Journal of Ship Research, Vol. 23, No. 3, September 1979.
17. Newman, J.N., "Second Order Slowly Varying Forces on Vessels in Irregular Waves", International Symposium on the Dynamics of Marine Vehicles and Structures in Waves, University College, London, April 1974.
18. Pinkster, J.A. and van Oortmerssen, G., "Computation of the First and Second Order Wave Forces on Bodies Oscillating in Regular Waves", Proceedings of the Second International Conference on Numerical Ship Hydrodynamics, University of California, pp. 136-156, September 1977.
19. Tasai, F. and Koteratama, W., "Non-linear Hydrodynamic Forces Acting on Cylinders Heaving on the Surface of a Fluid", Reports of the Research Institute For Applied Mechanics, Vol. XXIV, No. 77, 1976.
20. Dalzell, J.F., "A Note on the Form of Ship Roll Damping", SIT-DL-76-1887, Davidson Laboratory, Stevens Institute of Technology, May 1976, (Also: Journal of Ship Research, Vol. 22, No. 3, September 1978).
21. Dalzell, J.F., "Estimation of the Spectrum of Non-linear Ship Rolling: The Functional Series Approach". SIT-DL-76-1894, Davidson Laboratory, Stevens Institute of Technology, May 1976, AD-A031 055/761.
22. Rugh, W.J., "Nonlinear System Theory; The Volterra/Wiener Approach," Johns Hopkins University Press, 1981.
23. Dalzell, J.F., "A Note on the Distribution of Maxima of Ship Rolling," Journal of Ship Research, Vol. 17, No. 4, December 1973.
24. Bendat, J.S. and Piersol, A.G., "Random Data: Analysis and Measurement Procedures," John Wiley & Sons, 1971.
25. Laning, J.H., and Battin, R.H., "Random Processes in Automatic Control," McGraw-Hill, 1956.
26. Dalzell, J.F., "Some Further Experiments on the Application of Linear Superposition Techniques to the Responses of a Destroyer Model in Extreme Irregular Long-Crested Head Seas," Davidson Laboratory Report 918, September 1962.

27. Brillinger, D.R. and Rosenblatt, M., Two Papers: "Asymptotic Theory of Estimates of  $k$ th Order Spectra," and "Computation and Interpretation of  $k$ th Order Spectra," Proceedings of an Advanced Seminar on Spectral Analysis of Time Series, Edited by B. Harris, October 1966, John Wiley & Sons, New York.
28. Lii, K.S., Rosenblatt, M., and Van Atta, C., "Bi-Spectral Measurements in Turbulence," Journal of Fluid Mechanics, Vol. 77, Part 1, 1976.

## APPENDIX A

EXPECTED VALUES OF PRODUCTS OF  
ZERO MEAN GAUSSIAN EXCITATION

The autocorrelation function or second moment of the zero mean Gaussian excitation,  $X(t)$ , is defined in Equation 35 as:

$$R_{XX}(\tau) = \overline{X(t) X(t - \tau)}$$

By definition of a zero mean process:

$$\overline{X(t)} = 0 \quad (A-1)$$

From the development of Reference 25, pages 82-85:

$$\overline{X(t_1) X(t_2) \cdots X(t_n)} = 0 \quad \text{for } n \text{ odd} \quad (A-2)$$

In the present work occasion is found for the manipulation of up to sixth order expectations. Equations 35 of the text and Equations A-1 and A-2 define all but the fourth and sixth order expectations. The fourth order case is given in numerous texts including Reference 25, and may be written:

$$\begin{aligned} \overline{X(t_1) X(t_2) X(t_3) X(t_4)} &= R_{XX}(t_1 - t_2) R_{XX}(t_3 - t_4) \\ &+ R_{XX}(t_1 - t_3) R_{XX}(t_2 - t_4) \\ &+ R_{XX}(t_1 - t_4) R_{XX}(t_2 - t_3) \end{aligned} \quad (A-3)$$

where the zero mean assumption has been utilized.

The sixth order expectation as derived from the general treatment in Reference 25 for the zero mean process may be written in present notation as:

$$\begin{aligned}
& \overline{X(t_1) X(t_2) X(t_3) X(t_4) X(t_5) X(t_6)} \\
&= R_{XX}(t_1 - t_2) R_{XX}(t_3 - t_4) R_{XX}(t_5 - t_6) \\
&+ R_{XX}(t_1 - t_2) R_{XX}(t_3 - t_5) R_{XX}(t_4 - t_6) \\
&+ R_{XX}(t_1 - t_2) R_{XX}(t_3 - t_6) R_{XX}(t_4 - t_5) \\
&+ R_{XX}(t_1 - t_3) R_{XX}(t_2 - t_4) R_{XX}(t_5 - t_6) \\
&+ R_{XX}(t_1 - t_3) R_{XX}(t_2 - t_5) R_{XX}(t_4 - t_6) \\
&+ R_{XX}(t_1 - t_3) R_{XX}(t_2 - t_6) R_{XX}(t_4 - t_5) \\
&+ R_{XX}(t_1 - t_4) R_{XX}(t_2 - t_3) R_{XX}(t_5 - t_6) \\
&+ R_{XX}(t_1 - t_4) R_{XX}(t_2 - t_5) R_{XX}(t_3 - t_6) \\
&+ R_{XX}(t_1 - t_4) R_{XX}(t_2 - t_6) R_{XX}(t_3 - t_5) \\
&+ R_{XX}(t_1 - t_5) R_{XX}(t_3 - t_4) R_{XX}(t_2 - t_6) \\
&+ R_{XX}(t_1 - t_5) R_{XX}(t_3 - t_2) R_{XX}(t_4 - t_6) \\
&+ R_{XX}(t_1 - t_5) R_{XX}(t_3 - t_6) R_{XX}(t_2 - t_4) \\
&+ R_{XX}(t_1 - t_6) R_{XX}(t_3 - t_4) R_{XX}(t_5 - t_2) \\
&+ R_{XX}(t_1 - t_6) R_{XX}(t_3 - t_5) R_{XX}(t_4 - t_2) \\
&+ R_{XX}(t_1 - t_6) R_{XX}(t_3 - t_2) R_{XX}(t_4 - t_5)
\end{aligned} \tag{A-3}$$

## APPENDIX B

## THE n-DIMENSIONAL PARSEVAL FORMULA

The n-dimensional form of Parseval's formula finds application in the present work. It is as follows (Reference 4):

$$\begin{aligned} & \iint \cdots \int f_1(t_1, t_2, \cdots t_n) f_2(t_1, t_2, \cdots t_n) dt_1 dt_2 \cdots dt_n \\ &= \frac{1}{(2\pi)^n} \iint \cdots \int F_1^*(\omega_1, \omega_2, \cdots \omega_n) F_2(\omega_1, \omega_2, \cdots \omega_n) d\omega_1 d\omega_2 \cdots d\omega_n \end{aligned} \quad (B-1)$$

where the (\*) denotes complex conjugate and  $f_j(t_1 \cdots)$  and  $F_j(t_1 \cdots)$  are Fourier Transform pairs defined:

$$\begin{aligned} F_j(\omega_1, \omega_2, \cdots \omega_n) &= \iint \cdots \int f_j(t_1, t_2, \cdots t_n) \text{Exp}(-i \sum_{r=1}^n \omega_r t_r) dt_1 dt_2 \cdots dt_n \\ f_j(t_1, t_2, \cdots t_n) &= \frac{1}{(2\pi)^n} \iint \cdots \int F_j(\omega_1, \omega_2, \cdots \omega_n) \text{Exp}(i \sum_{r=1}^n \omega_r t_r) d\omega_1 \cdots d\omega_n \end{aligned} \quad (B-2)$$

## PRINCIPAL NOTATION

$A, A_j$	Constants
$B_j$	Constants
$C_j$	Constants
$D_n(\alpha)$	Auxilliary function = $A_n\alpha^2 + B_n\alpha + C_n$
$g_1(t)$	Linear impulse response
$g_2(t_1, t_2)$	Quadratic impulse response
$g_3(t_1, t_2, t_3)$	Cubic impulse response
$g_j^1$	Digital impulse response (linear)
$g_{jk}^2$	Digital impulse response (quadratic)
$g_{jkl}^3$	Digital impulse response (cubic)
$G_1(\omega)$	Linear frequency response function
$G_2(\omega_1, \omega_2)$	Quadratic frequency response function
$G_3(\omega_1, \omega_2, \omega_3)$	Cubic frequency response function
$j, k, \ell$	Time increments
$N$	Number of points in a time series
$p, q, r$	Frequency increments
$P_{yx}(j)$	Second order periodogram
$P_{yxx}(j, k)$	Third order periodogram
$P_{yxxx}(j, k, \ell)$	Fourth order periodogram
$R_{xx}(t)$	Autocorrelation function
$R_{yx}(t)$	Cross correlation function
$R_{yxx}(t_1, t_2)$	Third order correlation
$R_{yxxx}(t_1, t_2, t_3)$	Fourth order correlation

$S_{xx}(\omega)$	Two sided spectrum, excitation
$S_{yy}(\omega)$	Two sided spectrum, response
$S_{yx}(\omega)$	Cross spectrum
$S_{yxx}(\omega_1, \omega_2)$	Cross-bi-spectrum
$S_{yxxx}(\omega_1, \omega_2, \omega_3)$	Cross-tri-spectrum
$t, t_j$	Time
$U_{xx}(\omega)$	One sided spectrum, excitation
$U_{yy}(\omega)$	One sided spectrum, response
$\bar{W}(k)$	FFT of squared excitation
$X(t)$	Excitation
$\hat{X}(t)$	Periodic excitation
$\bar{X}(k)$	FFT of excitation
$Y(t)$	Response
$\hat{Y}(t)$	Response to periodic excitation
$\bar{Y}(k)$	FFT of response
$\bar{Z}(k)$	FFT of cubed excitation
$\Delta t$	Sampling interval
$\epsilon, \epsilon_j$	Phase angles
$\omega, \omega_j$	Circular frequency

## INITIAL DISTRIBUTION LIST

Contract N00014-81-K-0231

15	<p>Commander David W. Taylor Naval Ship Research and Development Center Attn: Code 1505 Bldg. 19, Rm. 129B Bethesda, MD 20084</p>	<p>Commander Naval Ocean Systems Center Attn: Library San Diego, CA 92152</p>
8	<p>Commander Naval Sea Systems Command Washington, DC 20362 Attn: 05R22 (J. Sejd) 55W (R. Keane, Jr.) 55W3 (W. Sandberg) 50151 (C. Kennell) 56X1 (F. Welling) 63R31 (T. Pierce) 55X42 (A. Paladino) 99612 (Library)</p>	<p>Library Naval Underwater Systems Center Newport, RI 02840</p> <p>Research Center Library Waterways Experiment Station Corp of Engineers P.O. Box 631 Vicksburg, MI 39180</p> <p>Charleston Naval Shipyard Technical Library Naval Base Charleston, SC 29408</p> <p>Norfolk Naval Shipyard Technical Library Portsmouth, VA 23709</p> <p>Puget Sound Naval Shipyard Engineering Library Bremerton, WA 98314</p> <p>Long Beach Naval Shipyard Technical Library (246L) Long Beach, CA 90801</p> <p>Mare Island Naval Shipyard Shipyard Technical Library (202.3) Vallejo, CA 94592</p> <p>Assistant Chief Design Engineer for Naval Architecture Code 250 Mare Island Naval Shipyard Vallejo, CA 94592</p>
12	<p>Director Defense Documentation Center 5010 Duke Street Alexandria, VA 22314</p> <p>Library of Congress Science &amp; Technology Division Washington, DC 20540</p> <p>Naval Ship Engineering Center Norfolk Division Combatant Craft Engineering Dept. Attn: D. Blount (6660) Norfolk, VA 23511</p> <p>Naval Underwater Weapons Research and Engineering Station (Library) Newport, RI 02840</p> <p>Commanding Officer (L31) Naval Civil Engineering Laboratory Port Hueneme, CA 93043</p>	

U.S. Naval Academy  
Annapolis, MD 21402  
Attn: Technical Library

Naval Postgraduate School  
Monterey, CA 93940  
Attn: Library (2124)

Study Center  
National Maritime Research Center  
U.S. Merchant Marine Academy  
Kings Point, LI, NY 11024

The Pennsylvania State University  
Applied Research Laboratory (Library)  
P.O. Box 30  
State College, PA 16801

Dr. B. Parkin, Director  
Garfield Thomas Water Tunnel  
Applied Research Laboratory  
P.O. Box 30  
State College, PA 16801

Bolt, Beranek & Newman (Library)  
50 Moulton Street  
Cambridge, MA 02138

Bethlehem Steel Corporation  
25 Broadway  
New York, NY 10004  
Attn: Library - Shipbuilding

Cambridge Acoustical Associates, Inc.  
54 Rindge Avenue Extension  
Cambridge, MA 02140

R&D Manager  
Electric Boat Division  
General Dynamics Corporation  
Groton, CT 06340

Gibbs & Cox, Inc.  
Technical Information Control  
119 West 31st Street  
New York, NY 10001

Hydronautics, Inc.  
Library  
Pindell School Road  
Laurel, MD 20810

Newport News Shipbuilding and  
Dry Dock Company  
Technical Library  
4101 Washington Avenue  
Newport News, VA 23607

Mr. S. Spangler  
Nielsen Engineering & Research, Inc.  
510 Clyde Avenue  
Mountain View, CA 94043

Society of Naval Architectures &  
Marine Engineers  
Technical Library  
One World Trade Center  
Suite 1369  
New York, NY 10048

Sun Shipbuilding & Dry Dock Co.  
Attn: Chief Naval Architect  
Chester, PA 19000

Sperry Systems Management Division  
Sperry Rand Corporation  
Attn: Library  
Great Neck, NY 11020

Stanford Research Institute  
Attn: Library  
Menlo Park, CA 94025

2 Southwest Research Institute  
P.O. Drawer 28510  
San Antonio, TX 78284  
Attn: Applied Mechanics Review  
Dr. H. Abramson

Tracor, Inc.  
6500 Tracor Lane  
Austin, TX 78721

Mr. Robert Taggart  
9411 Lee Highway, Suite P  
Fairfax, VA 22031

Ocean Engineering Department  
Woods Hole Oceanographic, Inc.  
Woods Hole, MA 02543

Worcester Polytechnic Institute  
Alden Research Laboratory  
Attn: Technical Library  
Worcester, MA 01609

Applied Physics Laboratory  
University of Washington  
Attn: Technical Library  
1013 N.E. 40th Street  
Seattle, WA 98105

4 University of California/Berkeley  
Naval Architecture Department  
Berkeley, CA 94720  
Attn: Prof. W. Webster  
Prof. J. Paulling  
Prof. J. Wehausen  
Library

California Institute of Technology  
Attn: Library  
Pasadena, CA 91109

Engineering Research Center  
Reading Room  
Colorado State University  
Foothills Campus  
Fort Collins, CO 80521

Florida Atlantic University  
Ocean Engineering Department  
Attn: Technical Library  
Boca Raton, FL 33432

Gordon McKay Library  
Harvard University  
Pierce Hall  
Cambridge, MA 02138

Department of Ocean Engineering  
University of Hawaii  
Attn: Library  
2565 The Mall  
Honolulu, HI 96822

2 Institute of Hydraulic Research  
The University of Iowa  
Iowa City, IA 52240  
Attn: Library  
Dr. L. Landweber

Prof. O. Phillips  
Mechanics Department  
The Johns Hopkins University  
Baltimore, MD 21218

Kansas State University  
Engineering Experiment Station  
Seaton Hall  
Attn: Prof. D. Nesmith  
Manhattan, KS 66502

University of Kansas  
Chm Civil Engr Department Library  
Lawrence, KS 60644

Fritz Engr. Laboratory Library  
Department of Civil Engineering  
Lehigh University  
Bethlehem, PA 18015

2 Department of Ocean Engineering  
Massachusetts Institute of Tech.  
Cambridge, MA 02139  
Attn: Prof. P. Leehey  
Prof. J. Kerwin

Engineering Technical Reports  
Room 10-500  
Massachusetts Institute of Tech.  
Cambridge, MA 02139

Office of Naval Research  
800 N. Quincy Street  
Attn: Dr. C. Lee, Code 432  
Arlington, VA 22217

2 St. Anthony Falls Hydraulic Laboratory  
University of Minnesota  
Mississippi River at 3rd Avenue S.E.  
Minneapolis, MN 55414  
Attn: Dr. Roger Arndt  
Library

Davidson Laboratory  
Stevens Institute of Technology  
711 Hudson Street  
Hoboken, NJ 07030  
Attn: Library

Department of Naval Architecture  
and Marine Engineering-North Campus  
University of Michigan  
Ann Arbor, MI 48109  
Attn: Library

Applied Research Laboratory Library  
University of Texas  
P.O. Box 8029  
Austin, TX 78712

Stanford University  
Attn: Engineering Library  
Stanford, CA 94305

Webb Institute of Naval Arch.  
Attn: Library  
Crescent Beach Road  
Glen Cove, LI, NY 11542

National Science Foundation  
Engineering Division Library  
1800 G Street N.W.  
Washington, DC 20550

Mr. John L. Hess  
4338 Vista Street  
Long Beach, CA 90803

Science Applications, Inc.  
134 Holiday Court, Suite 318  
Annapolis, MD 21401

Dr. Tuncer Cebeci  
Mechanical Engineering Dept.  
California State University  
Long Beach, CA 90840